

**RE-EVALUATION OF METALS TRANSPORT AT BEAR CREEK URANIUM
CONVERSE COUNTY, WYOMING**

October 13, 2011

Prepared for:

Anadarko Petroleum Corporation
1201 Lake Robbins Drive
The Woodlands, Texas 77380

Attention: Harry Nagel

Prepared by:

Tetra Tech GEO
363 Centennial Parkway, Suite 210
Louisville, Colorado 80027



TETRA TECH GEO

TABLE OF CONTENTS

1.0 Introduction.....	1
1.1 Objectives and Approach.....	2
1.2 Site Description.....	3
2.0 Groundwater System.....	3
2.1 Geology of the Site	3
2.2 Site Hydrogeology	4
2.2.1 Groundwater Flow Paths.....	4
2.2.2 Temporal changes in water levels.....	4
2.3 Groundwater Chemistry.....	5
2.3.1 Uranium	6
2.3.2 Sulfate	7
2.3.3 Chloride.....	7
2.3.4 pH.....	8
2.3.5 Radium.....	8
2.3.6 Nickel.....	9
2.4 Site Geochemistry.....	9
2.4.1 Geochemical speciation results.....	9
3.0 Updated predictive transport modeling.....	11
3.1 Model construction and calibration	12
3.2 Model Results	13
3.2.1 Lang Draw	13
3.2.2 Northern Pathway	16
4.0 Conclusions.....	18
5.0 References.....	19

FIGURES

Figure 1	Location of the Bear Creek, Wyoming Disposal Site, Converse County
Figure 2	Aerial Photograph of the Disposal Site
Figure 3	Saturated Thickness of the N sand, June 1986
Figure 4	Saturated Thickness of the N sand, March 1996
Figure 5	Saturated Thickness of the N sand, February 2011
Figure 6	Water Level Elevations, June 1986
Figure 7	Water Level Elevations, June 1986
Figure 8	Water Level Elevations, June 1986
Figure 9	Measured Water Level Elevations, 1981 to 2011
Figure 10	A. Distribution of Uranium Concentrations, February 2011 B. Temporal Changes in Uranium Concentrations, Lang Draw C. Temporal Changes in Uranium Concentrations, Northern Pathway
Figure 11	A. Distribution of Sulfate Concentrations, February 2011 B. Temporal Changes in Sulfate Concentrations, Lang Draw C. Temporal Changes in Sulfate Concentrations, Northern Pathway
Figure 12	A. Distribution of Chloride Concentrations, February 2011 B. Temporal Changes in Chloride Concentrations, Lang Draw

- Figure 13 C. Temporal Changes in Chloride Concentrations, Northern Pathway
 A. Distribution of pH, February 2011
 B. Temporal Changes in pH, Lang Draw
 C. Temporal Changes in pH, Northern Pathway
- Figure 14 A. Distribution of Radium Concentrations, February 2011
 B. Temporal Changes in Radium Concentrations, Lang Draw
 C. Temporal Changes in Radium Concentrations, Northern Pathway
- Figure 15 A. Distribution of Nickel Concentrations, February 2011
 B. Temporal Changes in Nickel Concentrations, Lang Draw
 C. Temporal Changes in Nickel Concentrations, Northern Pathway
- Figure 16 Simulated initial values along Lang Draw
 A. Uranium
 B. Sulfate
 C. Chloride
 D. pH
 E. Radium
 F. Nickel
- Figure 17 Simulated breakthrough along Lang Draw
 A. Uranium
 B. Sulfate
 C. Chloride
 D. pH
 E. Radium
 F. Nickel
- Figure 18 Predicted breakthrough along Lang Draw
 A. Uranium
 B. Sulfate
 C. Chloride
 D. pH
 E. Radium
 F. Nickel
- Figure 19 Simulated initial values along Northern Pathway
 A. Uranium
 B. Sulfate
 C. Chloride
 D. pH
 E. Radium
 F. Nickel
- Figure 20 Simulated breakthrough along Northern Pathway
 A. Uranium
 B. Sulfate
 C. Chloride
 D. pH
 E. Radium
 F. Nickel
- Figure 21 Predicted breakthrough along Northern Pathway
 A. Uranium
 B. Sulfate

C. Chloride
D. pH
E. Radium
F. Nickel

TABLES

Table 1	Results of monitoring wells samples, February 10 through February 12, 2011
Table 2	Saturation indices for water samples on Lang Draw Flow path, 2011
Table 3	Saturation indices for water samples on Northern Pathway, 2011

ATTACHMENTS

- I. Temporal plots of chemical parameters measured in monitoring wells
- II. Input PHREEQC data set for Lang Draw
- III. Input PHREEQC data set for Northern Pathway
- IV. Modifications to the Thermodynamic Database for Uranium and Radium

Re-evaluation of Metals Transport at Bear Creek Uranium Converse County, Wyoming

1.0 Introduction

The former Bear Creek Uranium Mine and milling operations are located in Converse County, Wyoming (Figure 1). Tailings were placed in an impoundment formed by a dam constructed across Lang Draw, west of the former mill. The milling operation was shut down in 1986, beginning a period of reclamation for the tailings impoundment.

A groundwater recovery system was operated beneath and downgradient of the tailings impoundment. Recovered water was pumped into the impoundment and allowed to evaporate. Later evaporation occurred within clay-lined impoundments, which had been constructed on top of the tailings.

In 1995, GeoTrans, Inc. (now called Tetra Tech GEO) performed a geochemical evaluation (GeoTrans, Inc., 1995) of the future transport of uranium, radium, and nickel, based on chemical conditions that existed at that time. An important consideration at that time was prediction of the neutralization of acidic water found beneath and a short distance downgradient of the tailings impoundment as the water moved downgradient through alluvium and rock that contained calcite. Measurements of the acidity of the water and the neutralization capacity of the alluvium and rock were made, and calculations indicated that the movement of low pH water would be slower than the movement of the water because of the neutralization reactions. For Lang Draw, the 1995 study estimated that the retardation factor of the pH front would be approximately 10 for the area upgradient of the seepage control dam, and approximately 15 for the area downgradient of it. The study also found that the concentrations of metals As, Be, Cd, Cl, Th, and Ra all decreased sharply as the pH increased above approximately 4.5, as did the concentrations of Fe and Al. This behavior was interpreted as being indicative of coprecipitation of the former list of metals with iron and aluminum hydroxides. During the 1995 modeling effort, GeoTrans used MINTEQA2 (Allison et al, 1991) to perform the geochemical speciation modeling to estimate retardation coefficients of uranium and nickel, and other laboratory measurements for Ra and Th. These values indicated that the metals would move more quickly than the pH front, and therefore one-dimensional transport models using linear sorption theory were prepared to predict future movement. Predictions of peak uranium concentrations at the property line at that time (near MW-14) were between approximately 50 and 70 pCi/L, depending on the amount of dilution from convergent flow into Lang Draw, with the peak occurring approximately 80 years after 1995, or in 2075. Nickel was estimated to travel more slowly, with the peak concentration ranging between approximately 0.05 and 0.85 mg/L in about 2250. These modeling predictions were used in an application to set Alternate Concentrations Limits (ACLs) in 1997. The ACLs for U, Ra, and Ni were set at 2038 pCi/L, 46 pCi/L, and 3.8 mg/L, respectively, with the points of compliance established at MW-12 for Lang Draw and MW-74 for the northern flow path. These ACLs were based on the model results indicating that concentrations at the point of exposure wells for U, Ra, and Ni would be 45 pCi/L, 13 pCi/L, and 0.55 mg/L, respectively.

In the interim, the recovery well system was shut down in 1996, and all wells not to be used for monitoring were plugged and abandoned. A cover was placed over the tailings, and additional grading was performed to control surface-water flow.

Five wells along Lang Draw (MW-12, MW-9, MW-14, MW-108, and MW-109), and 4 wells along the "northern pathway" (MW-74, MW-43, MW-110, and MW-111) have been monitored. No other monitoring wells exist for monitoring.

In reviewing the monitoring data in preparation to the transfer of the site to the DOE for long-term care and surveillance, the NRC recently compared the monitoring data with the predictions from the modeling work done in 1995, and noticed that uranium concentrations in MW-14 had reached values of 520 pCi/L. As a result, the NRC requested that Anadarko Petroleum Corporation, current owner of Bear Creek Uranium, submit a revised ACL application. Anadarko has requested that Tetra Tech GEO, using the newer information collected since the cessation of the recovery well pumping, reevaluate the transport of the radionuclides and metals in support of a new ACL application.

1.1 Objectives and Approach

This re-evaluation of transport is being done to improve the prediction capability of the transport modeling, using information collected over the sixteen-year period since the last predictions were made. This work involves several steps:

- a) Collect additional water samples from available monitoring points for analysis of parameters important to understanding geochemical controls on metals transport. The standard suite of analytes includes the trace metals and radionuclides of interest, and limited geochemical parameters (sulfate, chloride, and pH). The additional sampling added other parameters such as major anions and cations, iron, manganese, phosphate, and silica.
- b) Evaluate water-level data to determine if flow directions have changed significantly from when the recovery wells were still pumping and the tailings were draining more rapidly than today.
- c) Evaluate the areal distribution of and the temporal changes in water chemistry parameters, to understand if there are changes in water chemistry that affect the transport of the radionuclides and metals.
- d) Perform geochemical speciation modeling, to determine whether there are changes in chemical behavior that have occurred over the last sixteen years.
- e) Re-evaluate the transport modeling that was done in 1995 to develop an understanding of why it underpredicted the transport of uranium.
- f) Develop an improved transport model calibrated against more recent information, and predict future movement of the parameters of interest. The model that was used is PHREEQC (Parkhurst and Appelo, 1999), which has the capability of performing one-dimensional transport calculations considering the chemistry of the water in the system and the chemical reactions that occur in the water and between the water and the soil and rock.

1.2 Site Description

As shown on Figure 2, the site currently consists of the following major features:

- A tailings impoundment with a riprap-armored tailings embankment (dam) on the northwest (downgradient) side;
- Diversion channels to direct runoff around the tailings impoundment; and
- A smaller dam for seepage control located in Lang Draw about 600 feet northwest of the main dam.

The site is about 8500 feet from north to south, with the tailings impoundment approximately in the center. Thus, the downgradient (northern) site boundary is between 2600 and 2900 feet from the tailings impoundment. The former uranium mine is located about 850 feet east of the tailings impoundment but is not considered to be part of the site.

Surface drainage is generally toward the north. Lang Draw emerges from the base of the impoundment and heads north to the property boundary, and an unnamed draw begins northeast of the impoundment and heads northwest toward the property boundary. These two draws continue off the property and ultimately join some distance north of the property boundary.

2.0 Groundwater System

Information about the groundwater system consists of observations of the geology, hydrogeology, and geochemistry observed at the site. Much of the basic information used during the current model update was presented in the previous modeling report, and only the most relevant portions are repeated below. Since the modeling report was generated in 1995, a number of water level and groundwater quality data collection events have occurred. Trends will be discussed where appropriate, and the most recent data set (collected in February 2011) will be presented.

2.1 Geology of the Site

The tailings basin is underlain by sandstone, shales, and lignites of the Wasatch Formation. The uppermost sandstones have been named the K and N sands. The depositional environment appears to have been one of rivers carrying fine- to coarse-grained materials in a coastal or deltaic plain setting. The numerous shale deposits indicate that the river gradient was low. The massive thickness of the K sand suggests that it may have been deposited by a meandering river of moderate size. The underlying N sand is less consistent and of variable thickness. Drill hole information shows that it changes from a small channel sand into several sands splaying out into an overbank environment. Laterally continuous lignites and coals are present, and further suggest a meandering river through a low gradient wet overbank environment.

The K and N sands crop out within and underlie the tailings basin. The K sand is the upper sandstone and is exposed at the surface and on the sides of Lang Draw. In some places, the K sand has been eroded away. Within Lang Draw, the K sand has been eroded and replaced by up to 20 to 40 feet of alluvial sand, silt, and clay deposits. The K sand is separated from the N sand by a claystone that varies in thickness between 5 and 50 feet. The N sand tends to be thicker to the northeast near the unnamed draw than toward Lang Draw (S.M. Stoller, 1997) and dips to the

east north east. The N sand outcrops in Lang Draw north of MW-108, and in the unnamed draw about 500 feet northwest of MW-111.

2.2 Site Hydrogeology

The site hydrogeology will be discussed in two parts: groundwater flow paths and individual well hydrographs showing changes over time.

2.2.1 Groundwater Flow Paths

The primary focus of this report is on flow occurring in the N sand, since that is the permeable unit in which groundwater contamination has been found to occur. Saturated thickness maps have been prepared for the N sand based on the June 1986, March 1996, and February 2011 groundwater elevation data sets. These maps are provided as Figures 3 to 5. In addition, Figures 6 to 8 illustrate the potentiometric surface maps from the same time frames. The potentiometric surface and saturated thickness maps illustrate the two groundwater flow paths present at the site: the Lang Draw and Northern flow paths.

Water level data have consistently indicated a convergence of flow toward Lang Draw. The N sand is normally unsaturated on the east side of Lang Draw (see Figures 3 to 5), creating an area of decreased permeability. Coupled with the higher permeability of the alluvial sediments, there is a tendency for groundwater contour lines to indicate a strong flow component toward Lang Draw. East of Lang Draw (for example, near MW-74), flow appears to be toward the unnamed draw. Water-level data collected prior to installation of the groundwater recovery well system showed a flow pattern whereby groundwater east of the tailings dam had a northerly flow direction (GeoTrans, 1995, Figure 2-4). Recently, there are fewer wells for constraining the water-level elevation contour lines, but it does not appear that the presence of two separate flow paths has changed between 1986, 1996, and 2011.

The flow path along Lang Draw measures approximately 2700 feet from the tailings impoundment to the site boundary. The northern flow path measures approximately 3700 feet from the tailings impoundment to the site boundary along the unnamed draw in which MW-111 is installed. The gradients along these paths appear to have changed over time, likely due to the startup, then cessation, of the recovery pumping system.

2.2.2 Temporal changes in water levels

In discussing the temporal changes observed in water levels at the site, two events are important to consider. First, in 1986, a seepage recovery system using pumping wells was initiated downgradient of the tailings impoundment to intercept seepage and reapply it to the tailings impoundment for evaporation. Second, in 1996, the seepage recovery system was terminated (pumping ceased). These two events had an effect on water levels observed in a number of site wells.

Figure 9 shows the changes in water-level elevations through time for selected wells. Some of these wells are part of the current monitoring program (MW-9, -12, -14, -43, and -74). In addition, since some of the current wells were installed after major site changes occurred, some historical wells that have since been abandoned are included on Figure 9 (MW-22, -40, -41, and -42). There are two groups of data that are immediately apparent. The group with the higher elevations was measured in monitoring wells east of Lang Draw, and these wells will be called

the upland group. They are, generally speaking, located between the Lang Draw and the unnamed draw. The group with the lower groundwater elevations includes the wells along Lang Draw. Also noticeable on Figure 9 is the decline in water levels that began in about March of 1989. Recovery pumping had begun in 1986, and there was not a significant increase in pumping rate in the spring of 1989. The noticeable decrease in water levels that occurred in the upland group in 1989 may have been caused by redistribution of pumping. The rate of pumping from the recovery system was reduced in 1994 (and was turned off in 1996), and water levels began to recover.

MW-43 is an upland well that has been monitored during the entire period from the early 1980's to 2011. Water levels in this well were approximately 5098 ft when its record began in the early 1980's. Water levels rose and reached a peak in 1987. From the early 1980's until 1987, MW-43 was probably responding to rising levels in the tailings impoundment. With the beginning of recovery pumping, water levels began to decline, and continued to decline until 1994 when the recovery pumping decreased. Water levels then recovered until about 2000, when a period of declining levels began. The decline in water levels since 2000 is attributed to the reduction in seepage from the tailings as they dewatered in response to construction of a cover, which reduced the recharge rate. This trend of declining water levels will likely continue for several more years.

Another well shown on Figure 9 is MW-14, which is located along Lang Draw. While its behavior is similar to MW-43 with respect to the larger changes, its early behavior is somewhat different. When water levels were rising at the beginning of the record for MW-43, those in MW-14 were declining for a short period before beginning to rise. This different behavior is probably caused by the greater distance between MW-14 and the rising water levels in the tailings, and the greater isolation provided by the cut-off wall and recovery dam. With cessation of the operation of the recovery system, water levels increased in MW-14, but to higher levels than were present before recovery pumping began.

In summary, the cessation of the pumping in the recovery well system caused water levels to increase, and a change in the flow directions as the cones of depressions of the recovery wells dissipated. Water levels are now declining, assumed to be related to continued reduction in the rate of seepage from the tailings impoundment, and hydraulic gradients are decreasing.

2.3 Groundwater Chemistry

Since 1995, a number of groundwater sampling events have been completed. The most recent groundwater sampling event included wells MW-9, -12, -14, -43R, -74, -108, -109, -110, and -111. The analytes for each location are provided in Table 1. The following sub-sections discuss the February 2011 concentration data and provide a brief analysis of apparent trends, if any, observed in the data over time. The data are plotted on Figures 10 to 15. In each series, the "A" figure is a map illustrating the February 2011 concentrations, the "B" figure shows the historical data for the Lang Draw flow path, and the "C" figure shows the historical data along the Northern flow path.

Temporal plots separated by well and analyte are provided as Attachment I.

Predictions for beryllium, cadmium, chromium, molybdenum, and thorium-230 were not made because the concentrations of these parameters have remained below or very near their detection limits since the recovery system was turned off. GeoTrans (1995) found that concentrations of

Be and Cd have a strong dependence with pH, with very low concentrations at pH greater than 5. Molybdenum showed a similar dependence. The concentrations of beryllium, cadmium, and molybdenum measured since 1994 were reported by DOE to be less than the detection limit, or appeared to be less than the detection limit (based on the reported value and the reporting of identical values for MW-12 and MW-74). Chromium has been detected at concentrations as high as 0.04 mg/L, but concentrations have been typically less than 0.01 mg/L and were less than 0.001 mg/L when sampled in February 2011. Thus, these metals are not believed to be mobile under the current conditions, and the modeling, which will be discussed below, indicates that pH is unlikely to decrease below approximately 6.2, and will increase after the pH front moves through.

Thorium-230 could not be modeled because thermodynamic data were not available in the PHREEQC database. However, thorium should not be mobile under conditions of near-neutral pH. The sampling data demonstrate this. In the current monitoring wells, reported thorium-230 values have been low. The three highest reported values since the recovery system was turned off were 1.4 and 1 pCi/L in MW-43R in 1995 and 1996, and 1.1 pCi/L in MW-9 in 1996. In contrast, samples from TS-5 (pH 3.7) were as high as 14,000 pCi/L and MW-77 (pH 4.2 to 4.6) (downgradient of the tailings dam) had values as high as 31 pCi/L. Both of these sampling locations were characterized with low pH. Increasing the pH to above 6 has reduced the concentration of thorium-230 significantly. As a result, the higher values that were observed in the low pH waters are not expected to occur even in the upgradient monitoring wells, based on currently available measurements and the modeling predictions.

Most of the thorium-230 values that are reported in the DOE database are believed to be at or below the detection limits. Thorium-230 values are determined through counting. Most of the values reported in the DOE database are reported without information on the counting statistics. Where the counting statistics are provided, the detection limit is either at or greater than the reported value, suggesting that the concentration of thorium-230 for the samples without reported counting statistics or detection limits was at or below the detection limit. For samples collected from MW-74, MW-108, and MW-110 in July 2009, the reported values and detection limit were all 0.66 pCi/L. For these samples, the U flag was provided, but for most other sampling dates, the reported values were lower but no U flag was entered. Thus, the plots of thorium concentrations in Attachment I are believed to indicate the detection limits for the period after operation of the recovery system.

2.3.1 Uranium

Figure 10A provides a map of the February 2011 uranium concentrations. Uranium ranged from 1.6 pCi/L in MW-110 to 439 pCi/L in MW-14. The wells monitored are located along the Lang Draw and Northern flow paths.

Lang Draw Path: As indicated by Figure 10B, both MW-12 and MW-14 were increasing in concentration until late 1986, when the groundwater recovery system was started. Then, both wells experienced decreases in concentration, although there was a lag of a couple years between start of pumping and when concentrations began to decrease. Decreasing concentrations continued until 1994, when the groundwater recovery ceased. After that point, MW-12 and MW-14 both increased significantly in uranium concentration. The concentrations in MW-12

near the south end of the Lang Draw, nearest to the tailings impoundment, peaked after the groundwater recovery system was shut down in 1994, but are now decreasing. Similarly, concentrations at MW-14, located about 500 feet north of MW-12, peaked about two years ago and now appear to be decreasing. Concentrations at MW-108 are fairly stable, but concentrations at MW-109 are slightly increasing. This is because the peak has passed MW-12 and likely MW-14, and is moving northward in the direction of groundwater flow. Concentrations at MW-108 and MW-109 would therefore be expected to increase somewhat over the next few years, then decrease. It is noteworthy that MW-14 seems to have peaked at a concentration about 30% lower than was observed in MW-12. This would indicate that some natural attenuation or dilution is occurring along the Lang Draw flow path. Therefore, peaks observed at MW-108 and MW-109 would be expected to be significantly less than that observed at MW-14.

Northern Path: Figure 10C illustrates that peak concentrations have already passed MW-74 and MW-43. Concentrations at MW-110 and MW-111 appear to be fairly stable. As a result, it is not clear whether peak concentrations will actually reach MW-110 and MW-111. The highest concentrations observed along this flow path were prior to the shutdown of the groundwater recovery system in 1994. In addition, due to geologic and spatial heterogeneity, it appears that not all wells on this flow path are located in the plume center.

2.3.2 Sulfate

Figure 11A provides a map of the February 2011 sulfate concentrations. Overall, the sulfate concentrations ranged from 1190 mg/L in MW-111 to 2810 mg/L in MW-12 during the sampling event. The sulfate concentrations near the tailings impoundment are, in general, noticeably higher than the sulfate concentrations further downgradient.

Lang Draw Path: As indicated by Figure 11B, the sulfate concentrations have generally increased over time in wells MW-12 and MW-14, although they briefly decreased during the operation of the groundwater recovery system. The current sulfate concentrations in wells MW-12 and MW-14 continue to represent an increase over previous sampling events. The concentrations in well MW-9 began to increase after the shutdown of the groundwater recovery system in 1994. Wells MW-108 and MW-109 have had fairly constant sulfate concentrations since they were installed.

Northern Path: Figure 11C shows that sulfate concentrations in MW-43 increased steadily until at least the late 1990's, but have recently decreased. In addition, MW-74 has experienced increases in sulfate concentrations since the groundwater recovery system was shut down in 1994. Well MW-74 seems somewhat slower to reach its peak concentration than MW-43; possibly it is not located in the center of the plume due to geologic heterogeneity. Sampling in wells MW-110 and MW-111 since 2002 has indicated that sulfate concentrations are increasing in MW-111 but stable in MW-110.

2.3.3 Chloride

Figure 12A provides a map of the February 2011 chloride concentrations. Overall, the chloride concentrations ranged from 89 mg/L in MW-109 to 371 mg/L in MW-12 during the sampling event.

Lang Draw Path: Figure 12A shows that chloride concentrations decrease along the Lang Draw flow path from MW-12 (371 mg/L, nearest the tailings impoundment) to MW-14 (358 mg/L), MW-108 (302 mg/L), and MW-109 (89 mg/L). Concentrations in well MW-9 (334 mg/L) are also elevated, indicating that downward migration has occurred into this deeper-screened well. As indicated by Figure 12B, the chloride concentrations in MW-12 were increasing until the groundwater recovery system was implemented in 1986; after that, concentrations decreased until after the pumping ceased in 1994. Recent sampling events indicate that concentrations of chloride in well MW-12 have risen again. Chloride concentrations in well MW-14 seem to follow the same general pattern as in well MW-12, but delayed by about 5 years such that the decreases due to pumping are first seen in after 1991. Recent sampling shows that chloride concentrations in this well have increased since pumping ceased. Wells MW-108 and MW-109 have experienced steady increases since sampling began in 2002. Well MW-9 has experienced chloride concentration increases since about 1995, after the groundwater recovery system was shut down.

Northern Path: Figure 12A shows that MW-110 has the highest concentration (290 mg/L) and MW-111 has the lowest concentration (102 mg/L). Therefore, there is not a consistent decrease in chloride concentrations between the tailings impoundment and MW-111; this is likely due to some wells along this flow path not being located along the plume centerline as a result of geologic heterogeneity. As shown by Figure 12C, chloride concentrations in MW-43 increased steadily until reaching a peak in about 1994, and have since decreased. Chloride concentrations in well MW-110 have been on a decreasing trend since sampling began in 2002. Well MW-111 experienced some initial increase in chloride concentrations but has since been fairly stable.

2.3.4 pH

Figure 13A provides a map of the pH measured during the February 2011 sampling event. The measured pH ranged from 6.56 in MW-12 to 7.6 in MW-111 during the sampling event. These are all near neutral pH values and therefore do not indicate a significant low-pH plume emanating from the tailings impoundment.

Lang Draw Path: As indicated by Figure 13B, pH values along the Lang Draw flow path decreased slightly after the shutdown of the groundwater recovery system in 1994. The current sampling event seems to indicate a slight increase in most of the pH values; this potential new trend will continue to be monitored during future sampling events.

Northern Path: Figure 13C shows the pH values along the Northern flow path. Few monitoring points were available for this flow path prior to 2002. However, available data seem to indicate that a small decrease in pH may have occurred on the Northern flow path after the recovery system shutdown in 1994, though there seems to have been a lag of several years. The current sampling event appears to represent an increase in pH for most wells, but again, this potential trend will continue to be monitored during upcoming sampling events.

2.3.5 Radium

Figure 14A provides a map of the February 2011 combined radium-226 and radium-228 concentrations. The combined radium concentrations range from 0.9 pCi/L in well MW-9 to 10.5 pCi/L in MW-110.

Lang Draw Path: As indicated by Figure 14B, wells MW-12, MW-14, and MW-9 were increasing in concentration during the 1980's, and peaked after the start of pumping in 1986. Once the effects of pumping began to decrease concentrations in the late 1980's, concentrations have decreased fairly steadily over time. The highest concentration of radium in the Lang Draw flow path is still located at well MW-12 (3.0 pCi/L), though it has decreased significantly since the 1980's. Concentrations of radium in wells MW-108 and MW-109 have experienced slow increases since the wells were installed. These factors indicate that the peak has passed at MW-12 and MW-14, but has not yet reached MW-108 or MW-109.

Northern Path: Figure 14C indicates that concentrations are stable in well MW-74, decreasing in MW-43, possibly increasing in MW-110, and stable in MW-111. This pattern indicates that the plume peak has passed MW-74 and MW-43. The overall increasing trend in MW-110 seems to indicate that the peak has not yet passed this location. The low, stable concentrations at MW-111 indicate that the core of the plume has not reached this well.

2.3.6 Nickel

Figure 15A provides a map of the February 2011 nickel concentrations. The nickel concentrations range from 0.004 mg/L in well MW-111 to 0.043 mg/L in MW-108.

Lang Draw Path: Figure 15A indicates that the highest nickel concentrations on this flow path are near MW-14 and MW-108. Figure 15B shows that these two wells have experienced some increase in concentration over the last few years. Figure 15B also shows that overall concentrations in MW-12 and MW-14 have significantly decreased since the 1980's and 1990's. Nickel concentrations in MW-109 and MW-9 have remained fairly stable since 2002.

Northern Path: Figure 15A indicates that concentrations of nickel along the Northern flow path decrease as distance from the tailings impoundment increases, with the highest concentration being 0.042 mg/L in well MW-74. Figure 15C indicates that nickel concentrations in well MW-43 significantly decreased since the 1980's, but have slightly increased in recent years. Nickel concentrations in well MW-74 have increased since 2002, while concentrations in MW-110 and MW-111 have remained fairly stable since the wells were installed.

2.4 Site Geochemistry

2.4.1 Geochemical speciation results

Aqueous geochemical speciation models are computational tools for improving the understanding of the chemical reactions that occur in water and between constituents in the water and minerals that the water may contact or that may dissolve or precipitate. The models are based on equations that describe chemical reactions, thermodynamic data that collectively define equilibrium conditions, and the assumption that aqueous reactions are at equilibrium but reactions between the aqueous species and minerals may not be. These models are particularly useful for providing an understanding of the effects of reactions on chemical behavior of the water, and for predicting changes in water chemistry that may occur if conditions change. Changes can occur by many mechanisms, such as mixing of waters of different chemistry, and dissolution or precipitation of minerals.

One of the output parameters from a geochemical speciation model is known as the saturation index, or SI, that provides information on the state of saturation of minerals given the chemistry

of the water. Although complicated to calculate, the SI has a value of 0.0 when the water appears to be in equilibrium with a mineral. When the SI is 0, the mineral will neither precipitate nor dissolve unless conditions change. A value of SI greater than zero indicates that the water is supersaturated with respect to the mineral, and the mineral would have a tendency to precipitate. Conversely, a negative value for SI indicates that the mineral would have a tendency to dissolve, if it is present. Quite commonly, the chemical reactions do not occur rapidly enough for the water to be in equilibrium with the mineral. However, some minerals can dissolve or precipitate quite rapidly and exert controls on the chemistry of the water. Examples include the dissolution and precipitation of calcite, gypsum, and ferrihydrite, three minerals that are important in the chemical characteristics of the water in the groundwater system at Bear Creek.

The 1995 speciation model using MINTEQA2 indicated supersaturation with respect to a number of iron, aluminum, and sulfate minerals, with gibbsite, ferrihydrite, and gypsum identified as the most likely to control aqueous phase concentrations. The waters were found to be in equilibrium with calcite and undersaturated with respect to siderite. Four geochemically distinct pH zones were identified ranging from acidic (<3.5 pH) to neutral.

The 2011 speciation model using PHREEQC indicated many of the same conclusions. Low pH water was not observed, indicating that the pH front had not reached any of the monitoring wells, or that the neutralization capacity of the calcite in the rock is sufficiently high to maintain the pHs above 6. pH conditions beneath the impoundment are unknown, and may be acidic. Prior to dewatering of the tailings, the acid flux was great enough to overwhelm the neutralization capacity of the calcite in the soil and rock (i.e., the calcite that had been present in the soil and rock prior to disposal of the acidic tailings had been consumed). Currently, no data are available to indicate whether the influx of upgradient water is sufficient to neutralize any water which is draining or infiltrating through the tailings. As a result, the modeling (to be discussed later) will assume that low pH conditions continue to exist beneath the tailings to provide conservative results.

The water along the Lang Draw pathway is oversaturated with respect to calcite and the CO₂ pressures are greater than atmospheric CO₂ pressure (10^{-3.5} atmospheres) (Table 2). This indicates that the water has dissolved calcite, resulting in high CO₂ pressures, and is now trying to degas, which will cause precipitation of calcite. The waters are also supersaturated with ferrihydrite (iron hydroxide), indicating that it will tend to precipitate. Because uranium sorbs to ferrihydrite, the precipitation or dissolution of ferrihydrite affects the mobility of uranium. Waters along the flow path are at equilibrium with gypsum, the result of dissolution of calcite by sulfuric acid in the tailings seepage, with resultant precipitation of gypsum. One important outcome of the speciation modeling is that the waters are undersaturated with respect to all of the uranium minerals, and therefore uranium minerals have not been precipitating out of the groundwater. These results were also obtained when speciation modeling was performed using water-chemistry data from the 1980s and 1990s. Therefore, re-dissolution of uranium minerals is not expected. This result is expected, as the intent of the milling process is to mobilize the uranium from the ore, and remove it. Thus, the chemistry of the tailings solution does not favor precipitation of uranium bearing minerals for later remobilization. However, as will be seen later, the sorption of uranium onto ferrihydrite, followed by subsequent dissolution of the ferrihydrite as the pH front moves, can result in temporary remobilization.

Speciation modeling along the northern pathway produced similar results (Table 3).

In summary, the geochemical speciation modeling based on the recently collected samples produced the same conclusions as the earlier calculations with respect to mineralogic controls on the water chemistry. The low pH water from the tailings reacted with calcite, which raised the pH but caused gypsum to precipitate. The dissolved iron in the water precipitated as ferrihydrite when the pH increased. The waters have remained supersaturated with respect to ferrihydrite. Although not addressed by the speciation modeling, the uranium tends to sorb to ferrihydrite, which provides an attenuation/retardation mechanism for uranium.

3.0 Updated predictive transport modeling

The model that was developed in 1995 to predict transport of constituents in the water was performed using BIO1D, a one-dimensional transport code that uses linear sorption to simulate retardation. Because the pH front was estimated to move more slowly than other constituents in the water, the model was simulating transport downstream of the lower pH area. K_d values for uranium and other constituents were based on a combination of geochemical modeling and literature values. Initial concentrations were based on water samples collected as part of that study. The model assumed that water would begin moving down the flow paths when the groundwater recovery system was turned off. Capture of the COCs beneath and a short distance downgradient of the tailings impoundment would end, and impacted water would begin moving downgradient again.

As noted by NRC, the 1995 model under-predicted the U concentrations that would reach MW-14. The 1995 model in BIO1D used the observed concentrations as the modeling initial conditions downgradient from the low pH part of the plume. For the upstream boundary condition, it used the observed uranium concentration at the downstream edge of the pH front, 92 pCi/L. The assumption that was made was that this concentration was a good estimate of future uranium concentrations. As observed in Figure 10B, MW-12 had a uranium concentration of approximately 110 pCi/L in 1994, while MW-9 had a concentration of around 80 pCi/L. Because the modeling was only addressing transport downgradient of the pH front, these values appeared to be reasonable, based on the measurements.

What the modelers did not consider was the effect of dilution during the recovery pumping on the observed concentrations. The recovery pumping was causing steeper gradients west of Lang Draw than present after the pumping was stopped. The steeper gradients produced more water moving into the Lang Draw area than would occur after pumping stopped and water levels recovered. When pumping stopped, the dilution provided by this lateral inflow decreased. This water probably assisted in the neutralization of the acidic plume. The net result was that after water levels recovered, the uranium concentrations increased. Referring again to Figure 10B, the highest uranium concentration in MW-12 was approximately the same as was measured in this well in March 1989, before the full effects of the recovery system were apparent. Because the 1995 model used an upgradient boundary condition that was based on concentrations that were "artificially" low because of the recovery pumping, it underestimated the peak concentrations that were to develop.

The 1995 model estimated the future movement of uranium and other constituents using a K_d approach, in which the K_d values were estimated from speciation modeling and literature values for other locations and lithologies, and using estimates of groundwater flow velocities. There were no monitoring data with which to calibrate the models, as is normally done, and the more

recent monitoring data have indicated that the 1995 model overestimated the retardation of uranium, and thus underestimated the rate of its movement.

In response to NRC's request for a revised ACL application based on the additional 13 years of data, a new predictive transport model was developed. The new model has two significant advantages over the 1995 model. First, data are available regarding the transport of uranium and other constituents along Lang Draw and the Northern Pathway for use in calibration of the model. The 1995 model was performed in a purely predictive mode, without information on transport rates at the site. Second, modeling technology has improved allowing direct incorporation of the chemical reactions into the transport model. Separate models were constructed for Lang Draw and for the Northern Pathway.

3.1 Model construction and calibration

The current model in PHREEQC uses higher, undiluted source area concentrations and incorporates coefficients for U sorption onto ferrihydrite. The current model also assumes equilibrium with gypsum and supersaturation with respect to ferrihydrite. These assumptions are in keeping with the findings of the speciation model discussed above. The initial water concentrations at various points in model are adjusted to match observed concentrations during the earlier part of the simulation period, and concentrations upgradient of the pH front were adjusted to match observed breakthrough concentrations in downgradient monitoring wells. Further, the influx of water from tailings was decreased through time to reflect the decline in the rate of seepage from the tailings following construction of the cover. For example, the chemistry of the water for the upstream boundary of the Lang Draw model was calculated by mixing water from upgradient (represented by samples collected from MW-36) with MW-86, reflecting the tailings fluid. MW-86 had a pH of 4.5, a sulfate concentration of 9,040 mg/L, and iron concentration of 926 mg/L. Chemistries of downgradient water used in the model were based on samples that had been collected from monitoring wells at about the time that the recovery system was turned off.

The models were constructed to begin beneath the tailings impoundment and extend downgradient to the northern property boundary, along each flow path. Model lengths of 968 meters (3,175 ft) and 1,040 meters (3,412 ft) were used for Lang Draw and the Northern Pathway, respectively. The grid spacing was 4 meters, resulting in models with 242 cells and 260 cells, respectively. Time steps of approximately 1 month were used in each model. As would be expected with a reactive transport model with sharp changes in chemical parameters, especially pH, some minor numerical issues occurred early in the simulations. These quickly smoothed out both laterally and temporally as the sharp fronts were smoothed by the dispersive process that the model can simulate.

The model optimization code ucode (Poeter et al, 2005) was used to obtain initial estimates of various parameters (ferrihydrite concentration, water pore velocity, source decay rate, and concentration step factors). Concentration data for U, SO₄, Cl, Ra, and Ni observed in monitoring wells MW-12, -14, -108, and -109 were used as calibration targets for the Lang Draw flow path, and in wells MW-74, -43, -110, and -111 for the Northern flow path. Once a reasonable match to site data was obtained, hand calibration was used to fine tune parameters, such as the length of the low pH zone, which required adjustments to the model grid. Changes such as this are not easily made by ucode or other parameter-estimation approaches because of

the multiple steps involved in modifying the dataset, and the fact that cell designations can only be changed in integer steps.

During calibration of the models, the primary emphasis was on developing acceptable matches to the timing and magnitude of the breakthrough of uranium at the different monitoring wells, followed by simulating the sulfate and chloride concentrations. Other observations (radium for example) did not show a breakthrough pattern that could be used to assist the calibration of the model. A fact that became apparent early in the calibration process was that there was considerable spatial variability in the breakthrough behavior at different wells. MW-9 is a well that is completed at greater depth than MW-14, and even though MW-9 is closer to the tailings impoundment than MW-14 is, breakthrough occurs more slowly in MW-9. The breakthrough curves for chloride for MW-14 and MW-108 are nearly identical, even though they are nearly 700 feet apart. This complexity cannot be captured in a one-dimensional model. Because the peak uranium concentrations have already been observed in MW-12 and -14 along Lang Draw, the more recent data provide significant information on the rate of movement and the peak concentrations needed for predicting future movement.

For the Northern Pathway, the peak of the uranium breakthrough appears to have passed through MW-74. However, the data are noisier and the concentrations lower than in the wells along Lang Draw. The chloride peak appears to have already passed through MW-74, -4, and -110. As with Lang Draw, geologic variability will affect the actual movement of water and the constituents of interest, and therefore will affect the ability of the model to accurately predict the breakthrough of the constituents.

The input datasets for PHREEQC are provided in Attachments II and III for Lang Draw and the Northern Pathway, along with plots showing the initial concentrations for uranium, chloride, sulfate, pH, radium, and nickel.

For radium, the model considered only Ra-226 transport, because the great majority of the mass of radium is Ra-226, and the model is a chemical model that is based on the mass of the elements present. The activities presented assume that the radium is all Ra-226. Because Ra-226 and Ra-228 should be in secular equilibrium (and the monitoring data support this assumption), the total activity can be estimated by doubling the activities from the monitoring results.

An improved and expanded geochemical database for uranium and radium thermodynamic data was used. This dataset is described in Attachment IV.

3.2 Model Results

Modeling was performed based on two pathways, Lang Draw and the Northern Pathway. For each pathway, the calibration process will be discussed first. Predictions of future transport will then be presented. Data on concentrations of sulfate, chloride, uranium, radium, and nickel; and on pH were used for the calibration. Predictions for concentrations of these same parameters were also made.

3.2.1 Lang Draw

Calibration: The initial concentrations used for the Lang Draw model are shown in Figures 16A through 16F. The upgradient water was a mixture of MW-36 and MW-86 waters. MW-86 is characterized with low pH (4.5), high sulfate (9,040 mg/L), iron (926 mg/L), and high uranium

(2,038 pCi/L). The proportion of MW-86 water was decreased using an exponential function, in steps. Figures 17A through 17F present the simulated breakthrough curves and the measured values for uranium, sulfate, chloride, pH, Ni, and Ra. Uranium is presented first, as it is the constituent of primary interest. The groundwater pore velocity determined through the model calibration was 130 feet per year.

Uranium – Uranium is retarded in its movement by sorption to ferrihydrite, and its transport is therefore affected by the amount of ferrihydrite present in the aquifer solids, as well as by the rate of water movement and by dispersion. The amount of ferrihydrite is primarily determined by the amount of dissolved iron in the low pH water at the upgradient end of the pathway, and by the change in pH downstream of the pH front, which causes the dissolved iron to precipitate as ferrihydrite. At MW-12, the most upgradient monitoring well, uranium concentrations peaked at 731 pCi/L in July 2003. At MW-9, which is the next monitoring well down the flow path, concentrations are lower and it is not clear at this time whether they have peaked. MW-9 is monitoring bedrock beneath the alluvial channel, and thus the uranium breakthrough is different in this well than in the more rapid alluvial channel part of the flow system. Uranium concentrations in MW-14 have also peaked (July 2008) and are declining. This well is completed in the alluvial materials, and the breakthrough is similar to that observed in MW-12, but delayed. At MW-108 and -109, it is not clear whether the peak has arrived yet.

The calibrated model matches the observed uranium concentrations in MW-12 and -14 reasonably well. At MW-12, the simulated breakthrough occurs earlier than observed, and the concentrations drop off more quickly than observed. The tailing (slower decline than rise) in the data is probably caused by the heterogeneity in the sediments. Concentrations in the future will probably decrease more slowly than the model will predict. The model predicts peak concentrations should have already reached MW-9, where the data indicate that transport is occurring much more slowly. Because the model is addressing transport in the more permeable alluvial sediments, it predicts more rapid transport to this location than was observed. Similarly, the model has predicted much more rapid transport to MW-108 and -109, than has been observed. These wells are also completed in the bedrock, and thus would be expected to peak more slowly than predicted.

Sulfate - The movement of sulfate is determined by the water velocity and whether gypsum will dissolve or precipitate. As gypsum is composed of calcium and sulfate, the concentration of sulfate is inversely proportional to the concentration of calcium if gypsum is present. The geochemical speciation modeling discussed above indicated that gypsum is present throughout the area. The model simulates a peak for sulfate at MW-12 approximately 8 years after the pumping stopped. There is a gap in the measurements at about that time, but concentrations measured later are higher than the simulated values, suggesting that either breakthrough occurred more slowly than simulated, or that heterogeneity is causing tailing. The timing of the simulated peaks are coincident with those of uranium. At MW-12, the model matches the sulfate concentrations reasonably well, but over predicts them at other locations. This may indicate that the concentrations of calcium used in the model are too low.

Chloride – Chloride behaves conservatively. In other words, it is not retarded by a chemical mechanism such as sorption or precipitation. The peaks of the simulated breakthrough occur earlier than the peaks for uranium and sulfate. Although the data are quite variable, the model matches the breakthrough of chloride reasonably well except at MW-109. The difference in the measured breakthrough curves for MW-108 and -109 is surprising. Breakthrough of uranium

and sulfate has not occurred at these two wells, so it is surprising that chloride did breakthrough as early as it did. Peak chloride concentrations are matched well.

pH – The pH values varied over the range of approximately 6.1 to 7.5 in the data. The data indicate that pH has decreased in MW-12, -9, -14, -108, and perhaps -109. The lowest measured pH during the post-recovery system period was 6.1. The model simulates the pH over the same approximate range as the measurements with an initial decline followed by rising pH in the three most upgradient wells.

Radium – Concentrations of radium have been variable over this time frame, and may have peaked in approximately 2003. In MW-14, concentrations have generally been declining since the beginning of the period. Concentrations in MW-14 and MW-12 appear to have been higher than in MW-9, -108, and -109. Because radium concentration is determined by counting, and because the concentrations are low, the observed variability is likely due in large part by random counting error. There did not appear to be a reliable signal against which to calibrate the model. As a result, the timing of the peaks is essentially unconstrained, and determined by the groundwater velocity. In the resulting predictions, the range of concentrations is believed to be representative, but the timing of the breakthrough is not.

Nickel – Nickel appears to be increasing in concentration in MW-12 and -14, but concentrations have typically been higher in MW-14, the downgradient well. Some of the results at MW-109 have been nearly as high as those in upgradient wells. Thus, the high variability in the data made it difficult to select calibration targets. Nickel concentrations are lower than prior to the recovery system pumping, but may be trending upward. In the simulation, nickel is retarded by sorption onto ferrihydrite.

Predictions: For the predictions, the Lang Draw model was run until concentrations stopped changing. At that time, the water chemistry was primarily determined by the upgradient water chemistry and the simulated precipitation/dissolution reactions (i.e., equilibrium with calcite and gypsum, slight under saturation with aluminum hydroxide and supersaturation with ferrihydrite). The results are shown in Figures 18A through 18F.

Uranium – The uranium results show a double peak. The second peak is approximately one-third to one-half of the height of the first peak. The second peak is caused by the movement of the pH front. Even though the reduction in pH is small, it causes dissolution of ferrihydrite and releases some of the sorbed uranium which migrates downgradient creating the second peak. Because the model assumes homogeneity within different parts of the model, whereas the natural system is heterogeneous, the natural system may not show a clearly discernable second peak. It may create a long tailing effect, similar to what is shown for the most downgradient well, MW-109. The model predicts that uranium concentrations will be approaching background concentrations in approximately 2050; there is uncertainty in this estimate primarily because of heterogeneity, but also because there are many parameters, such as groundwater velocity, dispersion, and thermodynamic data that are uncertain. The availability of the uranium concentration data through and past the time when the first peak occurred provides a constraint on the calibration of the model, especially with respect to the peak concentration. While the timing of the return to background concentrations is not well-defined because the peak has just passed MW-12 and -14, it is unlikely that uranium concentrations will exceed the peak concentrations previously observed.

Sulfate – sulfate concentrations are predicted to have a single peak, as sulfate does not sorb to ferrihydrite. The model simulates that the sulfate peak will pass through the wells, and the concentration in each will then decline to a value of approximately 1,600 mg/L. This concentration is determined by the solubility of the gypsum that was precipitated, and the concentration of the dissolved calcium in the water, which is based on a sample from MW-36. If the simulation had been longer, it should show sulfate concentrations beginning to decrease again as the gypsum is dissolved from the upstream end.

Chloride – The breakthrough of chloride is also single-peaked. Concentrations decrease downgradient because of dispersion processes. The model predicts that concentrations at the monitoring wells will decline to the upstream input concentration within about 25 to 40 years after the pumping stopped, or in about 2025 to 2040. However, heterogeneity causes slower recovery than predicted by homogeneous models, and recovery may take longer than predicted.

pH – The model showed the pH front (from higher to lower pH) during the calibration period, with MW-12 and MW-9 showing increasing pH toward the end of it. In the longer run of the model, the pH increases at all locations to a value of approximately 7. The model predicts that about 4 decades will be required for the pH to become stable, but the range in pH over this period is small.

Radium – As discussed above, radium was assumed not to sorb because of the difficulty in interpreting the measurements. As a result, it is predicted to peak relatively quickly, with maximum concentrations between 2.0 and 2.5 pCi/L. This concentration is based on the observed concentrations over the previous 15 years. Radium concentrations had been as high as 18 pCi/L in the early 1990s, but have not risen much since pumping stopped. The simulations predict that the peak has already passed for many of the monitoring wells, but retardation of radium was not simulated because it does not sorb appreciably to ferrihydrite.

Nickel – Retardation of nickel was simulated using sorption to ferrihydrite. The model predicts that the nickel peak will pass through a little slower than that of chloride, with the concentrations not increasing appreciably above those seen today.

In summary, the modeling predictions for uranium are believed to be representative of the future transport of uranium, because the observed passage of peaks at two of the monitoring wells constrains the transport process. The variability (heterogeneity) of the properties of the soils and rocks further downgradient will cause the observed results to differ from the predicted results. A second peak is predicted for uranium due to pH changes. As ferrihydrite dissolves, sorbed uranium will be released into the groundwater. The second peak will be smaller than the first peak. Longer term sulfate concentrations are predicted to be controlled by the solubility of gypsum and the concentrations of calcium. The pH is expected to decline slightly, then return to present-day or slightly higher values. Predictions of the transport of radium and nickel are less certain, because of the variability in the data and the lack of current-day information on radium and nickel concentrations upgradient of MW-12.

3.2.2 Northern Pathway

Calibration: Figures 19A through 19E show the initial concentrations used in the model. The upgradient water was as described under the Lang Draw discussion. Results are shown in Figures 20A through 20E.

Uranium – Data variability at MW-74 makes it difficult to determine whether the uranium peak has passed this well. Concentrations at MW-43 were declining through the calibration period. Both MW-110 and -111 have low concentrations. The model simulates a peak for MW-74 that falls within the range of the observed data. The simulated peak for MW-43 occurred later than the data would suggest. Actual concentrations at MW-43 were much higher before the recovery system was installed and during its early operation. At MW-110 and -111, the model indicates slow breakthrough was occurring during the calibration period.

Sulfate – The measurements of sulfate concentrations for MW-74, -43, and -110 do not show appreciable changes during the calibration period, while MW-111 shows a slow increasing trend. The model shows slow upward trends at each location. Thus, the model probably over predicts sulfate concentrations during the coming several years.

Chloride - During the calibration period, chloride has been relatively constant in MW-74, has been declining in MW-43, may have peaked in MW-110, and may be slowly increasing in MW-111. The model simulates each of these trends, but is predicting higher concentrations at MW-111 than have been occurring.

pH – The pH measurements suggest that a weak acid front moved through the locations of MW-74 and -110. The pH in the intervening well, MW-43, has remained reasonably constant. The current measurements in MW-74 and MW-110 are higher than the previous values, and measurements over the next several years should indicate whether these values are likely to be representative. The model simulations indicate that all values are tending toward a pH of 6.5; this value is probably determined in the model by the water chemistry and the specification that the water is to be in equilibrium with calcite and gypsum.

Radium – The data for the wells indicate stable or slowly declining values. The model, on the other hand, predicts increasing concentrations in MW-74 and MW-43. A value of 6.8 pCi/L was assumed for the area upgradient of MW-74 and MW-43. No data are available on concentrations of Ra today beneath the tailings impoundment near these wells. If a lower value had been used for this segment of the model, the fit may have improved.

Nickel – It is difficult to discern whether there are trends in the nickel concentration data. Concentrations in MW-74 may have been increasing since 2005, and perhaps in MW-43. The concentrations are low and there appear to be some elevated detection limits. In the late 1980s, concentrations were as high as 0.33 in MW-43, but have been low since the recovery system was terminated. The model showed slow rises during the calibration period.

Predictions: The predictions were made by extending the time of the simulation until concentrations stabilized. One thing to note is the much longer time frame for the Northern Pathway for concentrations to become stable. This is a consequence of the slower velocity (65 ft/year) and longer flow path than for Lang Draw.

Uranium – The transport of uranium along the Northern Flowpath is similar to that along Lang Draw, except that the concentrations are lower and the rate of movement is slower. The second peak is predicted to occur along both flow paths, as described previously.

Sulfate – The breakthrough curves for sulfate are remarkably similar to those for Lang Draw, reaching the same long-term equilibrium concentration of approximately 1,600 mg/L. The peak concentrations for the Northern Pathway are slightly lower than those for Lang Draw.

Chloride – Peak concentrations for chloride are higher than those for Lang Draw because of the higher initial condition used.

pH – Both the Northern Pathway and Lang Draw models predict that pH will decrease, and then rise to a constant value. For the Northern Pathway, the lowest pH is predicted to be about 6.5, and the final pH will be about 6.9. These values are slightly different from those along Lang Draw (low of 6.4, long-term value of approximately 7.0).

Radium – Radium concentrations are predicted to peak above 6 pCi/L. This value is the result of the assumed concentration (6.8 pCi/L) in the water beneath the tailings impoundment. The double-peak feature of some of the breakthrough curves (MW-111 is the best example) was caused by having two areas of higher concentration in the initial concentrations dataset, and is not associated with dissolution of ferrihydrite. The lower concentration area was further downgradient, causing the first peak to be smaller than the second peak.

Nickel – The peak nickel concentration is predicted to be about 0.04 mg/L. It is sorbed slightly by ferrihydrite, causing the slight decrease in concentration below 0.01 mg/L before rising to 0.01 mg/L, the upgradient concentration used in the model.

4.0 Conclusions

The re-evaluation of the geochemistry of the groundwater at the Bear Creek Disposal Facility was based on monitoring data collected from the period of operation of the facility to the present. The geochemistry had previously been evaluated in 1987 and 1995. The chemical mechanisms controlling the groundwater chemistry identified in those previous investigations (namely, attenuation of the acid front by dissolution of calcite, and subsequent precipitation of gypsum and ferrihydrite) were found to remain true, based on new samples and geochemical modeling.

Monitoring data collected after cessation of the groundwater recovery system provided information with which to calibrate reactive transport models for predicting future movement of uranium, radium, and nickel along the Lang Draw and Northern pathways. When modeling was done in 1995, data to constrain the calibration did not exist. Estimates of the retardation factors were based on geochemical speciation modeling and on Kds (distribution coefficients) developed for other locations. The monitoring data that have been collected since 1995 have provided site-specific information with which to determine the retardation. For Lang Draw, which is the more significant of the two pathways, uranium concentrations have now peaked in two wells, providing information on the highest concentrations that might be expected in the future. The peaks observed in the data set also provided information on the rate of movement of uranium. For the Northern Pathway, uranium appears to have peaked in one, and perhaps two, of the monitoring wells, providing the same types of information.

The models predict that there will be a second peak of uranium that occurs in the monitoring wells, caused by movement of lower pH water that can dissolve the ferrihydrite that has sorbed uranium. The second peak would be caused by the release of the uranium through this process. The magnitude of the second peak is predicted to be less than that of the first peak. However, geologic heterogeneity and resulting dispersion may make the peaks difficult to distinguish in actual sample data.

The radium data that have been collected since cessation of the recovery pumping did not provide a clear indication of radium transport behavior. Therefore, radium was modeled as

essentially being conservative. Its sorption to ferrihydrite was considered in the model, but the mass sorbed was inconsequential. Radium is likely to be attenuated by ion exchange.

Information on the transport of nickel was also hard to discern in the data because of the low concentrations and the variability. Nickel attenuation was simulated through sorption on ferrihydrite. Thus, the movement of the pH front affects nickel transport behavior.

5.0 References

Allison, J.D., D.S. Brown, and K.J. Novo-Gradac, 1991. MINTEQA2/PRODEFA2: A geochemical assessment model for environmental systems, version 3.0 user's manual: EPA/600/3-91/021, USEPA, Athens, Georgia.

GeoTrans, Inc. (1995). *Hydrogeologic and Geochemical Transport Analyses Converse County, Wyoming*.

Parkhurst, D.L. and C.A.J. Appelo, 1999. *User's guide to PHREEQC (version 2) – a computer program for speciation, batch-reaction, one-dimensional transport, and inverse geochemical calculations*. USGS, Denver, Colorado, Water-Resources Investigations Report 99-4259, 312 pages.

Poeter, E.P; M.C. Hill, E.R. Banta, S. Mehl, and S. Christensen, 2008 revision. *UCODE_2005 and six other codes for universal sensitivity analysis, calibration, and uncertainty evaluation*. USGS, Reston, Virginia, Techniques and Methods 6-A11, 283 pages.

FIGURES

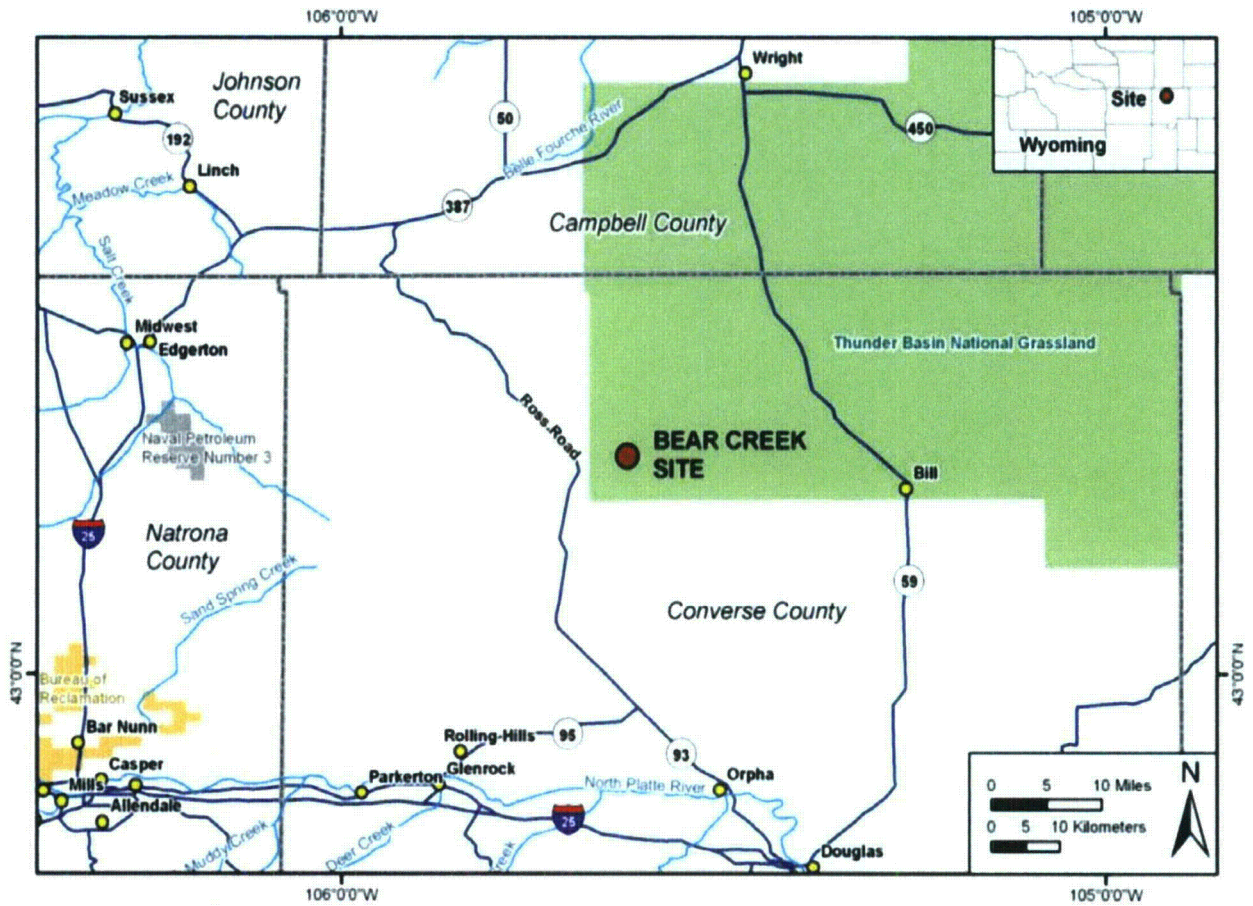
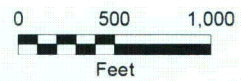


Figure 1. Bear Creek Uranium Mill Site Location

Source: 2009 NRC Information Sheet for Bear Creek Uranium Mill Site



Monitoring Wells, February 2011



ISSUED BY:



336 Centennial pkwy, Suite 210
Louisville, Colorado 80027

ISSUED FOR:

Bear Creek Disposal Site
Bear Creek, Wyoming

PROJECT NAME:

Bear Creek Uranium

DATE:

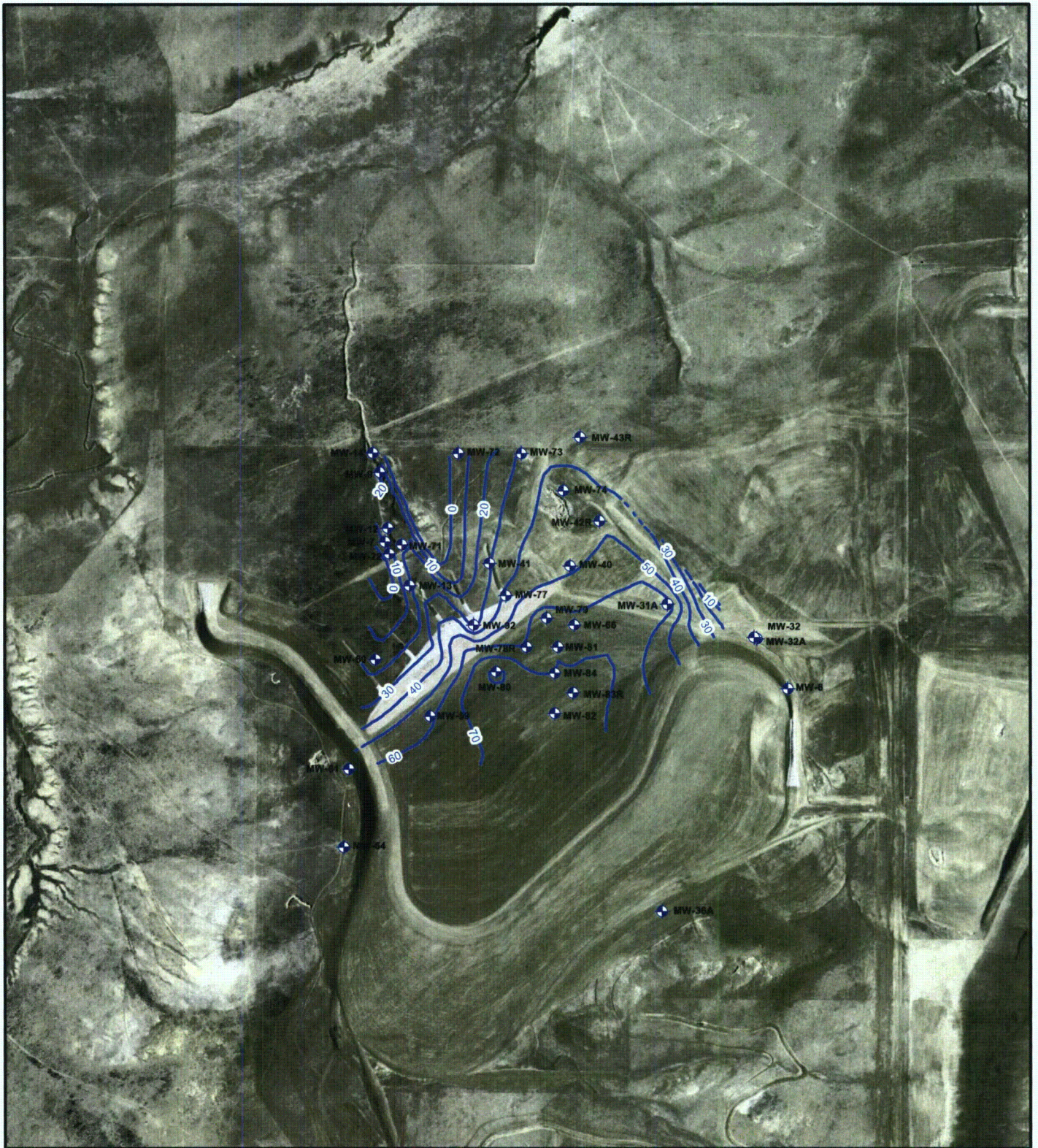
August 5, 2011

PROJECT NO.:

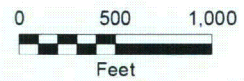
117-7252001

TITLE:

**Figure 2. Existing Site
Features**



 Monitoring Wells, June 1986
 Saturated Thickness, June 1986



ISSUED BY:



336 Centennial pkwy, Suite 210
Louisville, Colorado 80027

ISSUED FOR:

Bear Creek Disposal Site
Bear Creek, Wyoming

PROJECT NAME:

Bear Creek Uranium

DATE:

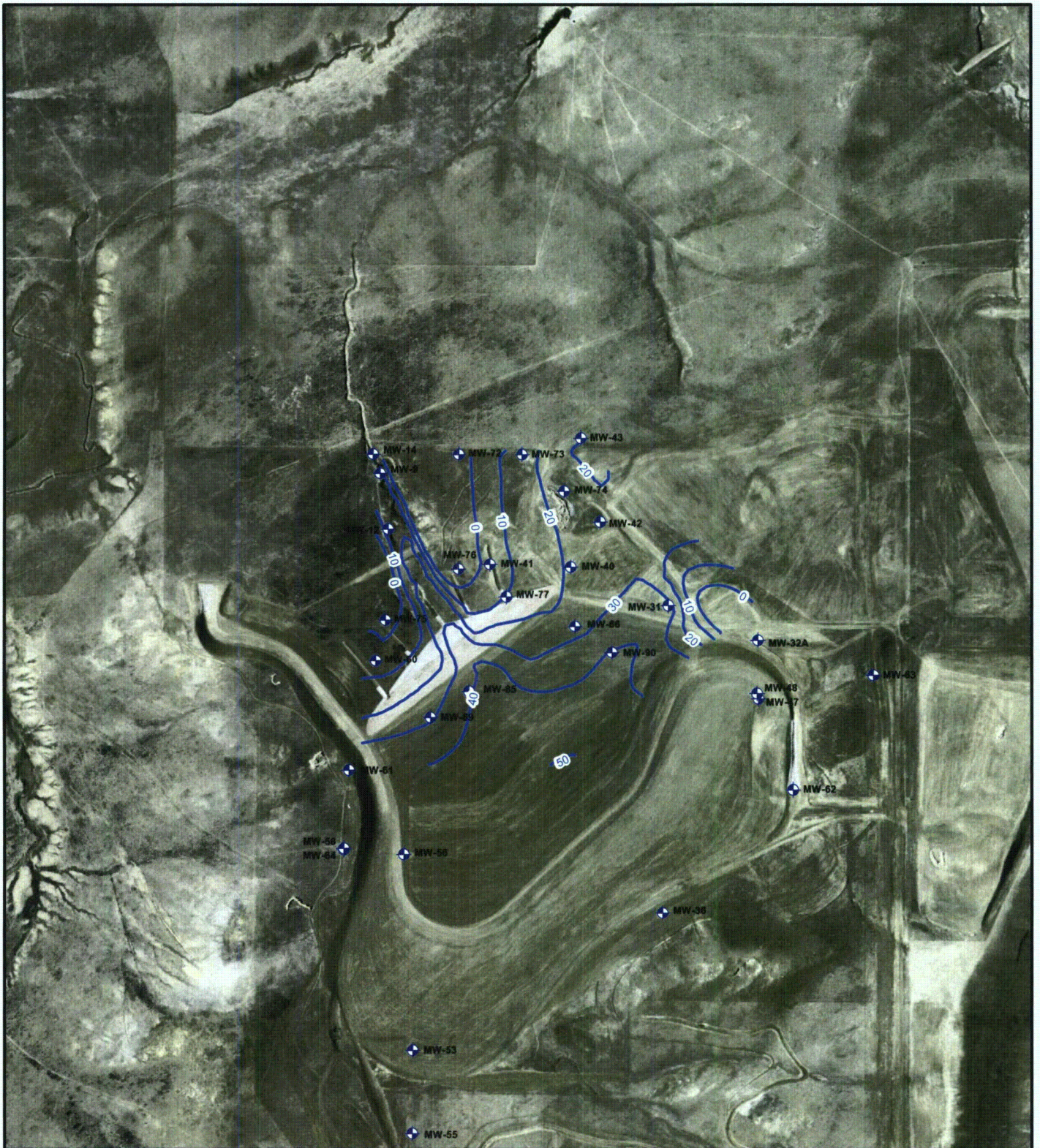
August 5, 2011

PROJECT NO.:

117-7252001

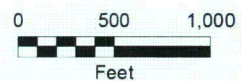
TITLE:

**Figure 3. Saturated
Thickness of N Sand,
June 1986**



 Monitoring Wells, March 1996

 Saturated Thickness, March 1996



ISSUED BY:



336 Centennial pkwy, Suite 210
Louisville, Colorado 80027

ISSUED FOR:

Bear Creek Disposal Site
Bear Creek, Wyoming

PROJECT NAME:

Bear Creek Uranium

DATE:

August 5, 2011

PROJECT NO.:

117-7252001

TITLE:

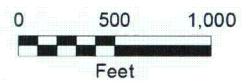
**Figure 4. Saturated
Thickness of N Sand,
March 1996**



Monitoring Wells, February 2011



Saturated Thickness, February 2011



ISSUED BY:



336 Centennial pkwy, Suite 210
Louisville, Colorado 80027

ISSUED FOR:

Bear Creek Disposal Site
Bear Creek, Wyoming

PROJECT NAME:

Bear Creek Uranium

DATE:

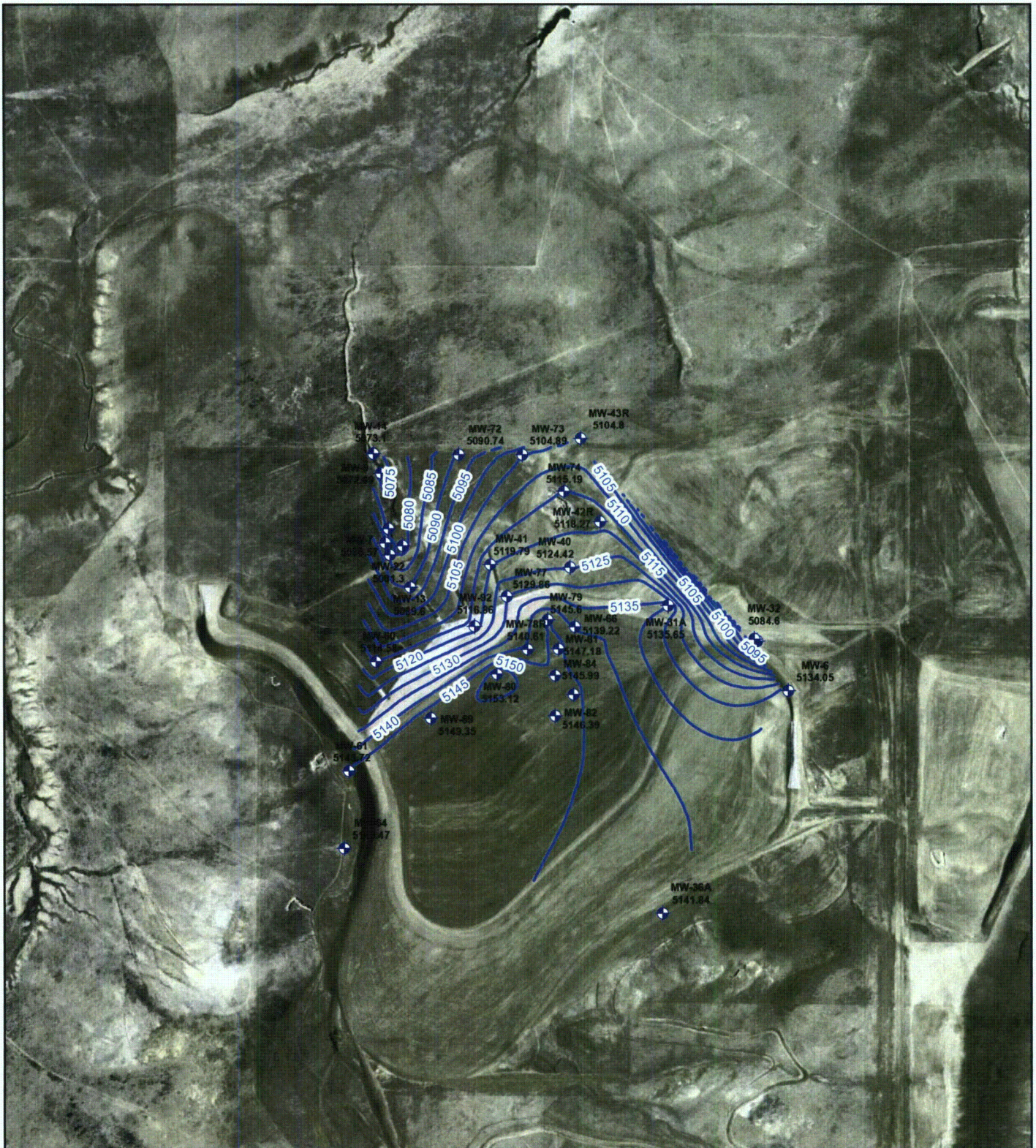
August 5, 2011

PROJECT NO.:

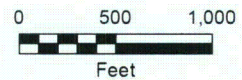
117-7252001

TITLE:

**Figure 5. Saturated
Thickness of N Sand,
February 2011**



Monitoring Wells, June 1986
Groundwater Elevation, June 1986



ISSUED BY:



336 Centennial pkwy, Suite 210
Louisville, Colorado 80027

ISSUED FOR:

Bear Creek Disposal Site
Bear Creek, Wyoming

PROJECT NAME:

Bear Creek Uranium

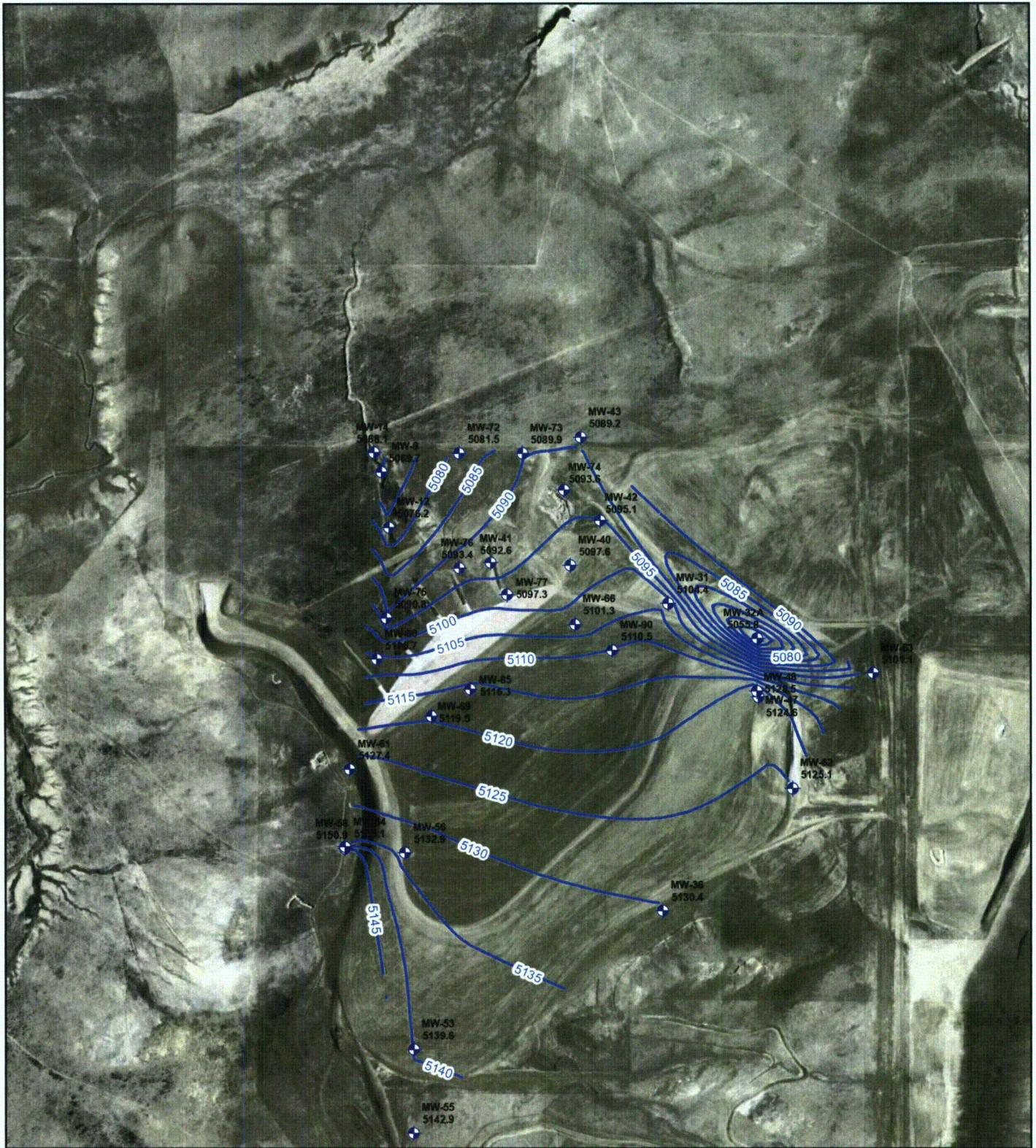
DATE:

August 5, 2011

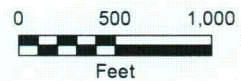
PROJECT NO.: 117-7252001

TITLE:

Figure 6. Water-Level Elevations, June 1986



Monitoring Wells, March 1996
Groundwater Elevation, March 1996



ISSUED BY:



336 Centennial pkwy, Suite 210
Louisville, Colorado 80027

ISSUED FOR:

Bear Creek Disposal Site
Bear Creek, Wyoming

PROJECT NAME:

Bear Creek Uranium

DATE:

August 5, 2011

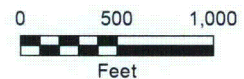
PROJECT NO.: 117-7252001

TITLE:

Figure 7. Water-Level Elevations, March 1996



Monitoring Wells, February 2011
Groundwater Elevation, February 2011



ISSUED BY:



336 Centennial pkwy, Suite 210
Louisville, Colorado 80027

ISSUED FOR:

Bear Creek Disposal Site
Bear Creek, Wyoming

PROJECT NAME:

Bear Creek Uranium

DATE:

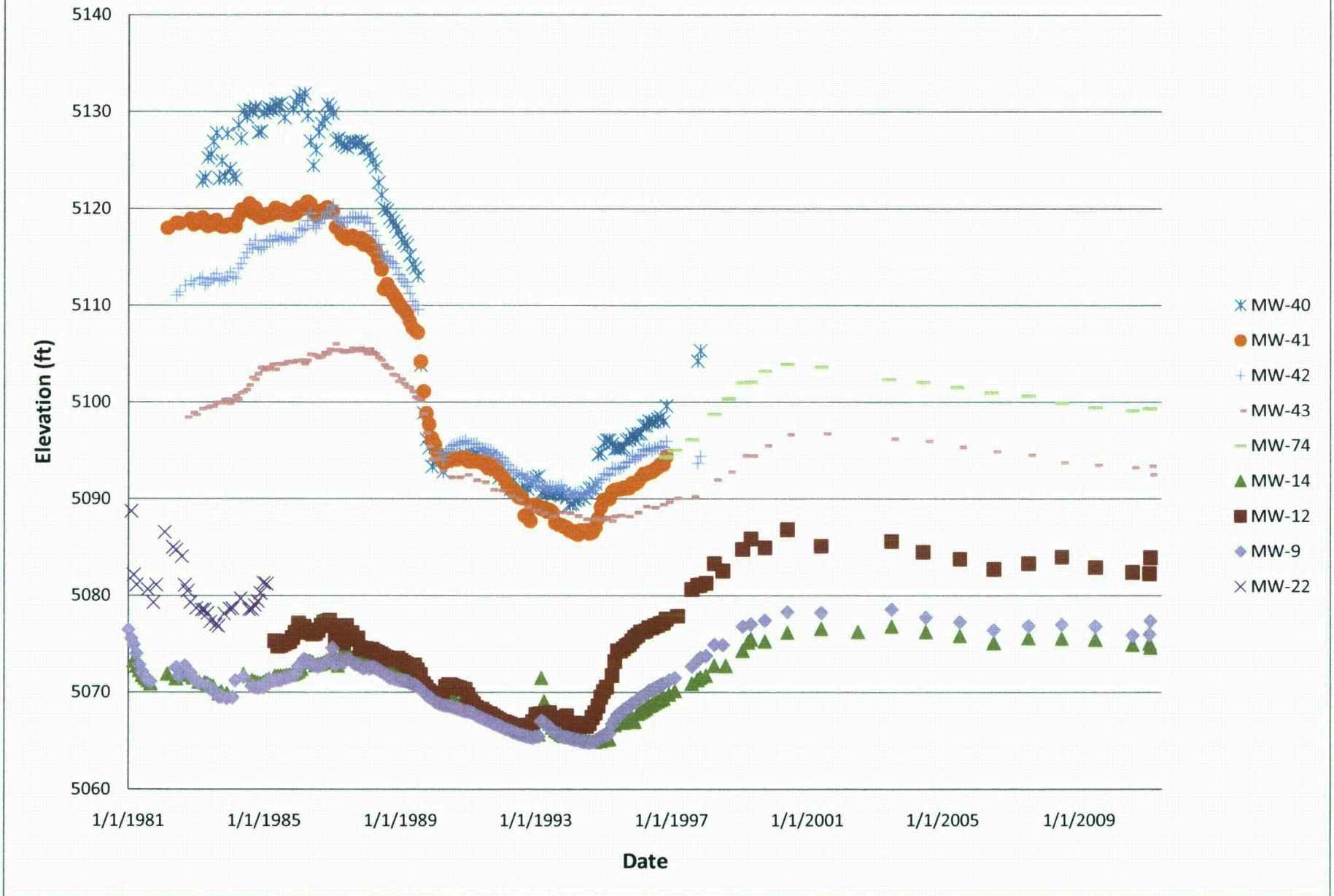
August 5, 2011

PROJECT NO.: 117-7252001

TITLE:

Figure 8. Water-Level Elevations, February 2011

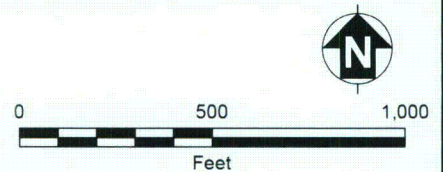
Figure 9. Measured Water-Level Elevations, 1981-2011





 Monitoring Well
 (17.6)

Concentrations are in pCi/L (picocuries per liter)
 ACL (alternate concentration limit) = 2,038 pCi/L



ISSUED BY:



336 Centennial pkwy, Suite 210
 Louisville, Colorado 80027

ISSUED FOR:

Bear Creek Disposal Site
 Bear Creek, Wyoming

PROJECT NAME:

Bear Creek Uranium

DATE:

August 5, 2011

PROJECT NO.: 117-7252001

TITLE:

**Figure 10A. Distribution
 of Uranium
 Concentrations,
 February 2011**

Figure 10B. Temporal Changes in Uranium Concentrations,
Lang Draw

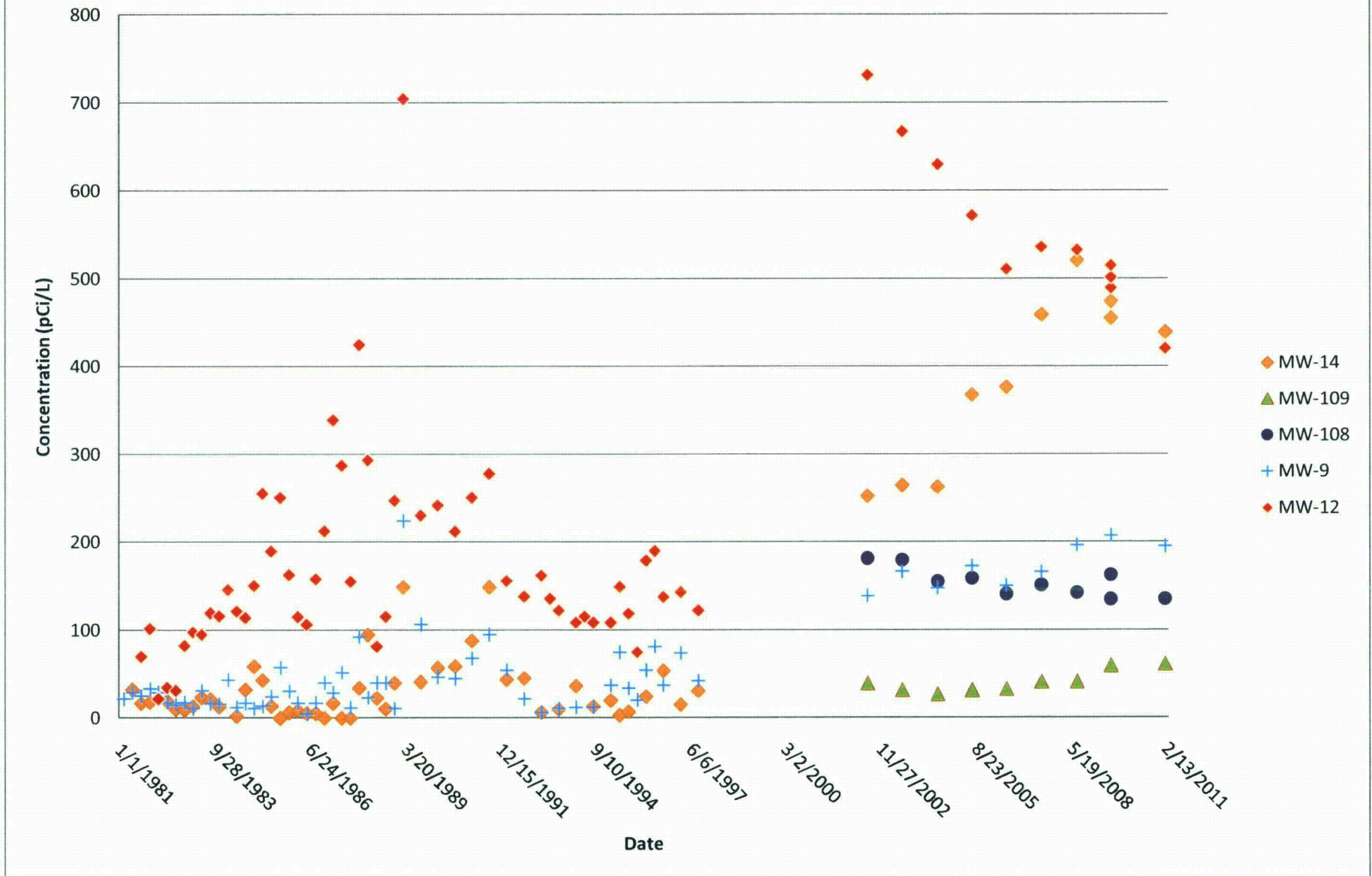
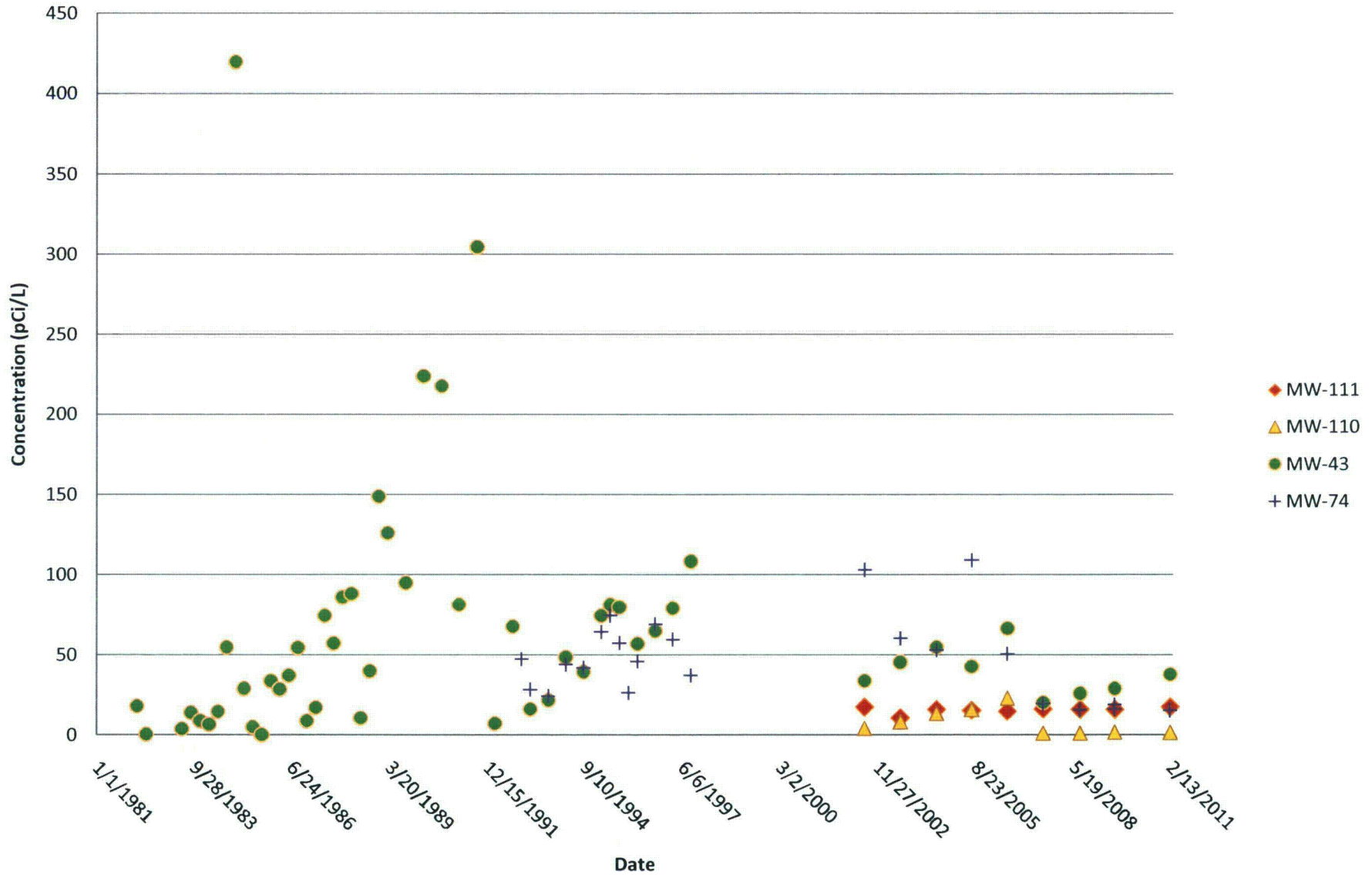


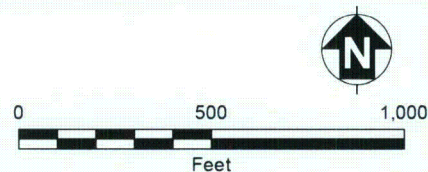
Figure 10C. Temporal Changes in Uranium Concentrations,
Northern Pathway





Monitoring Well
(1190)

Concentrations are in mg/L (milligrams per liter)
Groundwater Protection Standard = 3,000 mg/L



ISSUED BY:



336 Centennial pkwy, Suite 210
Louisville, Colorado 80027

ISSUED FOR:

Bear Creek Disposal Site
Bear Creek, Wyoming

PROJECT NAME:

Bear Creek Uranium

DATE:

August 5, 2011

PROJECT NO.: 117-7252001

TITLE:

**Figure 11A. Distribution
of Sulfate
Concentrations,
February 2011**

Figure 11B. Temporal Changes in Sulfate Concentrations,
Lang Draw

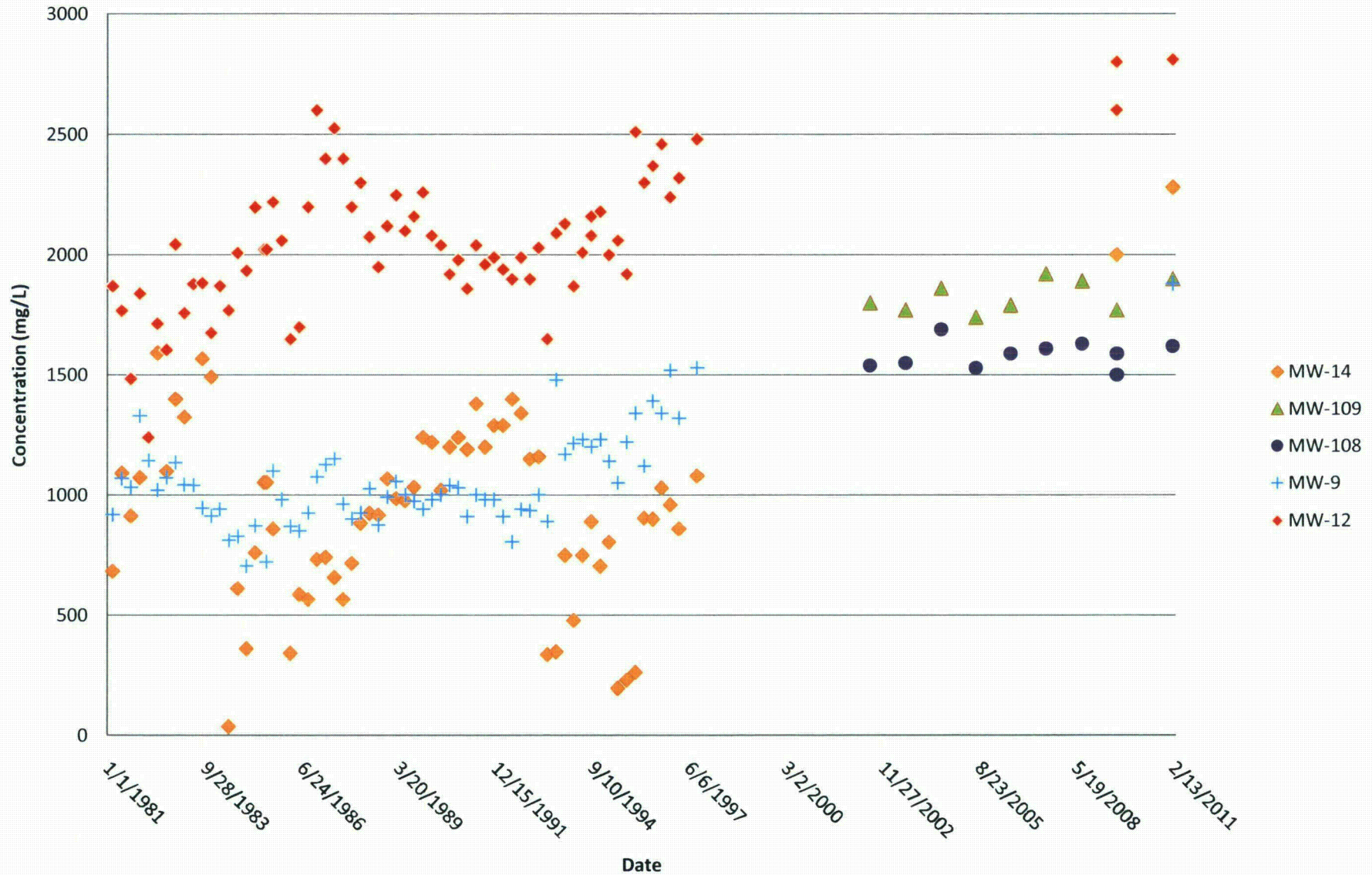
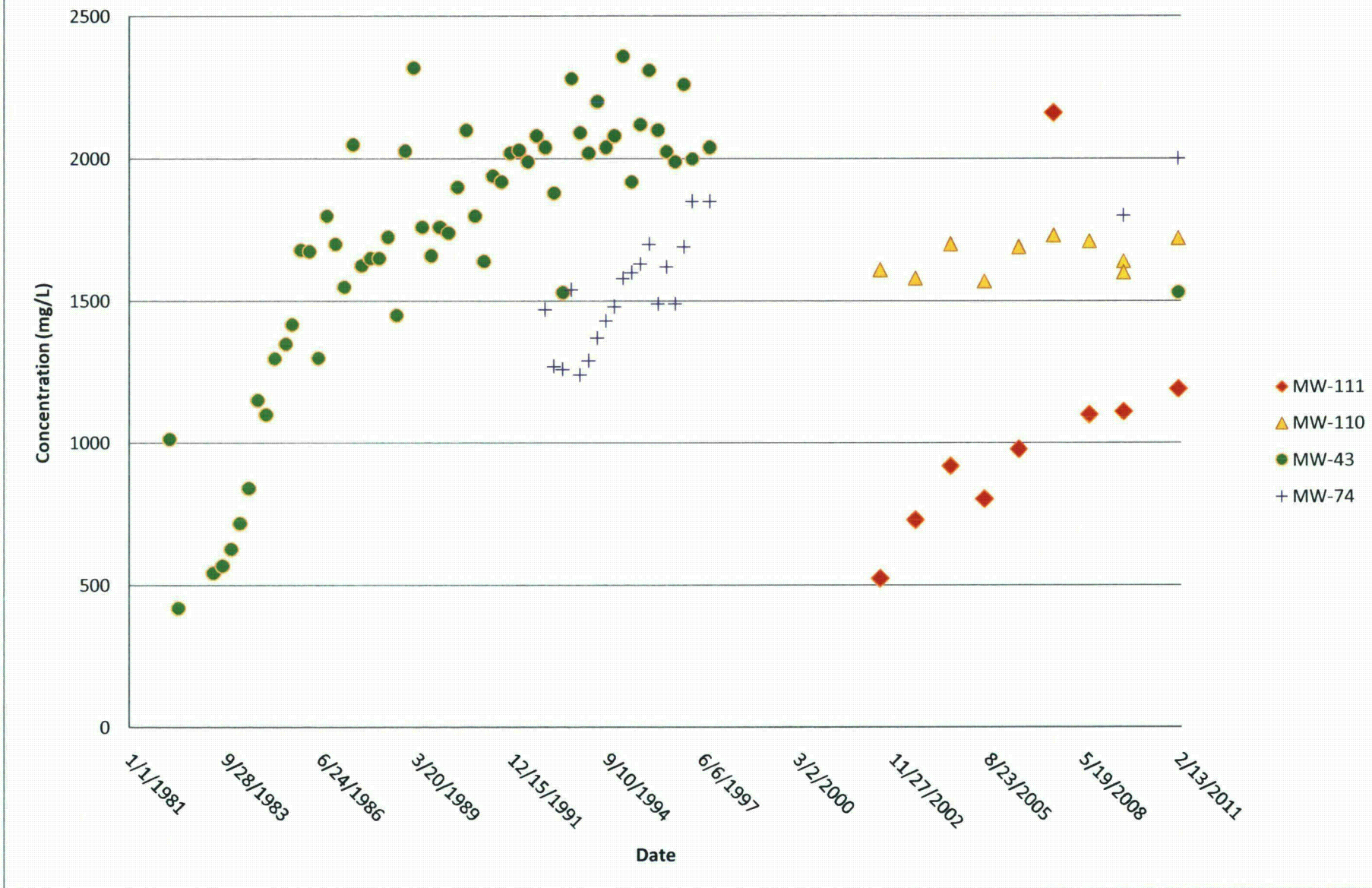
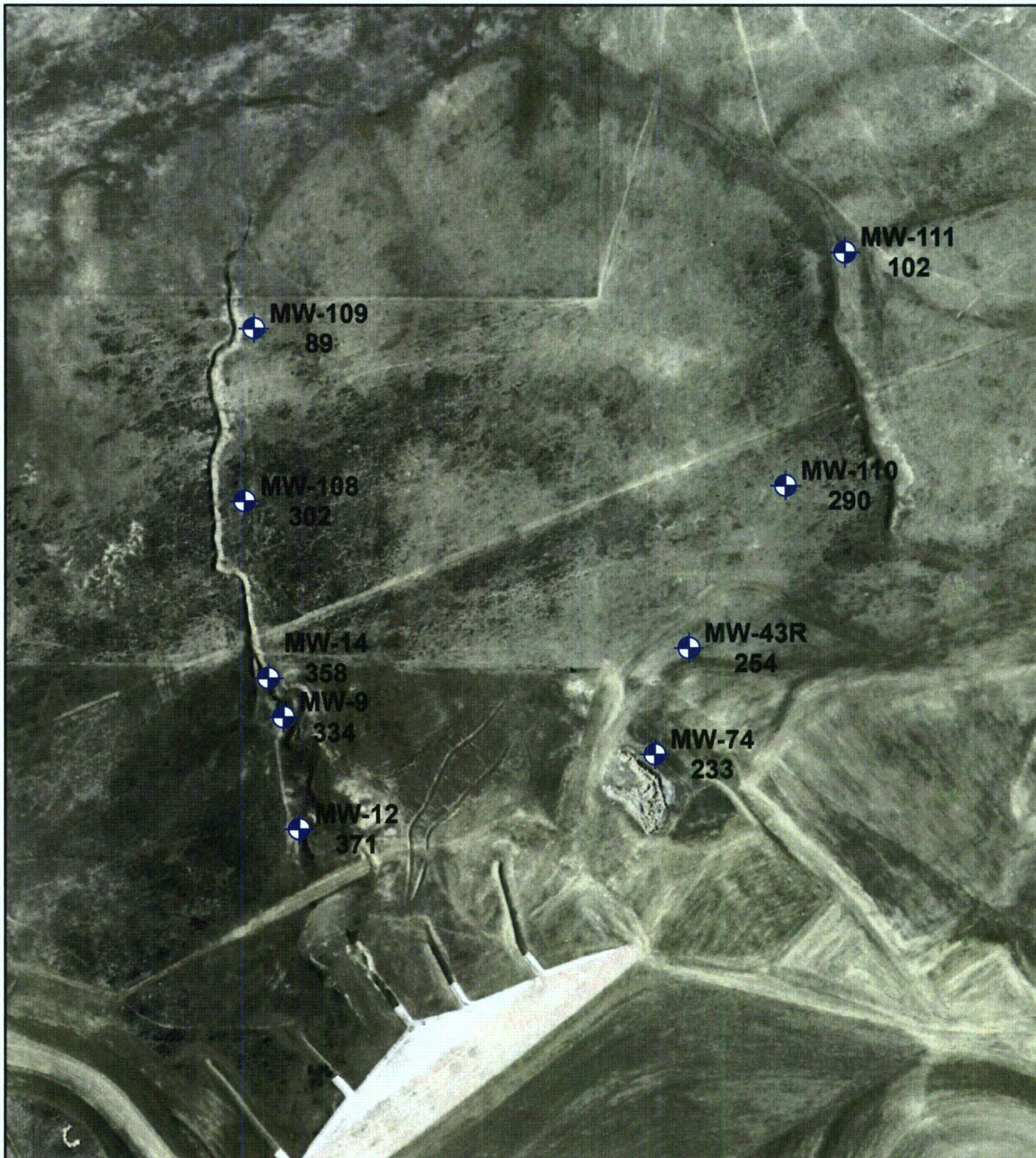


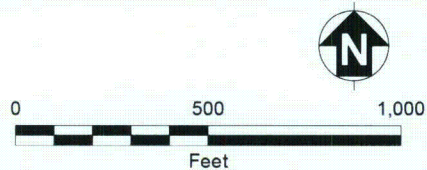
Figure 11C. Temporal Changes in Sulfate Concentrations,
Northern Pathway





 Monitoring Well
 (102)

Concentrations are in mg/L (milligrams per liter)
 Groundwater Protection Standard = 2,000 mg/L



ISSUED BY:



336 Centennial pkwy, Suite 210
 Louisville, Colorado 80027

ISSUED FOR:

Bear Creek Disposal Site
 Bear Creek, Wyoming

PROJECT NAME:

Bear Creek Uranium

DATE:

August 5, 2011

PROJECT NO.: 117-7252001

TITLE:

**Figure 12A. Distribution
 of Chloride
 Concentrations,
 February 2011**

Figure 12B. Temporal Changes in Chloride Concentrations,
Lang Draw

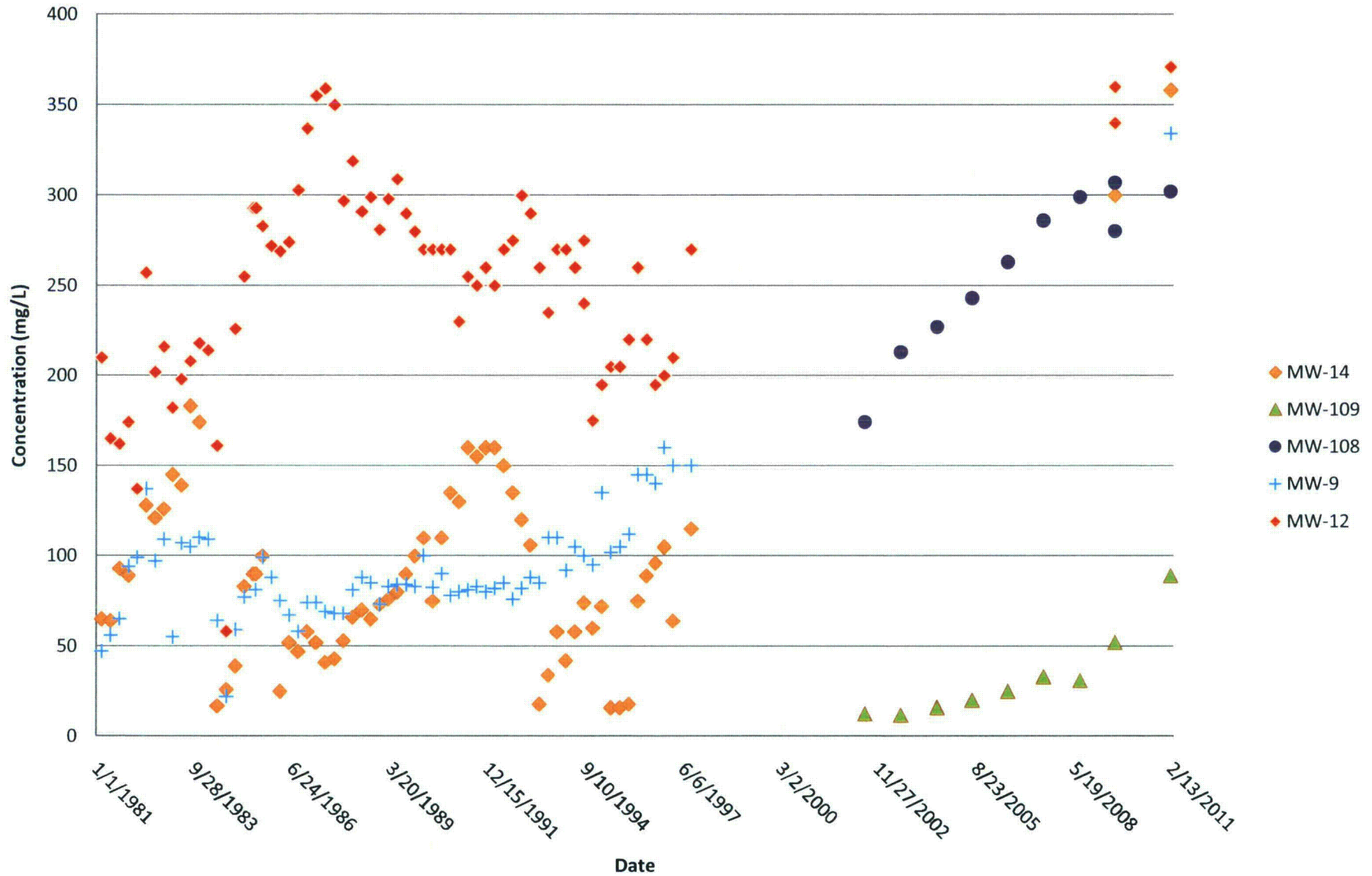
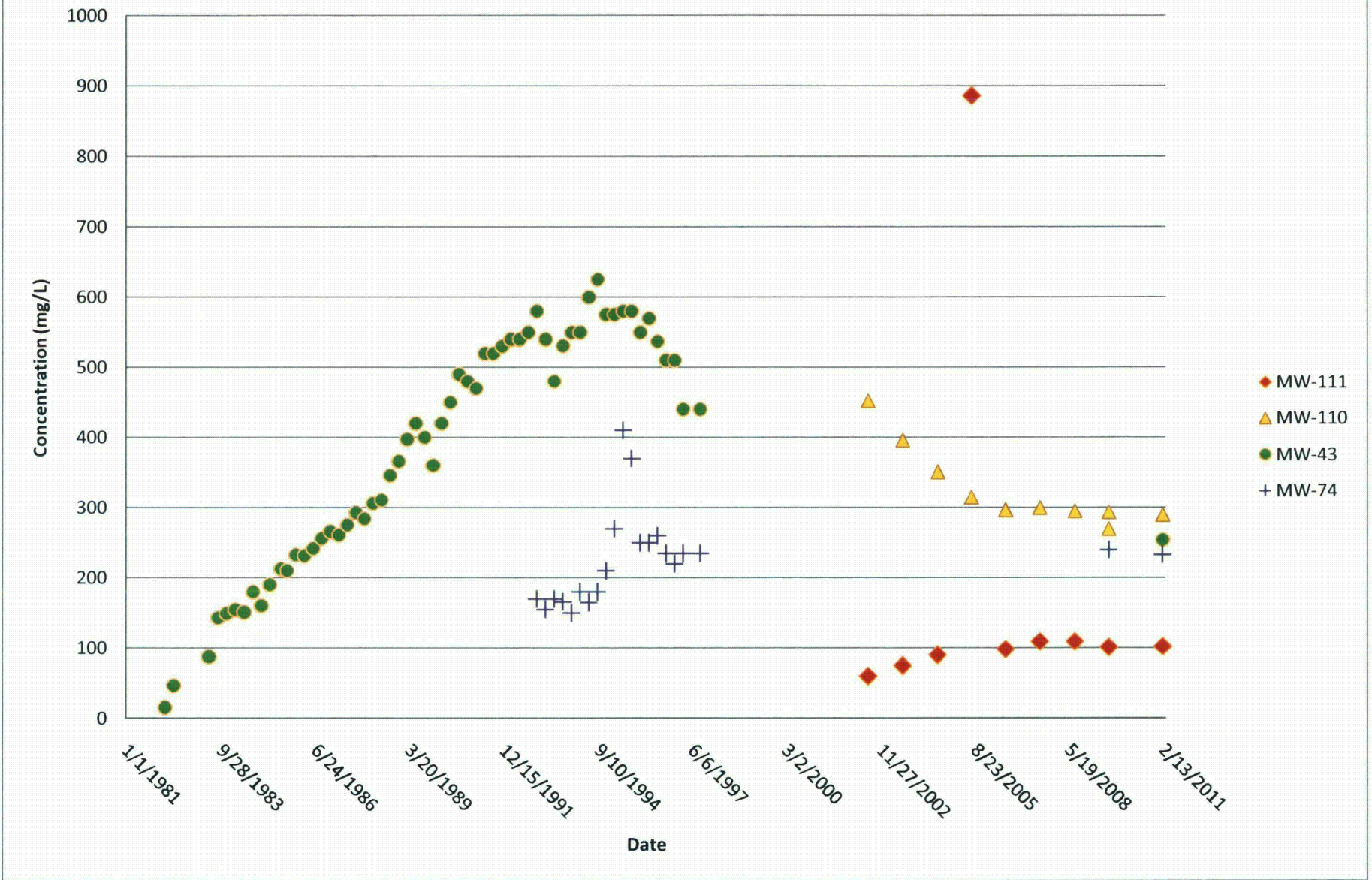


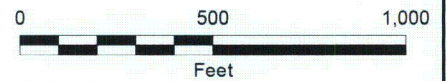
Figure 12C. Temporal Changes in Chloride Concentration,
Northern Pathway





 Monitoring Well
 (7.6)

Values are in pH units (s.u.)



ISSUED BY:



336 Centennial pkwy, Suite 210
Louisville, Colorado 80027

ISSUED FOR:

Bear Creek Disposal Site
Bear Creek, Wyoming

PROJECT NAME:

Bear Creek Uranium

DATE:

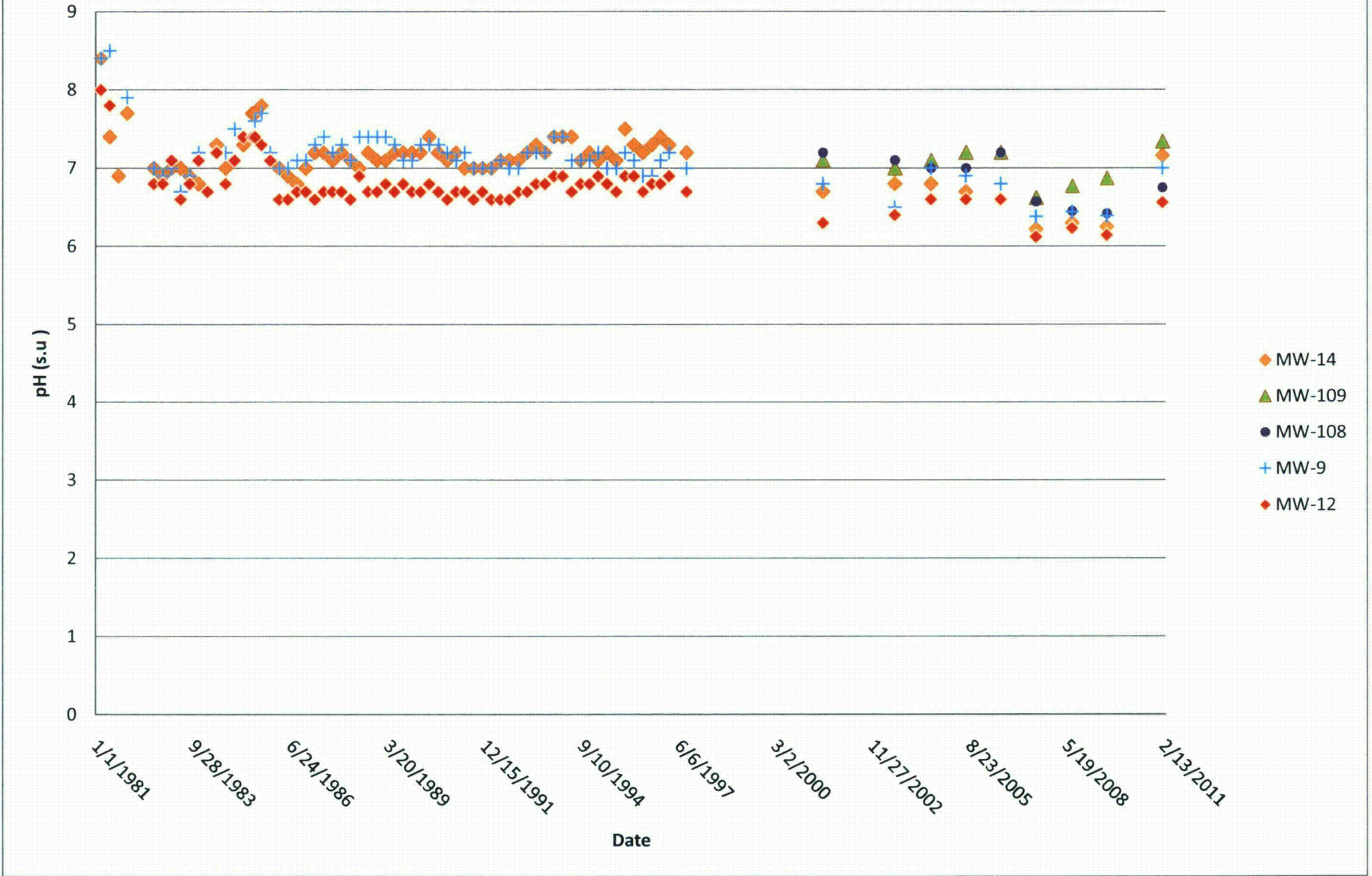
August 5, 2011

PROJECT NO.: 117-7252001

TITLE:

**Figure 13A. Distribution
of pH, February 2011**

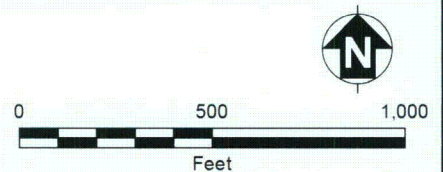
Figure 13B. Temporal Changes in pH,
Lang Draw





 Monitoring Well
 (1.8)

Concentrations are in pCi/L (picocuries per liter)
 ACL (alternate concentration limit) = 46 pCi/L



ISSUED BY:



336 Centennial pkwy, Suite 210
 Louisville, Colorado 80027

ISSUED FOR:

Bear Creek Disposal Site
 Bear Creek, Wyoming

PROJECT NAME:

Bear Creek Uranium

DATE:

August 5, 2011

PROJECT NO.: 117-7252001

TITLE:

**Figure 14A. Distribution
 of Radium
 Concentrations,
 February 2011**

Figure 14B. Temporal Changes in Radium Concentrations,
Lang Draw

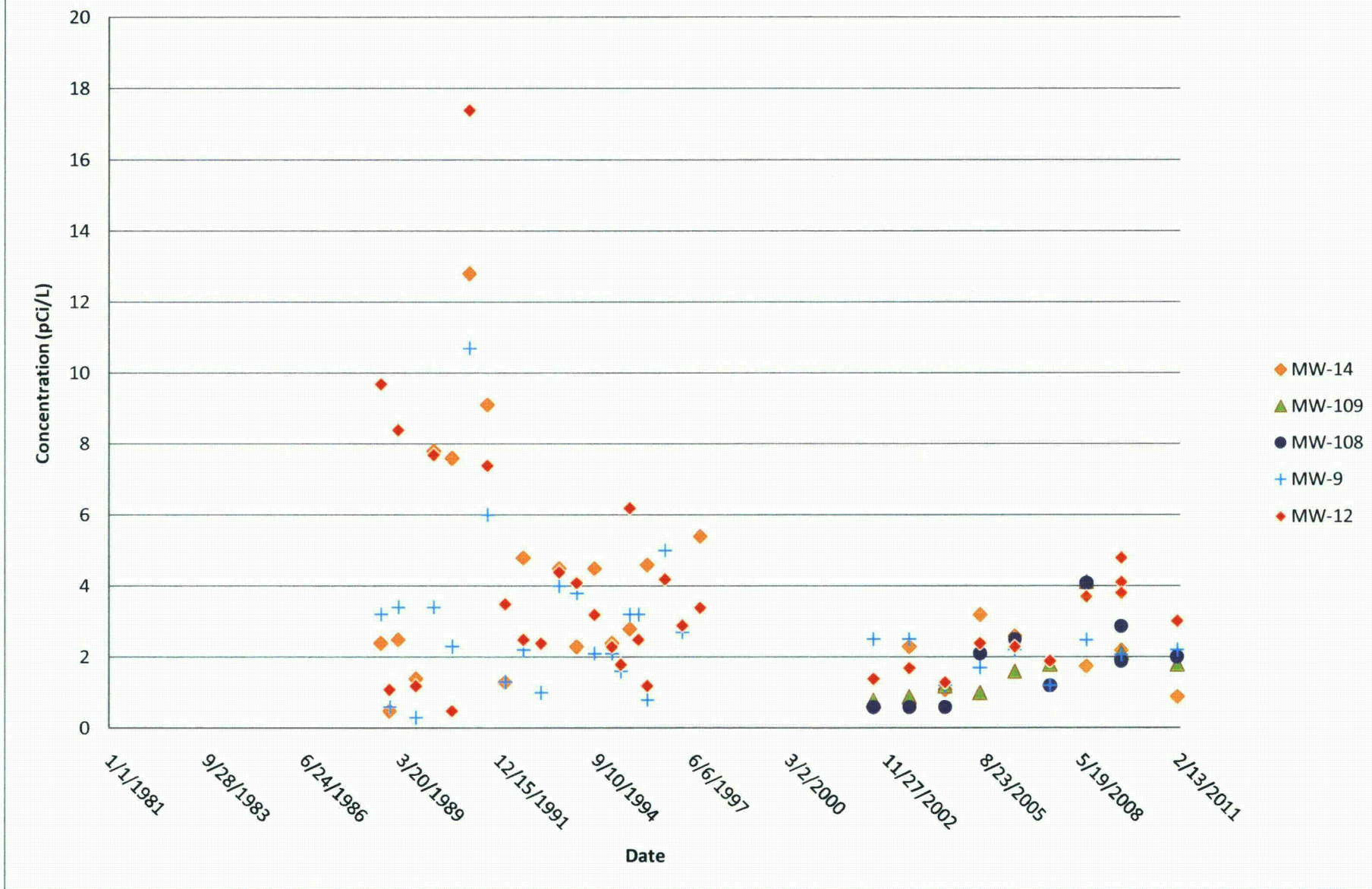
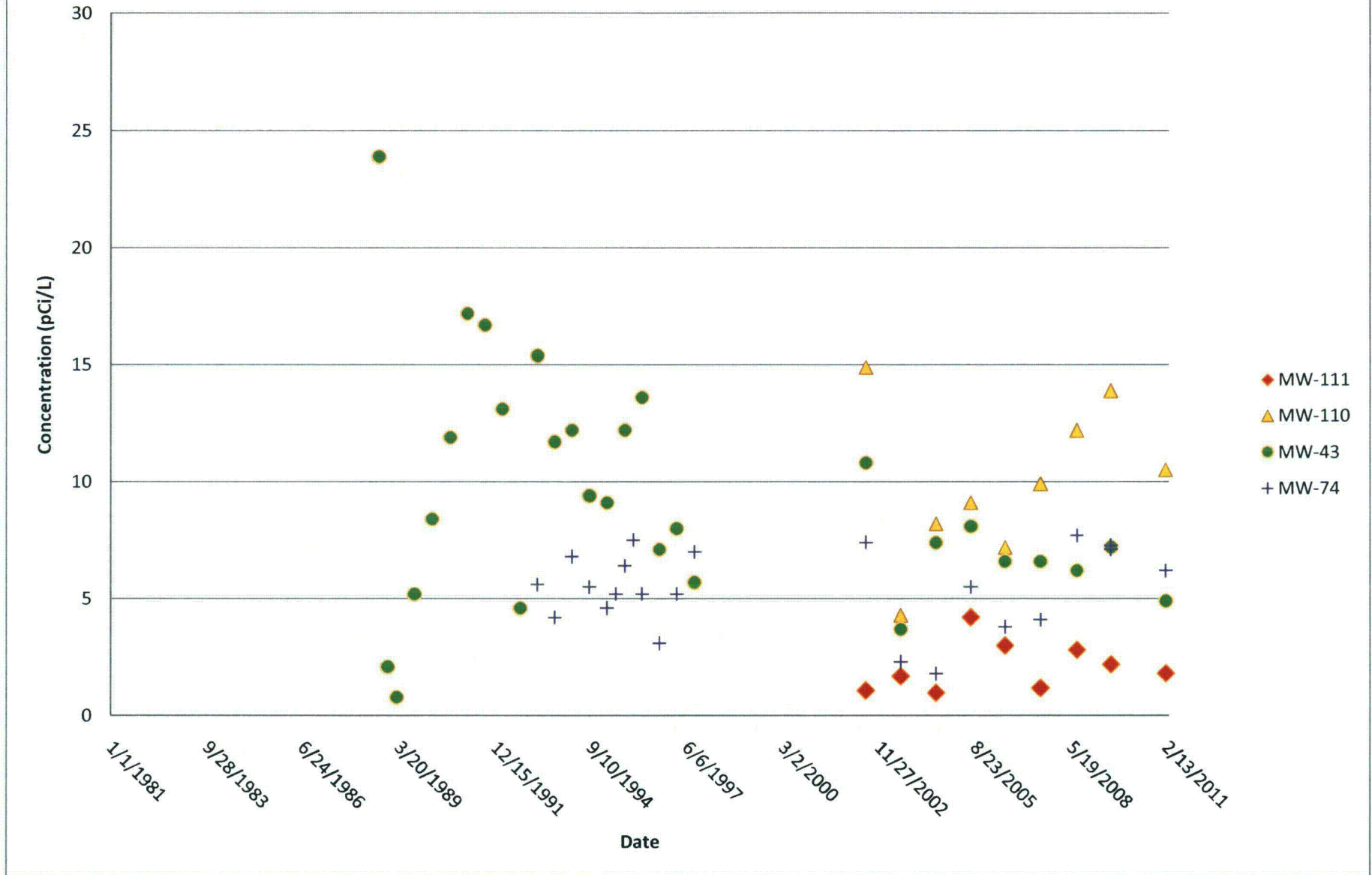


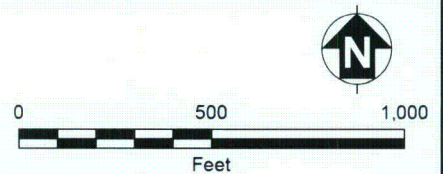
Figure 14C. Temporal Changes in Radium Concentrations,
Northern Pathway





 Monitoring Well
 (0.017)

Concentrations are in mg/L (milligrams per liter)
 ACL (alternate concentration limit) = 3.8 mg/L



ISSUED BY:



336 Centennial pkwy, Suite 210
 Louisville, Colorado 80027

ISSUED FOR:

Bear Creek Disposal Site
 Bear Creek, Wyoming

PROJECT NAME:

Bear Creek Uranium

DATE:

August 5, 2011

PROJECT NO.: 117-7252001

TITLE:

**Figure 15A. Distribution
 of Nickel
 Concentrations,
 February 2011**

Figure 15B. Temporal Changes in Nickel Concentrations,
Lang Draw

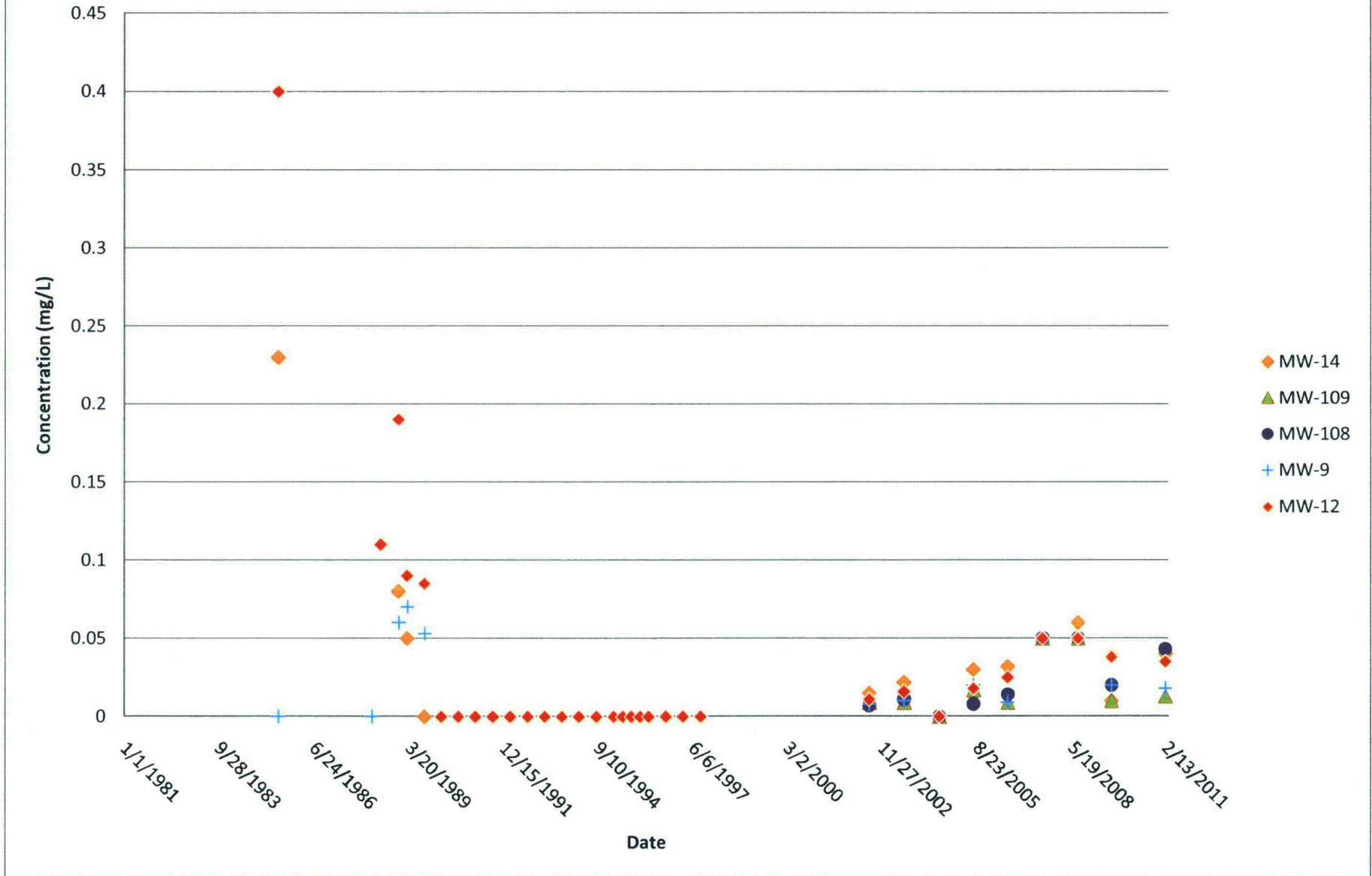
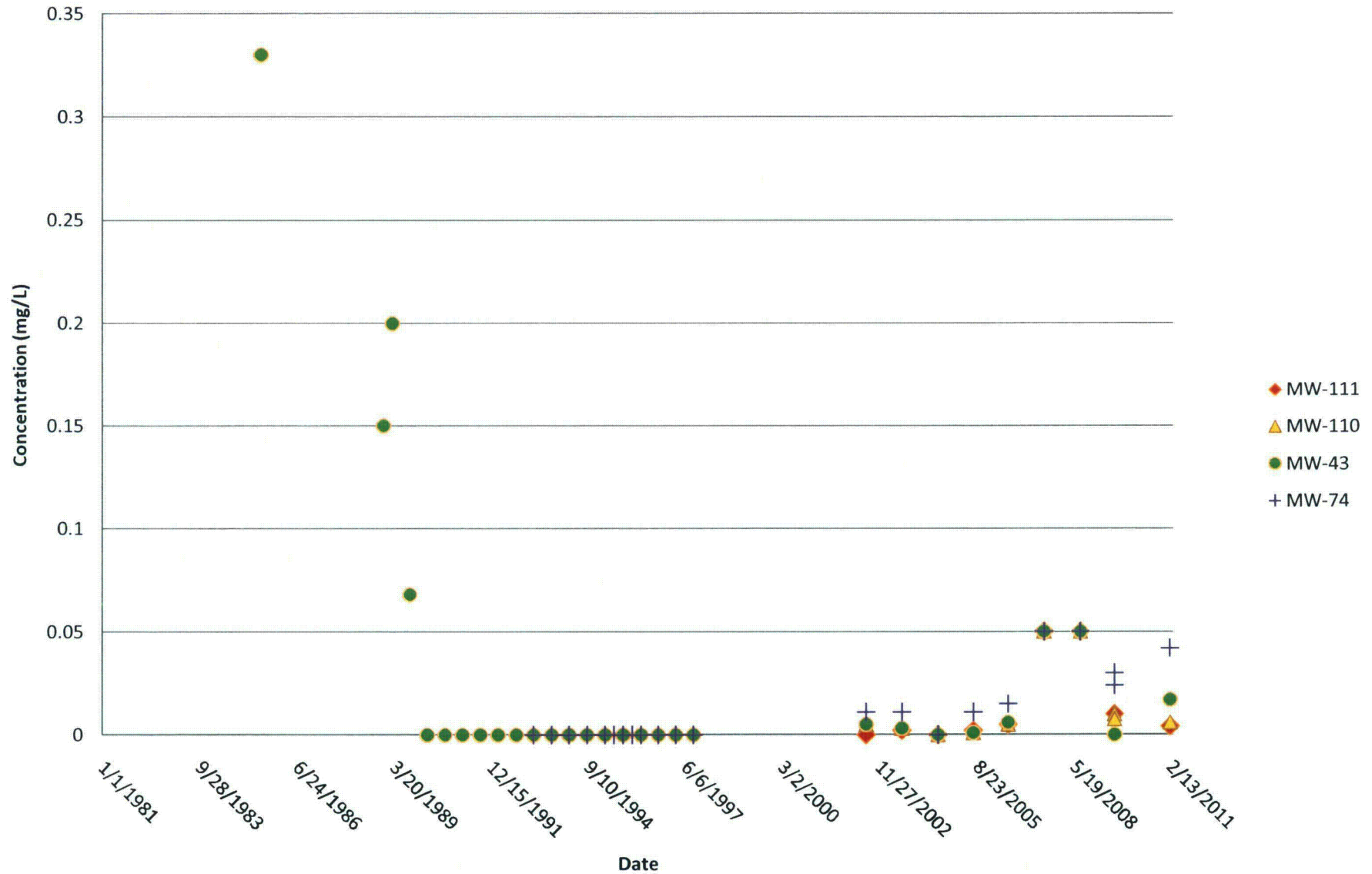
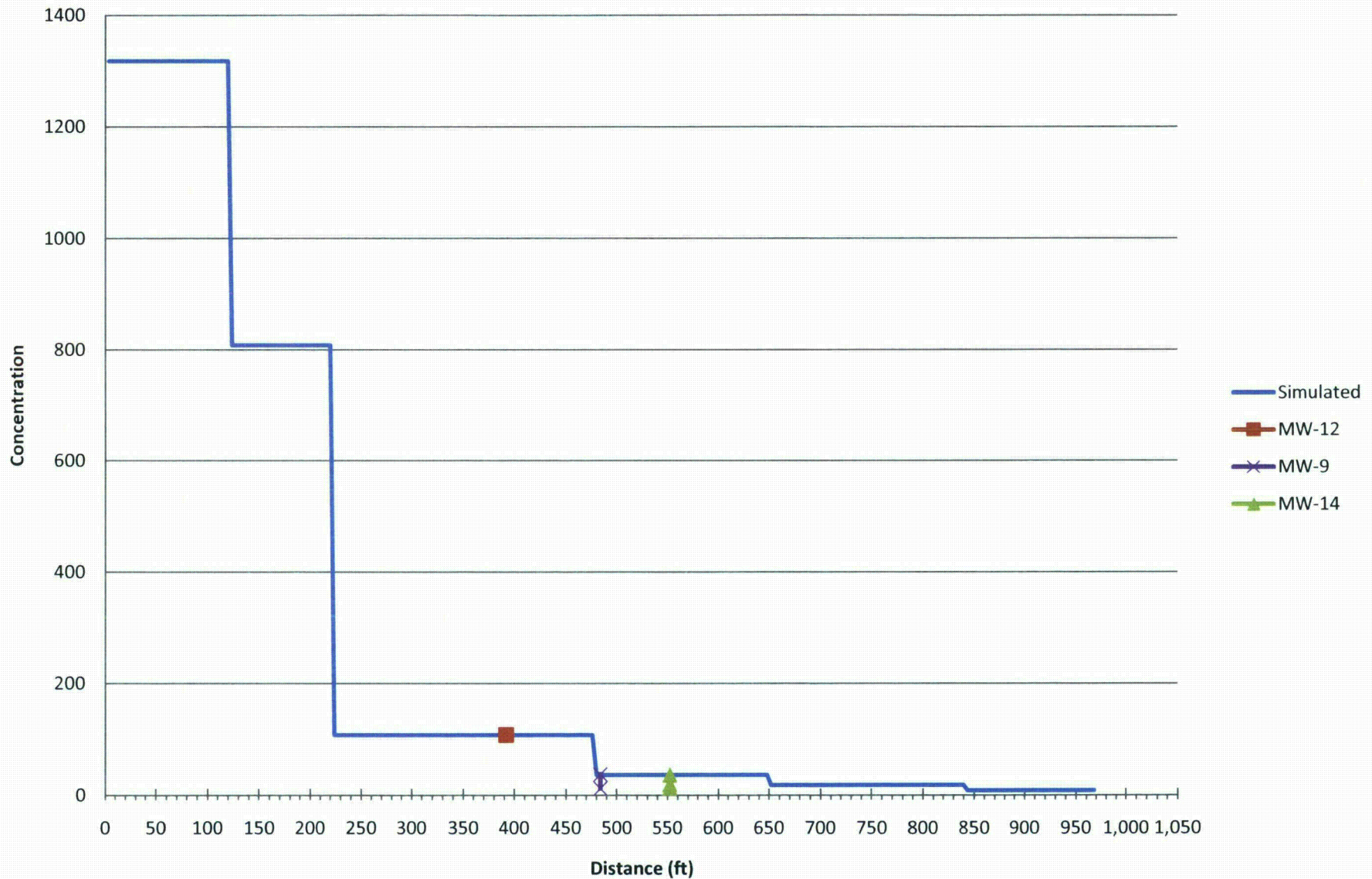


Figure 15C. Temporal Changes in Nickel Concentration,
Northern Pathway



**Figure 16A. Simulated Initial Values of Uranium
Lang Draw**



**Figure 16B. Simulated Initial Values of Sulfate
Lang Draw**

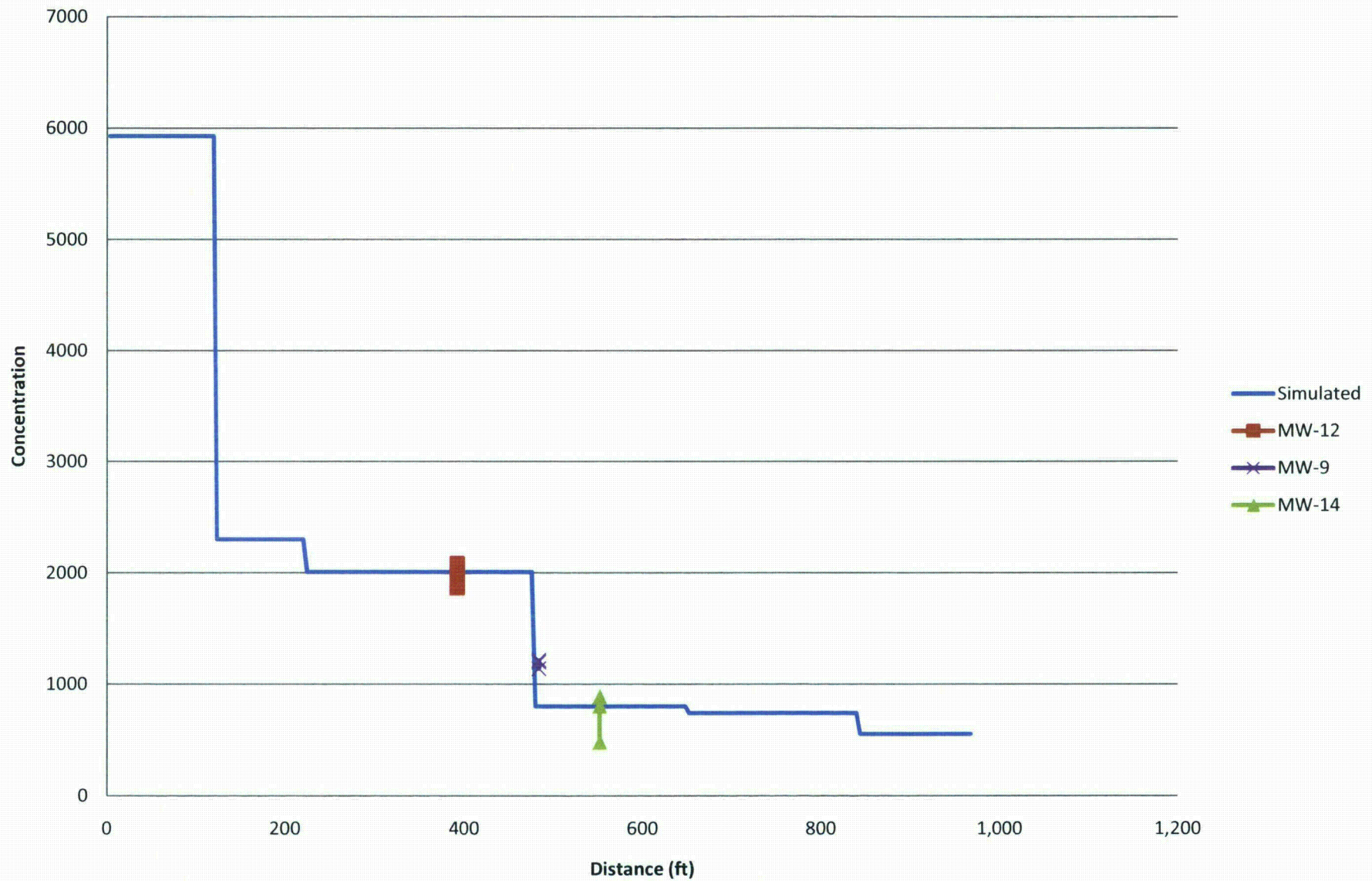


**Figure 16C. Simulated Initial Values of Chloride
Lang Draw**

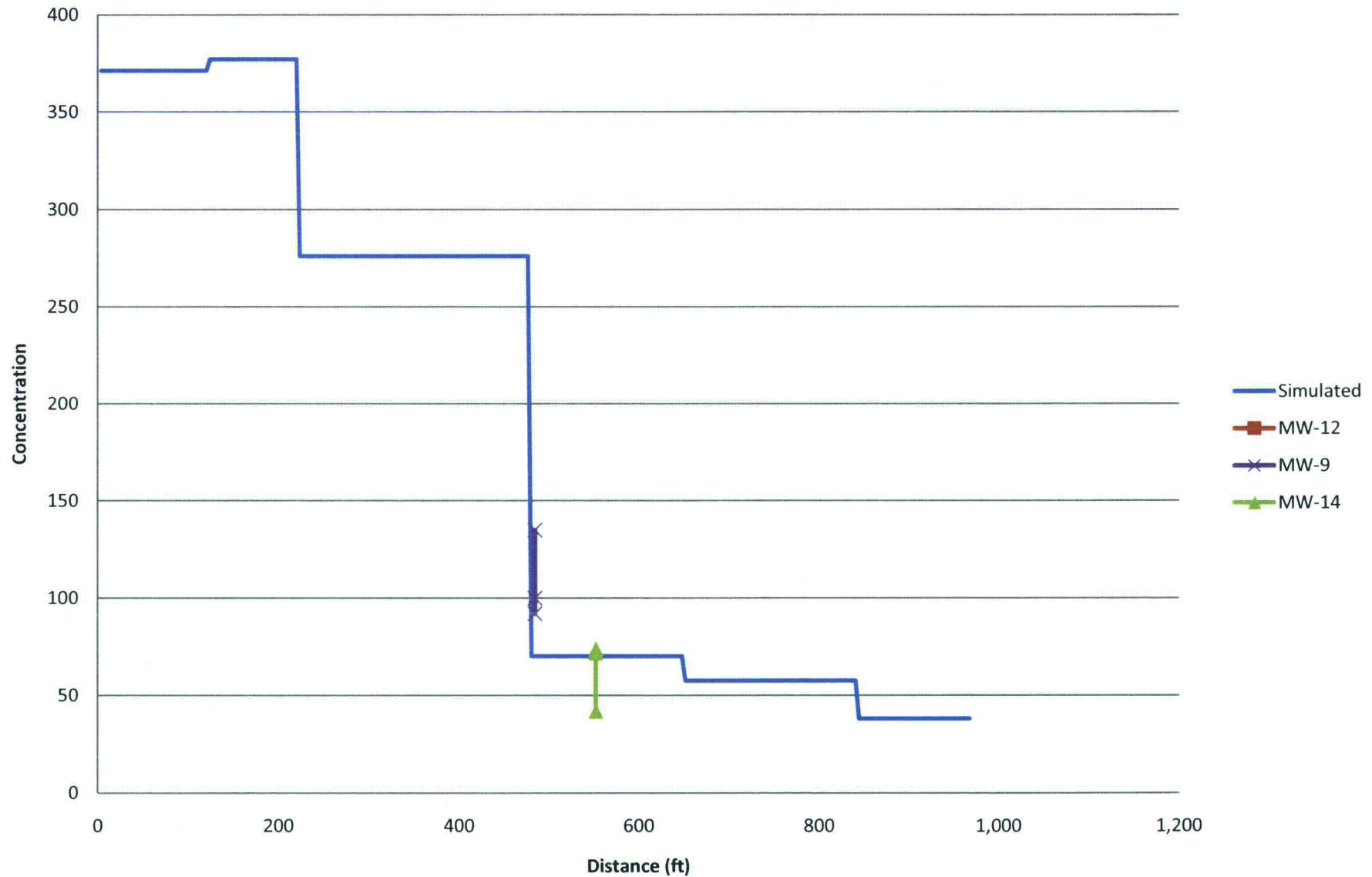


Figure 16D. Simulated Initial Values of pH
Lang Draw

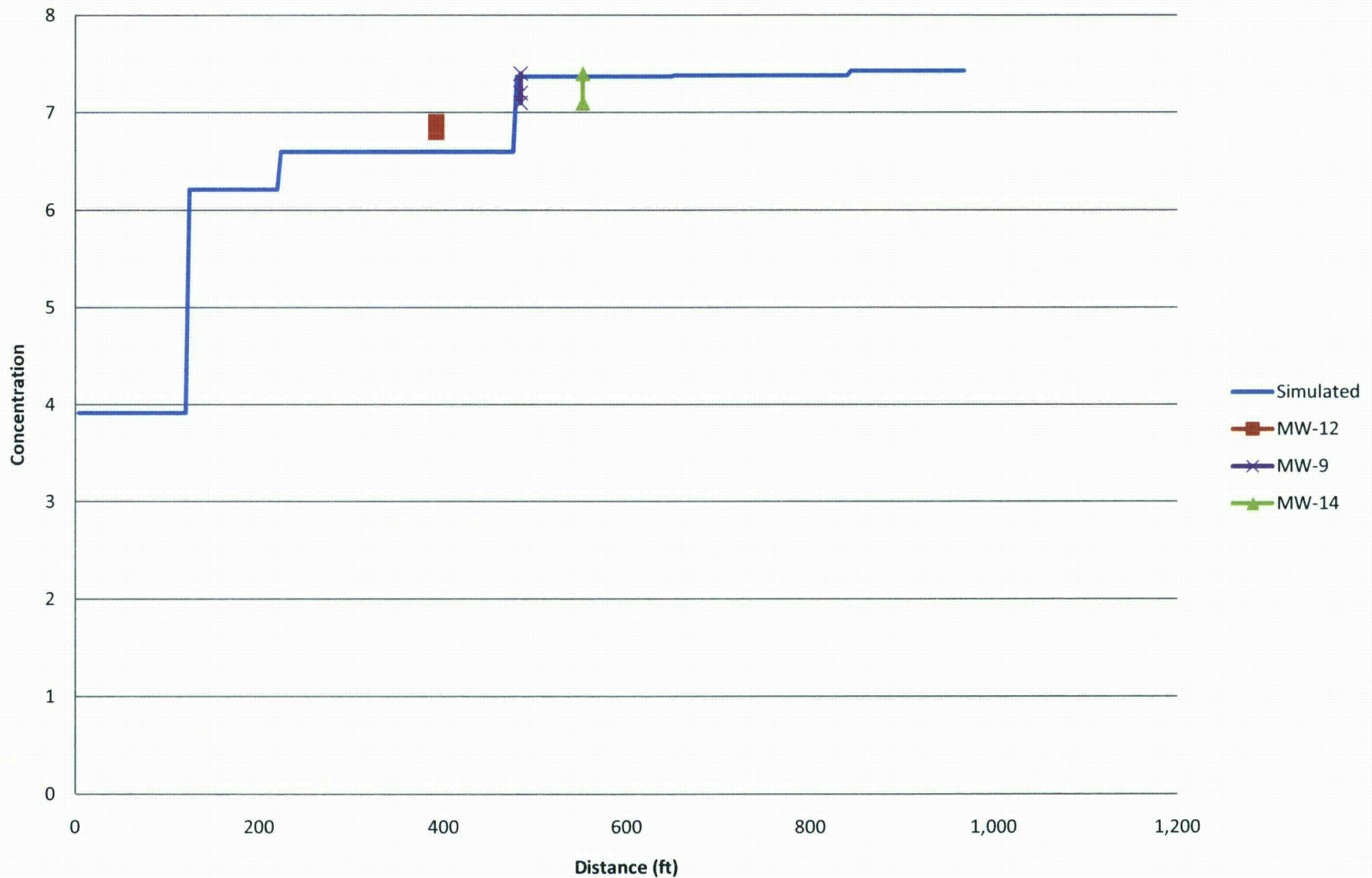
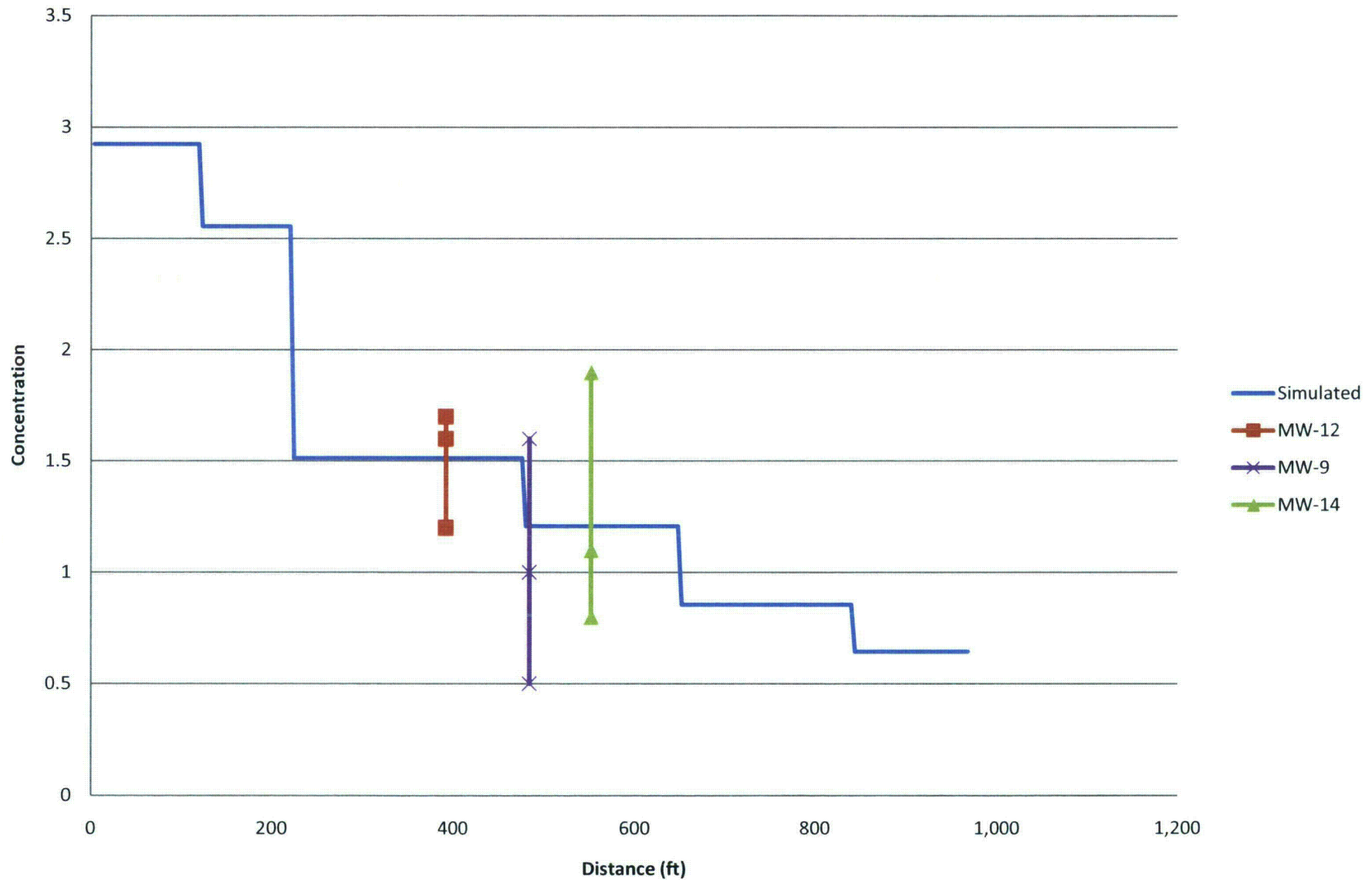
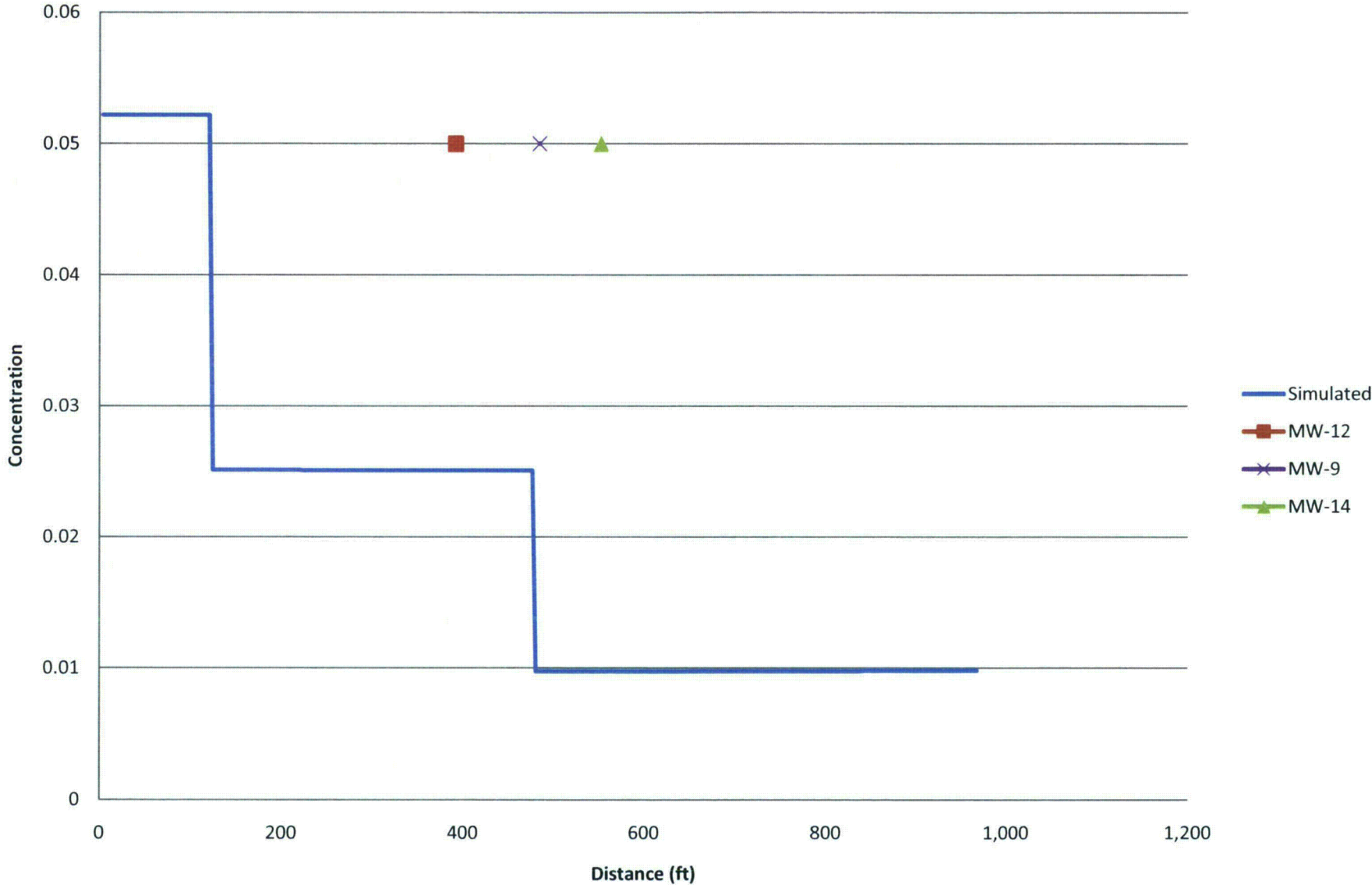


Figure 16E. Simulated Initial Values of Radium
Lang Draw



**Figure 16F. Simulated Initial Values of Nickel
Lang Draw**



**Figure 17 A. Simulated Breakthrough of Uranium
Lang Draw**

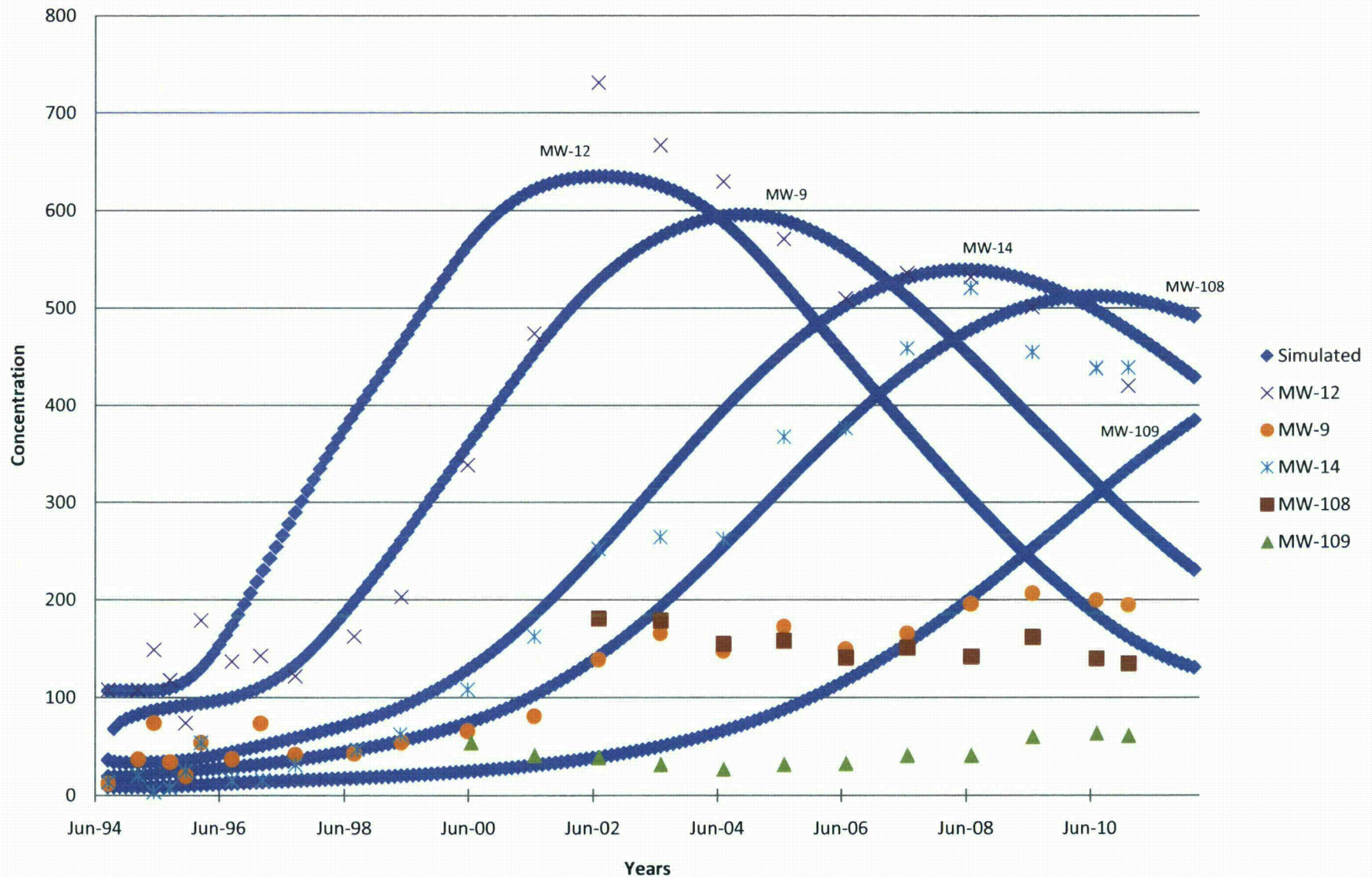


Figure 17B. Simulated Breakthrough of Sulfate Lang Draw

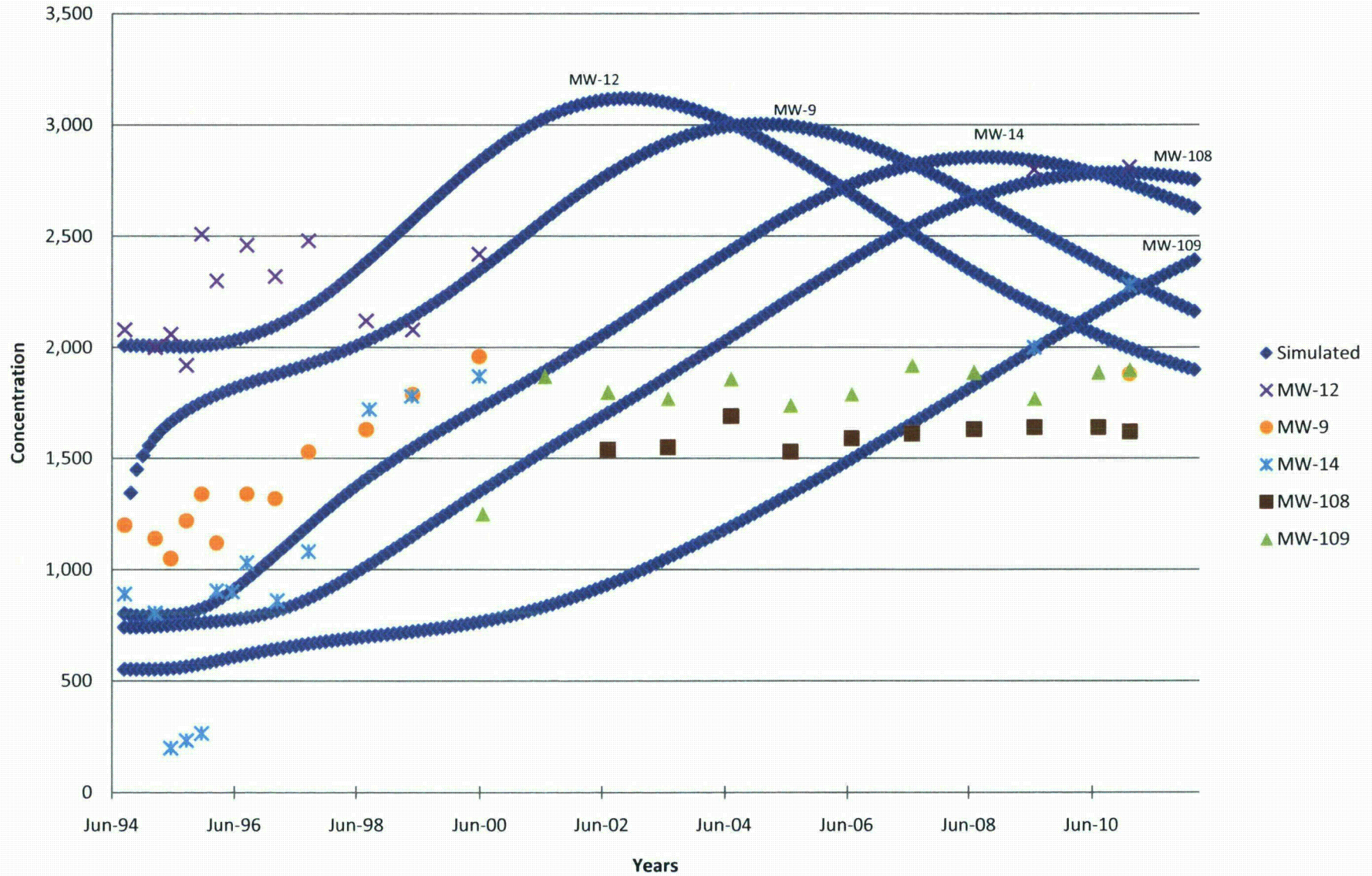


Figure 17C. Simulated Breakthrough of Chloride
Lang Draw

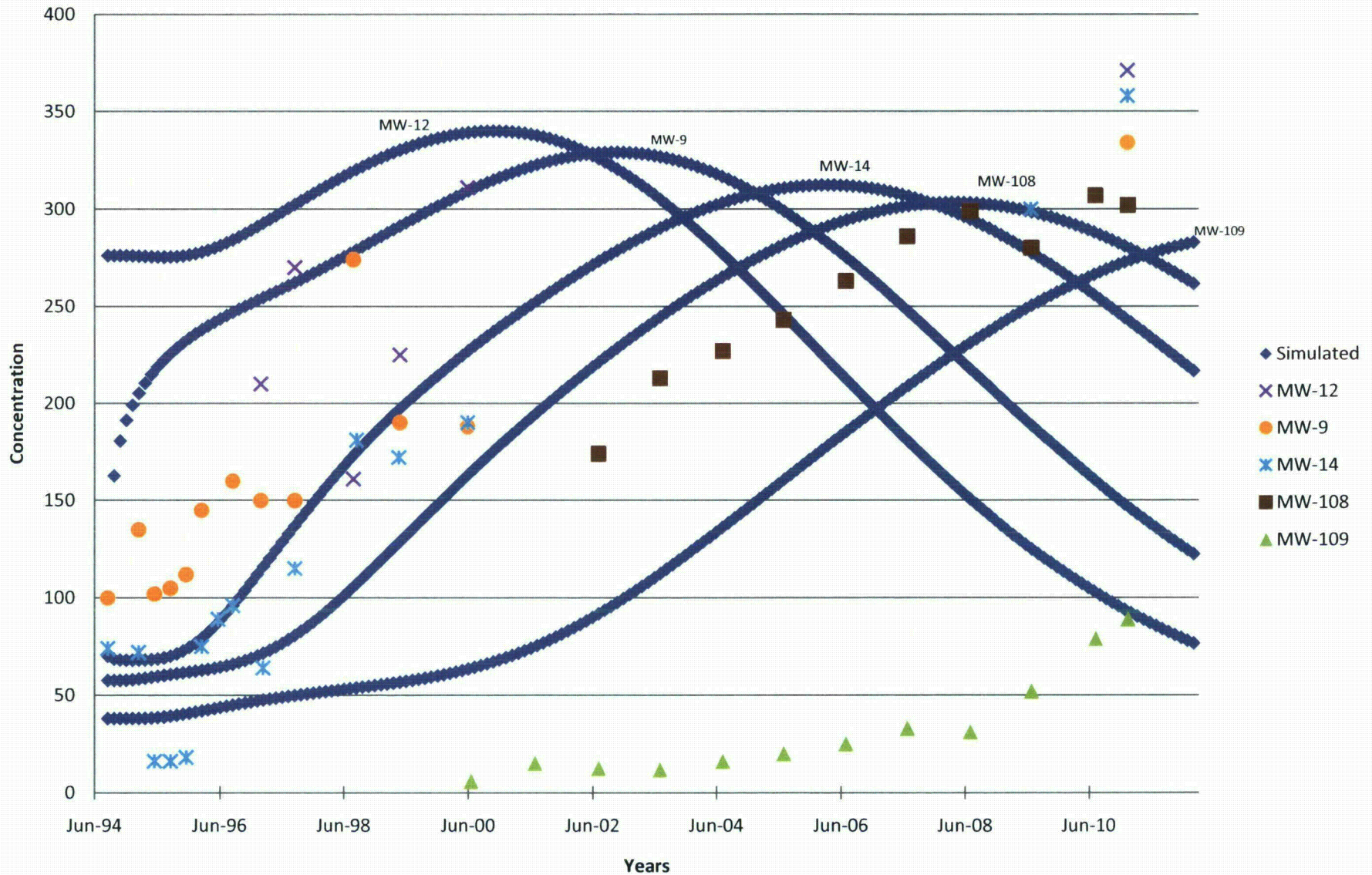


Figure 17D. Simulated Breakthrough of pH Lang Draw

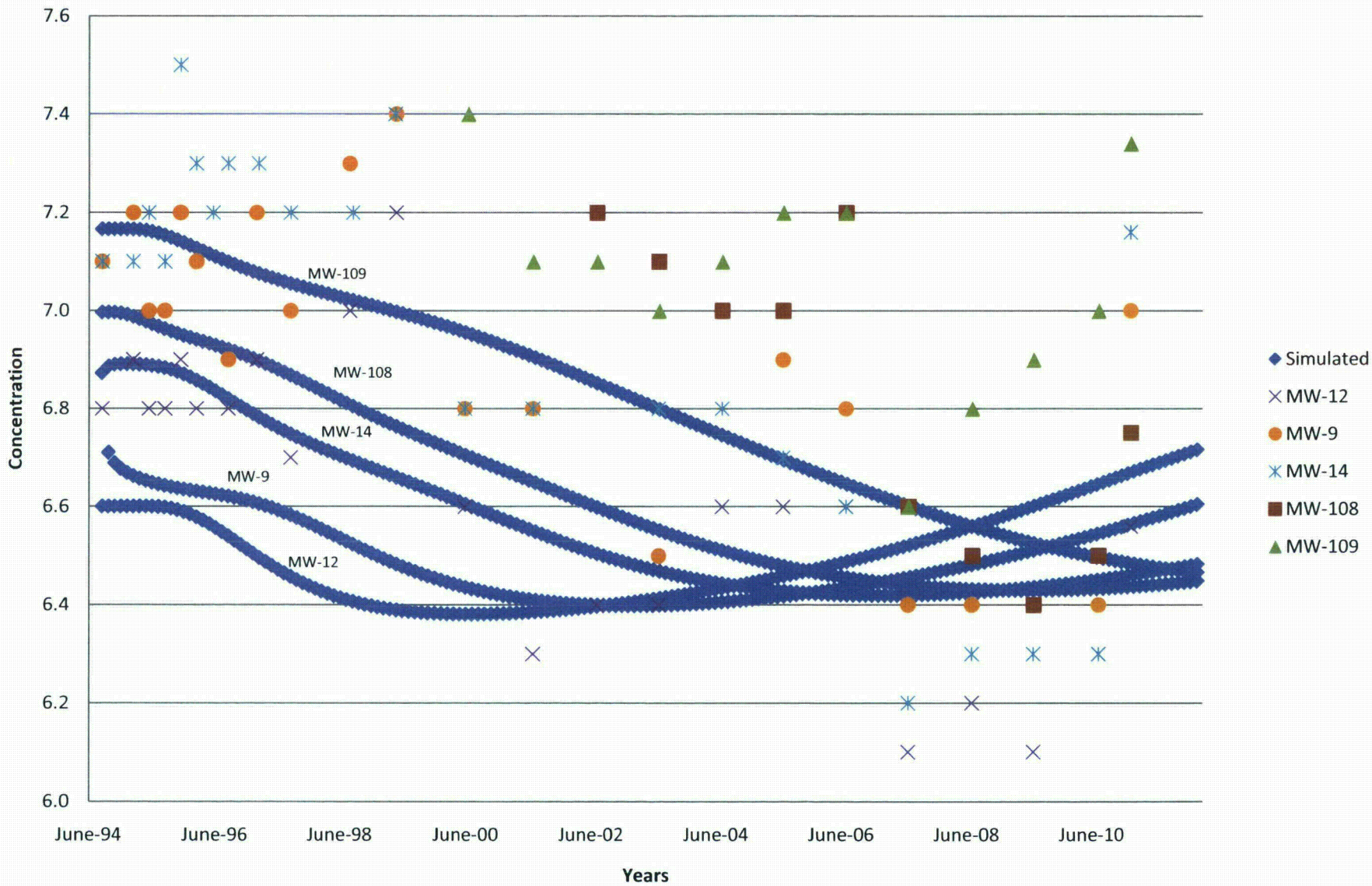


Figure 17E. Simulated Breakthrough of Radium
Lang Draw

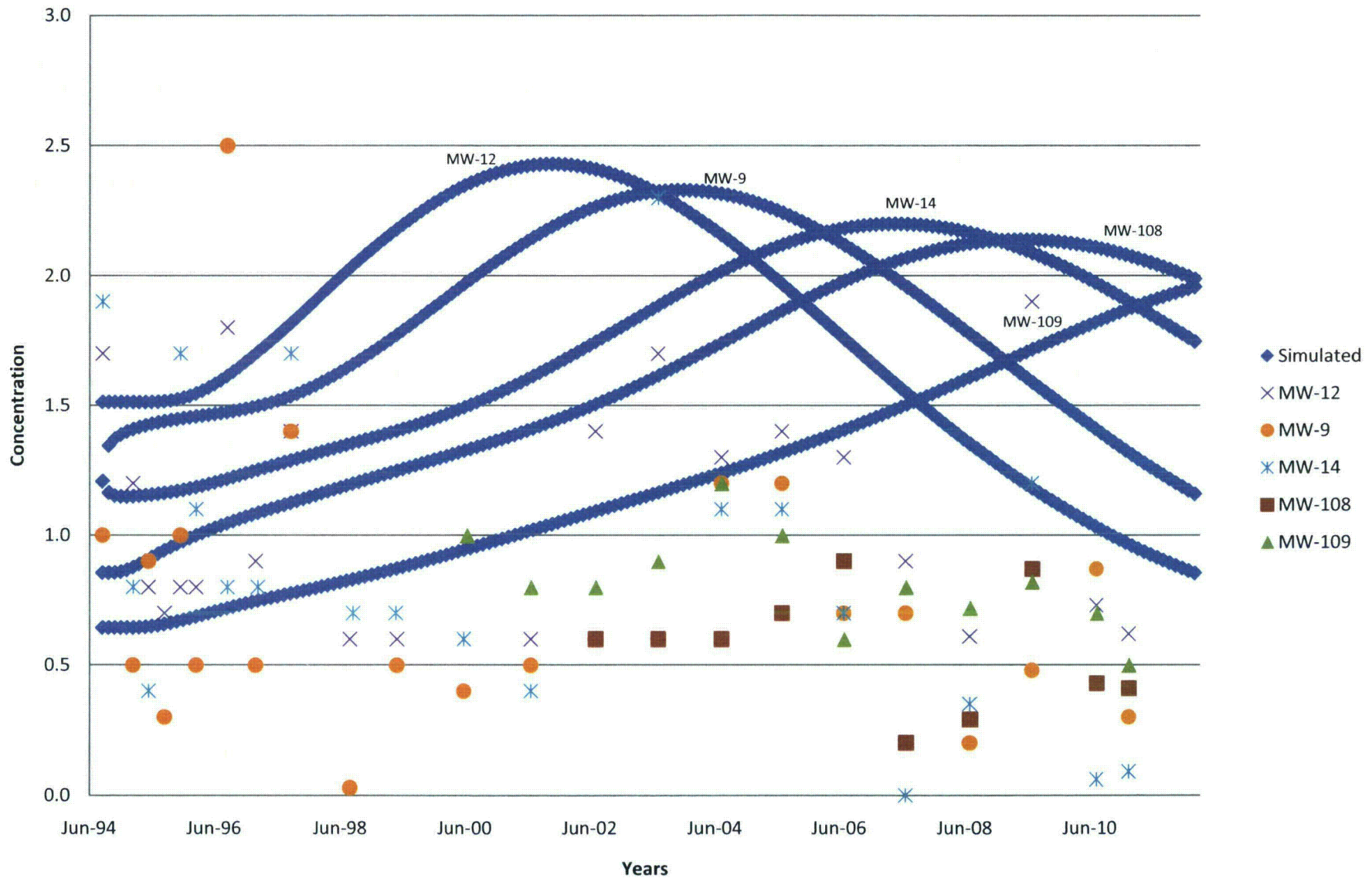
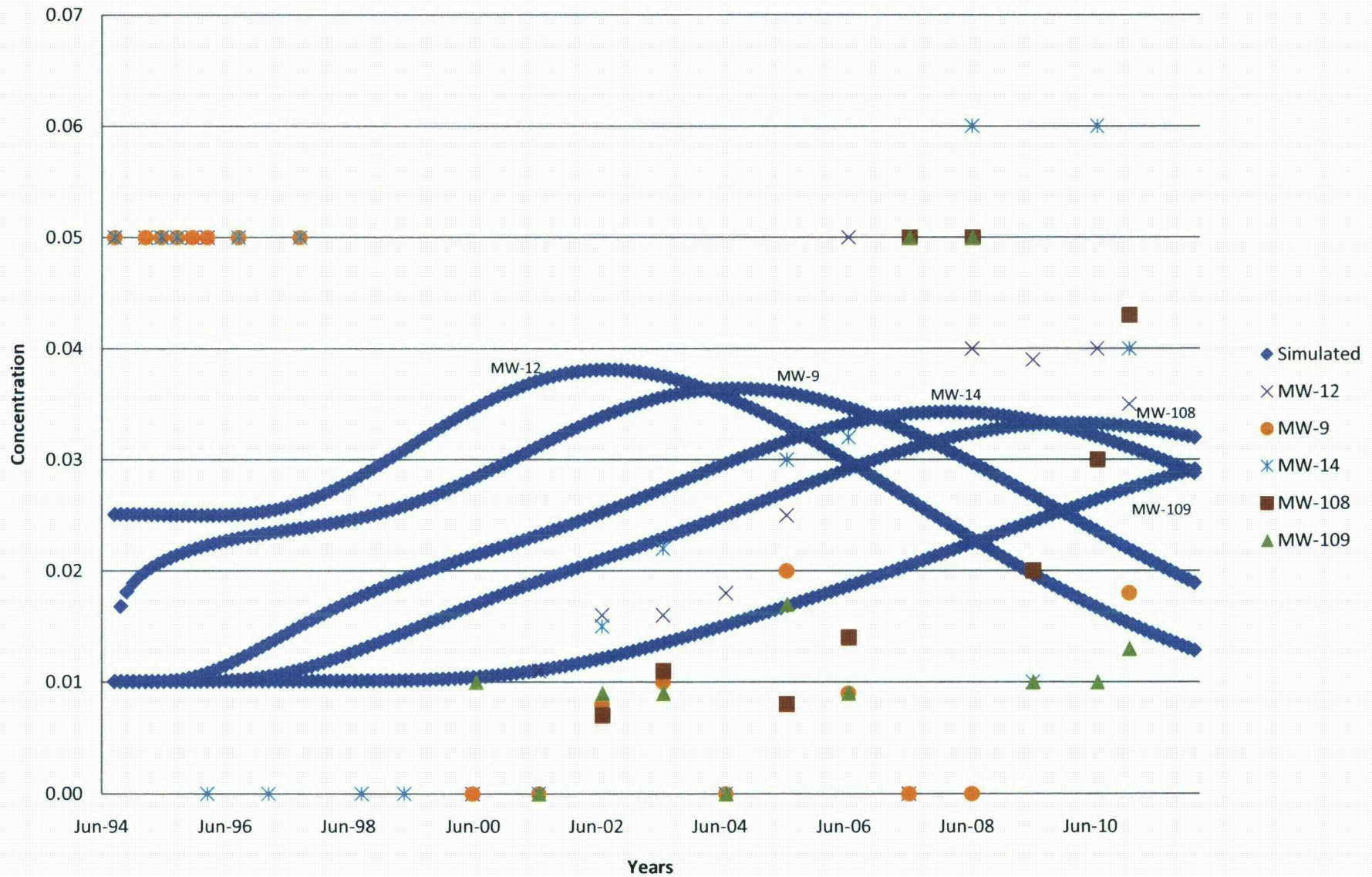
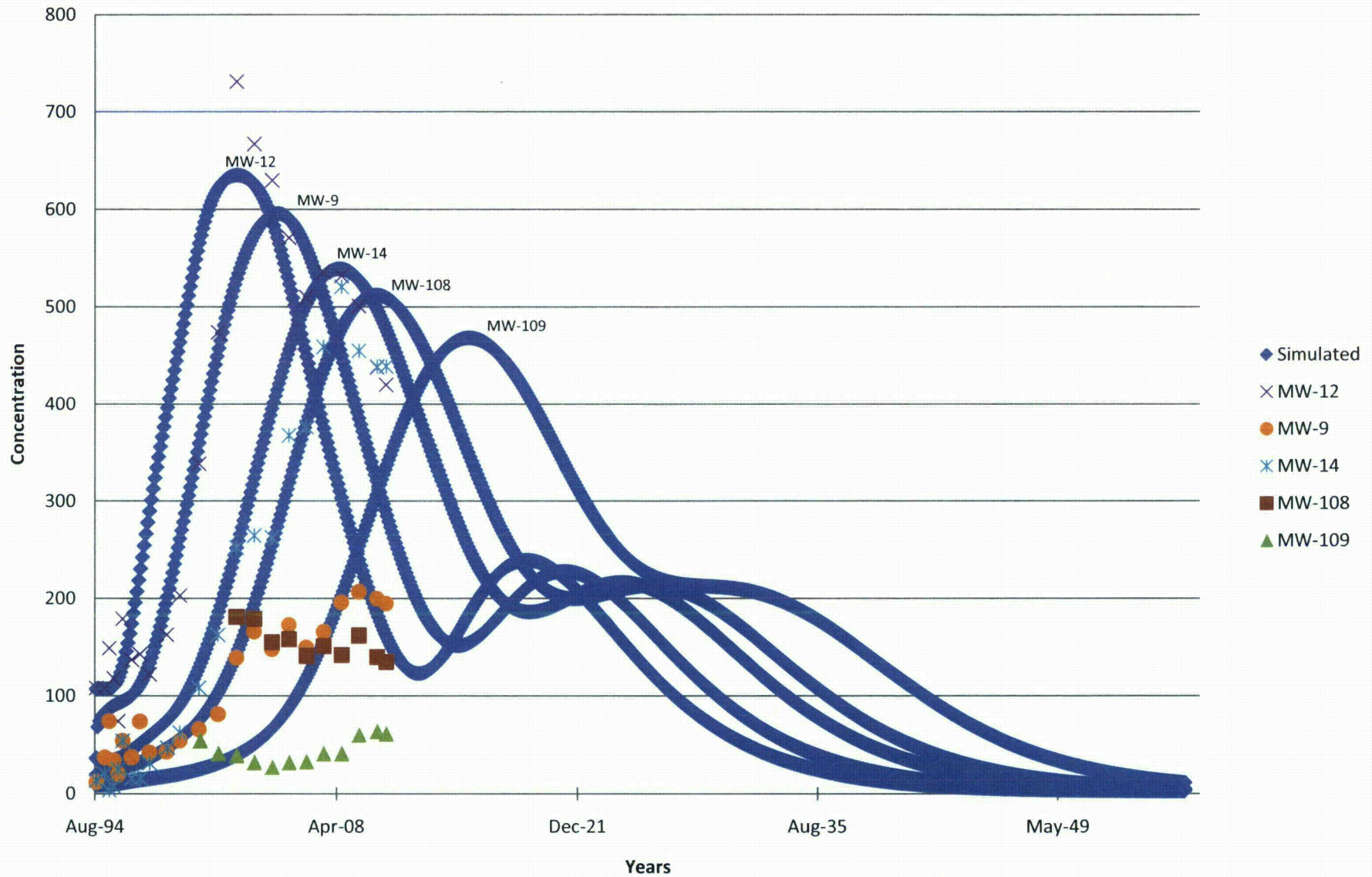


Figure 17F. Simulated Breakthrough of Nickel
Lang Draw



**Figure 18A. Predicted Breakthrough of Uranium
Lang Draw**



**Figure 18B. Predicted Breakthrough of Sulfate
Lang Draw**

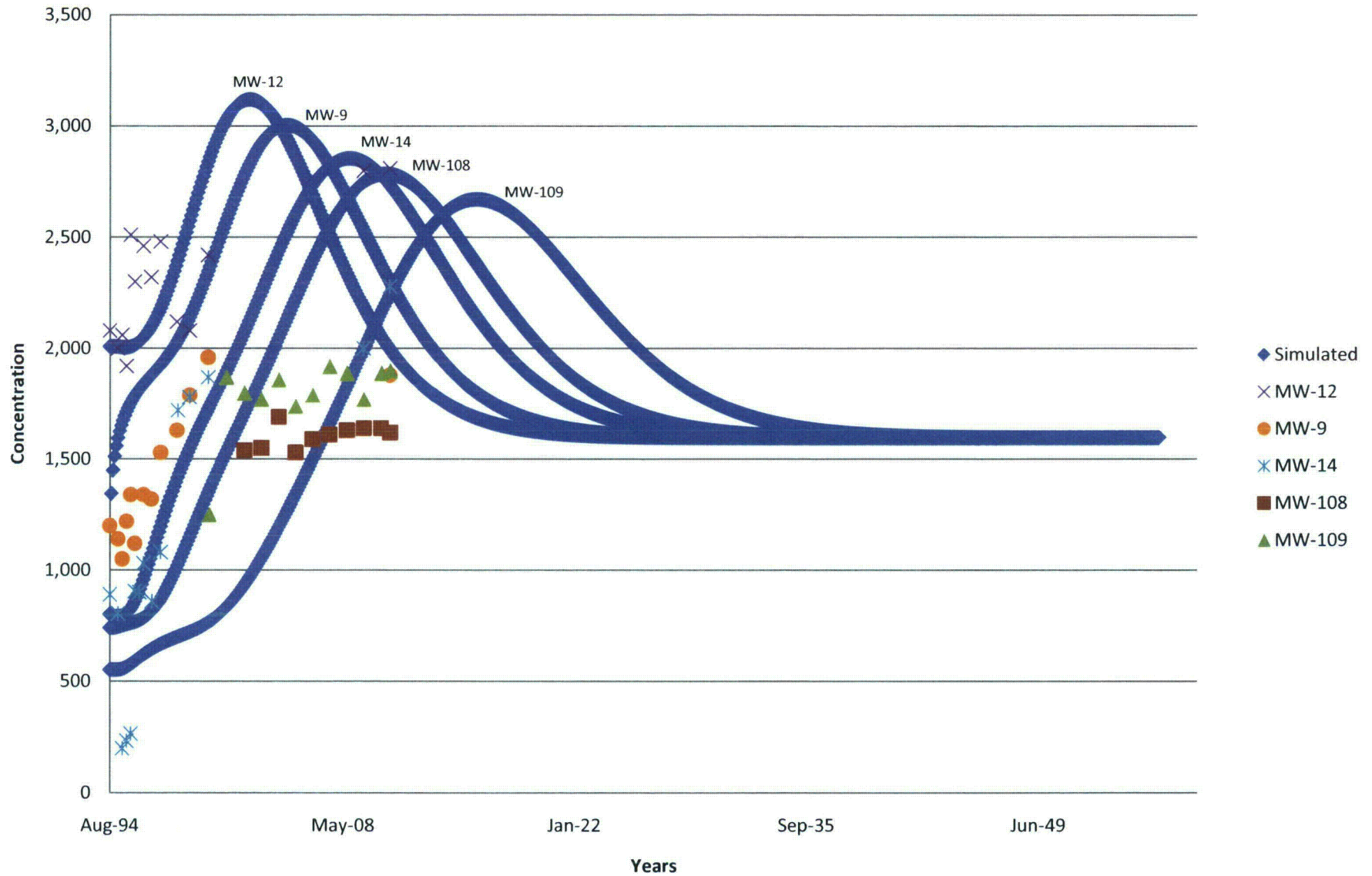
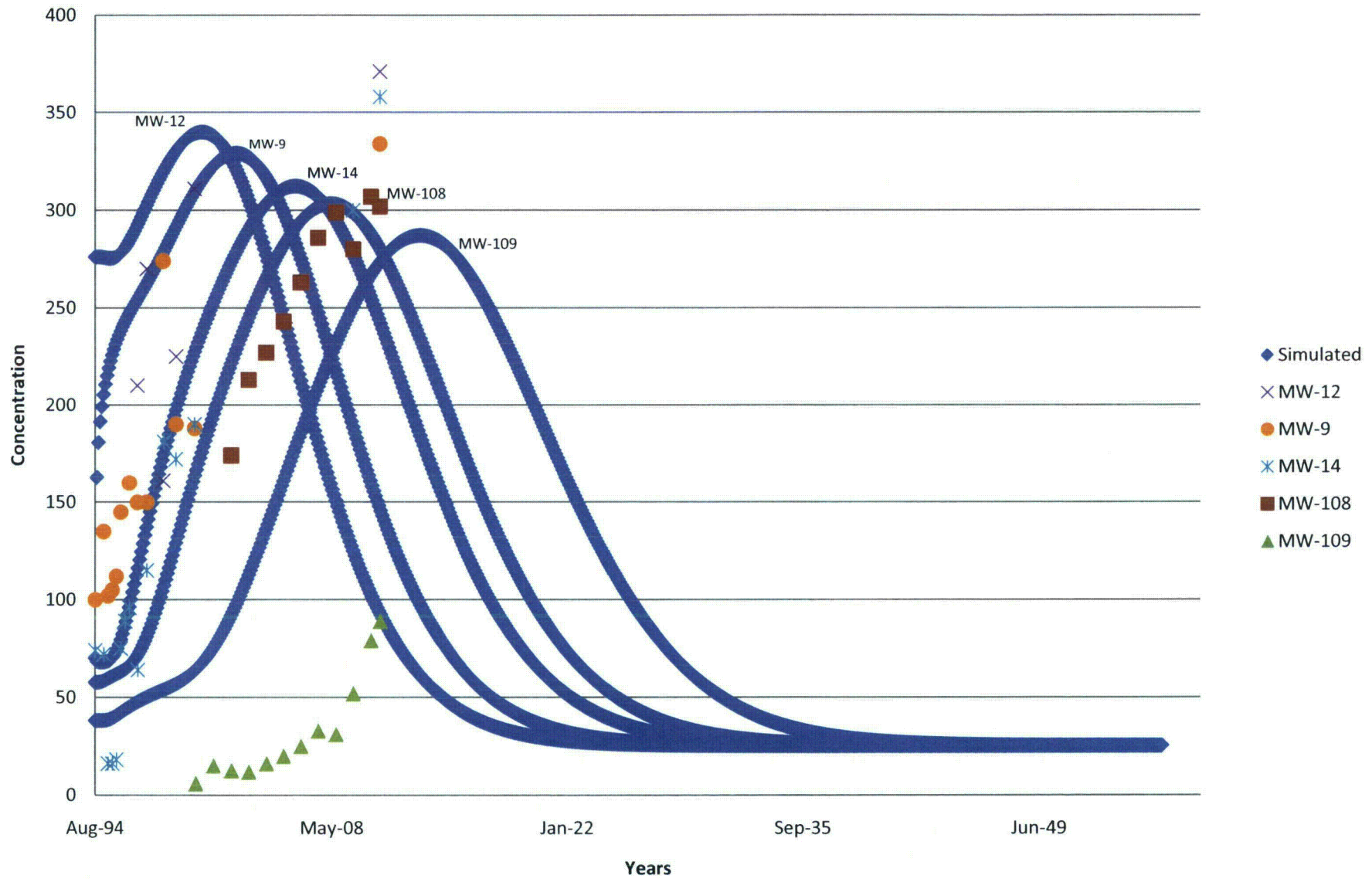


Figure 18C. Predicted Breakthrough of Chloride Lang Draw



**Figure 18D. Predicted Breakthrough of pH
Lang Draw**

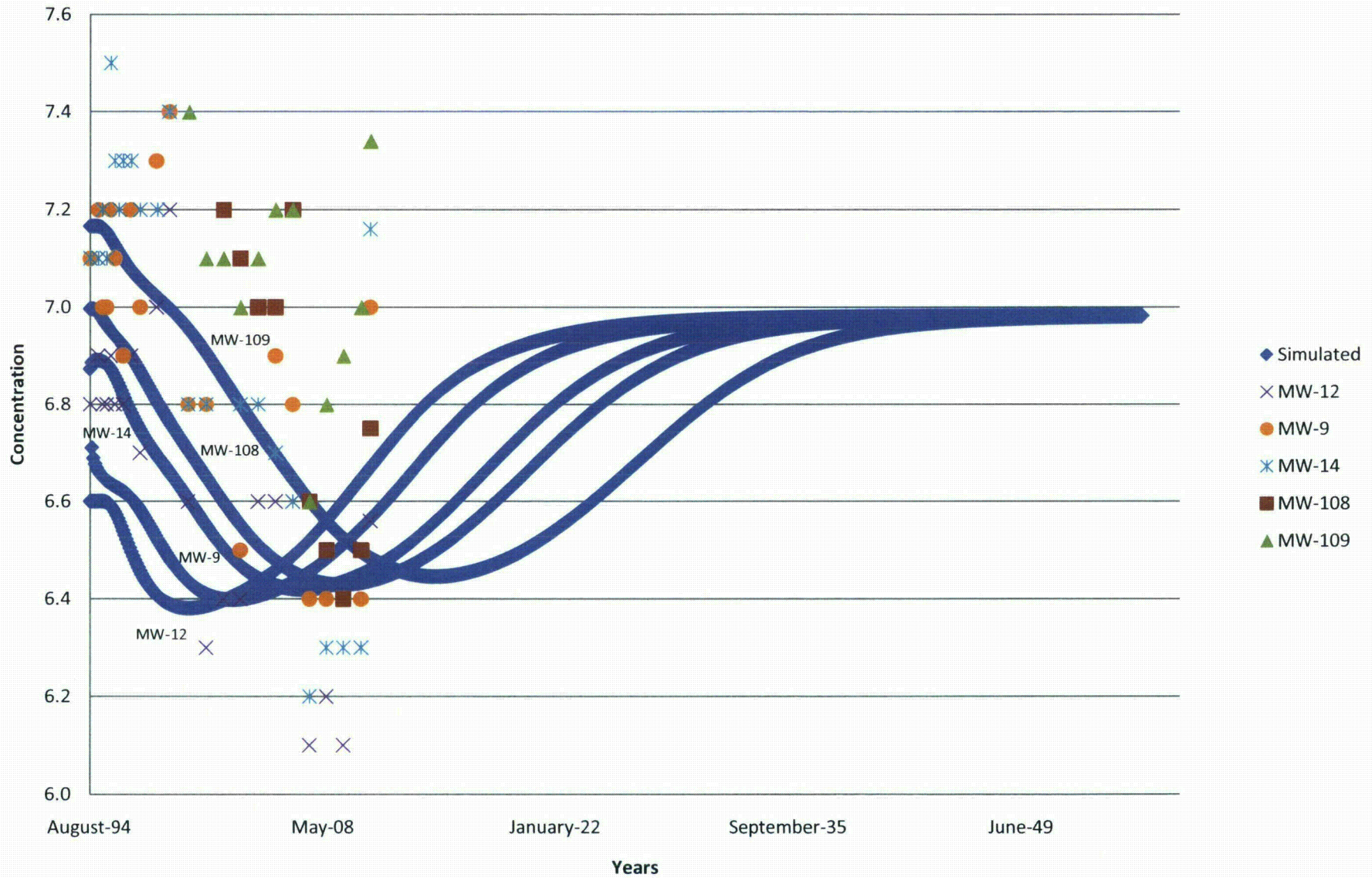


Figure 18E. Predicted Breakthrough of Radium Lang Draw

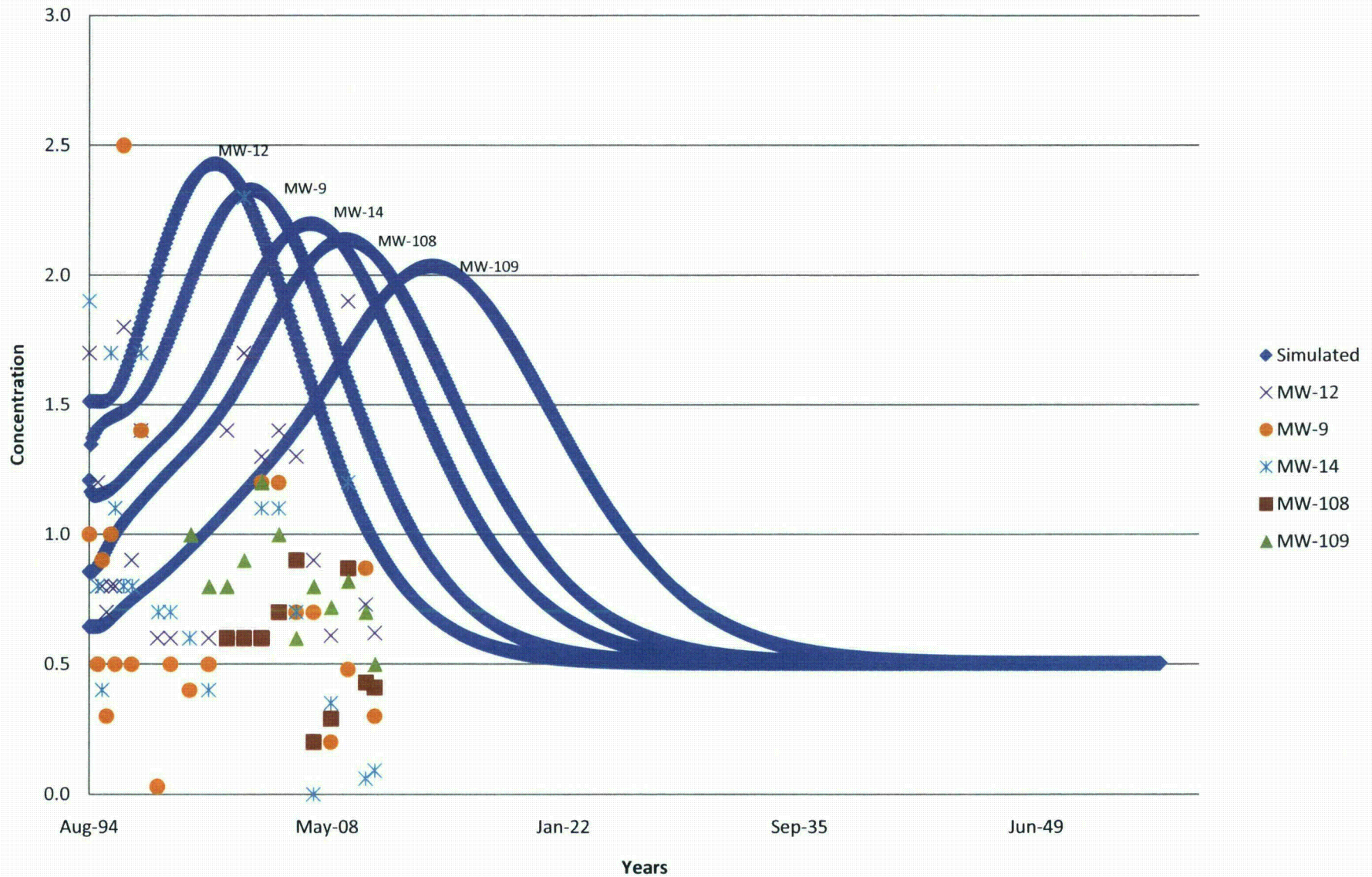
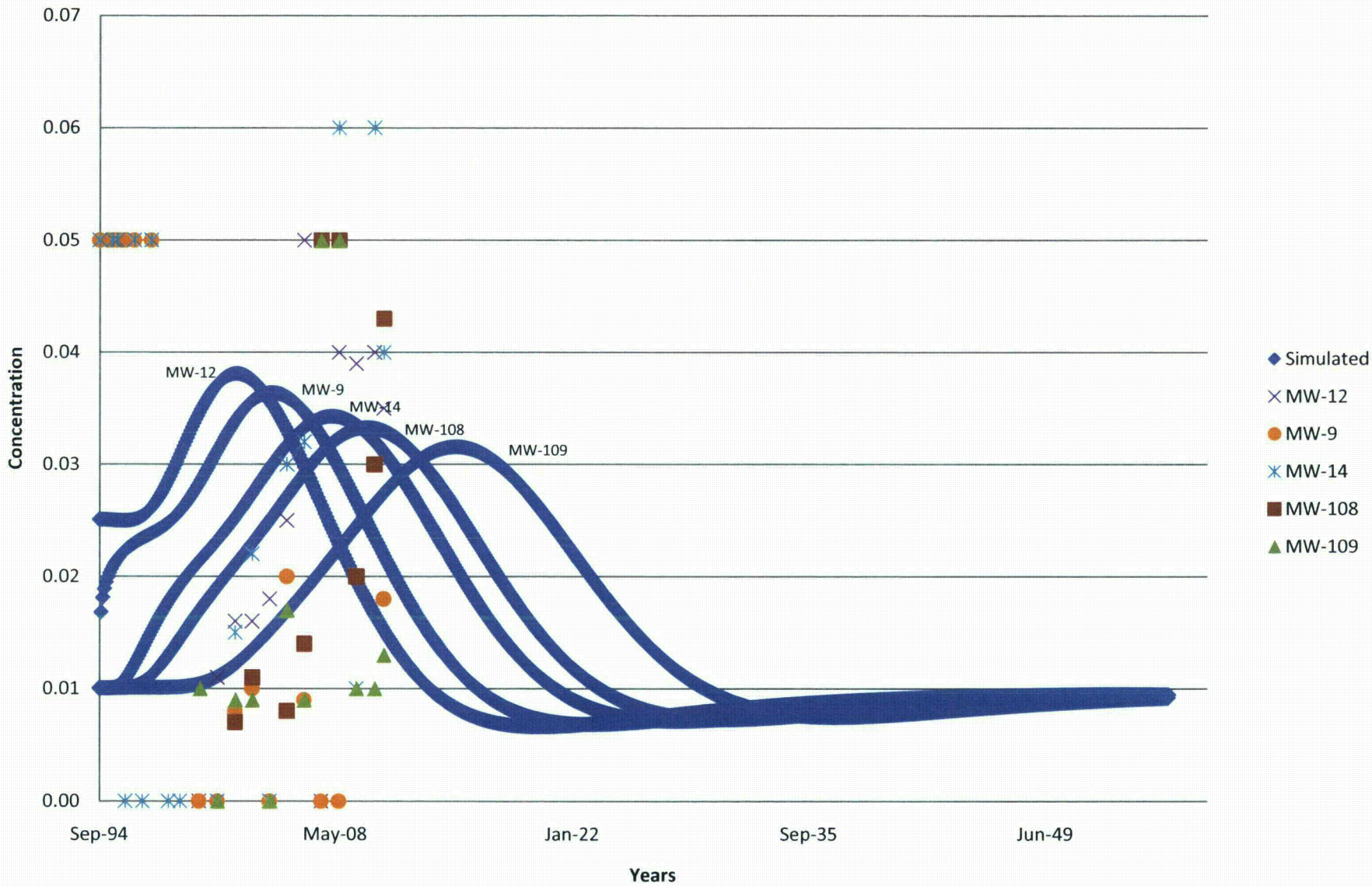
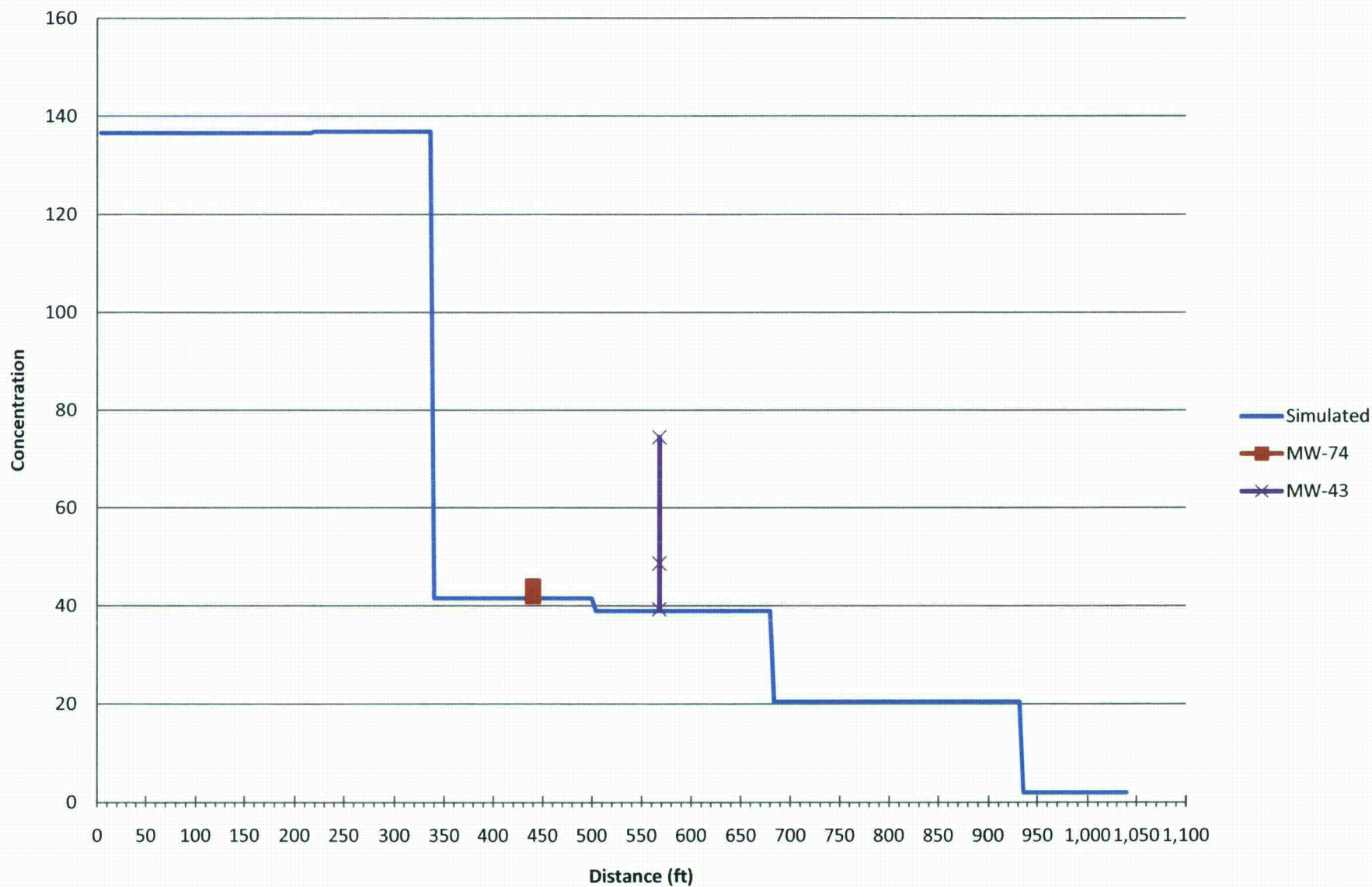


Figure 18F. Predicted Breakthrough of Nickel
Lang Draw



**Figure 19A. Simulated Initial Values of Uranium
Northern Pathway**



**Figure 19B. Simulated Initial Values of Sulfate
Northern Pathway**

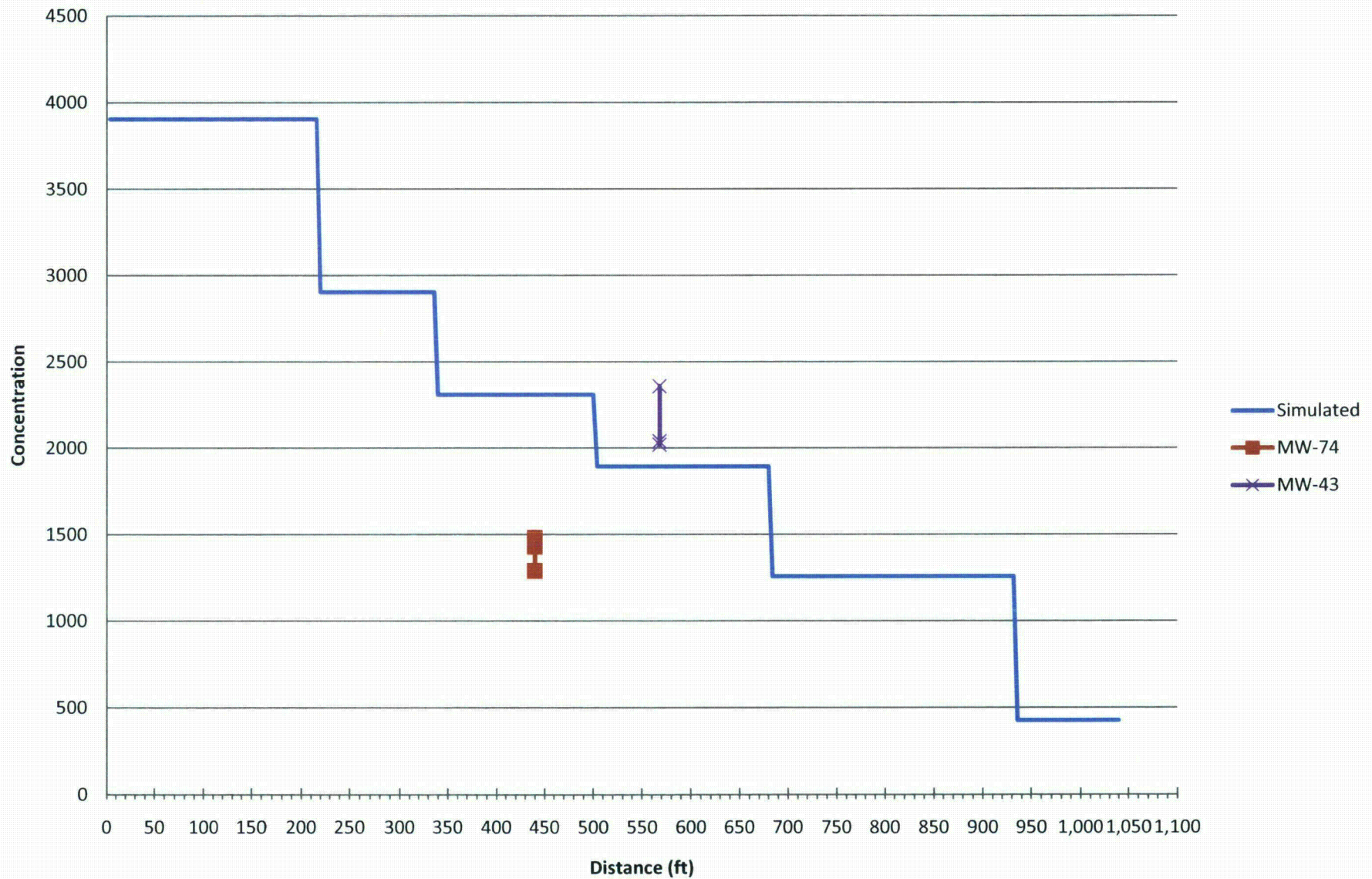


**Figure 19C. Simulated Initial Values of Chloride
Northern Pathway**

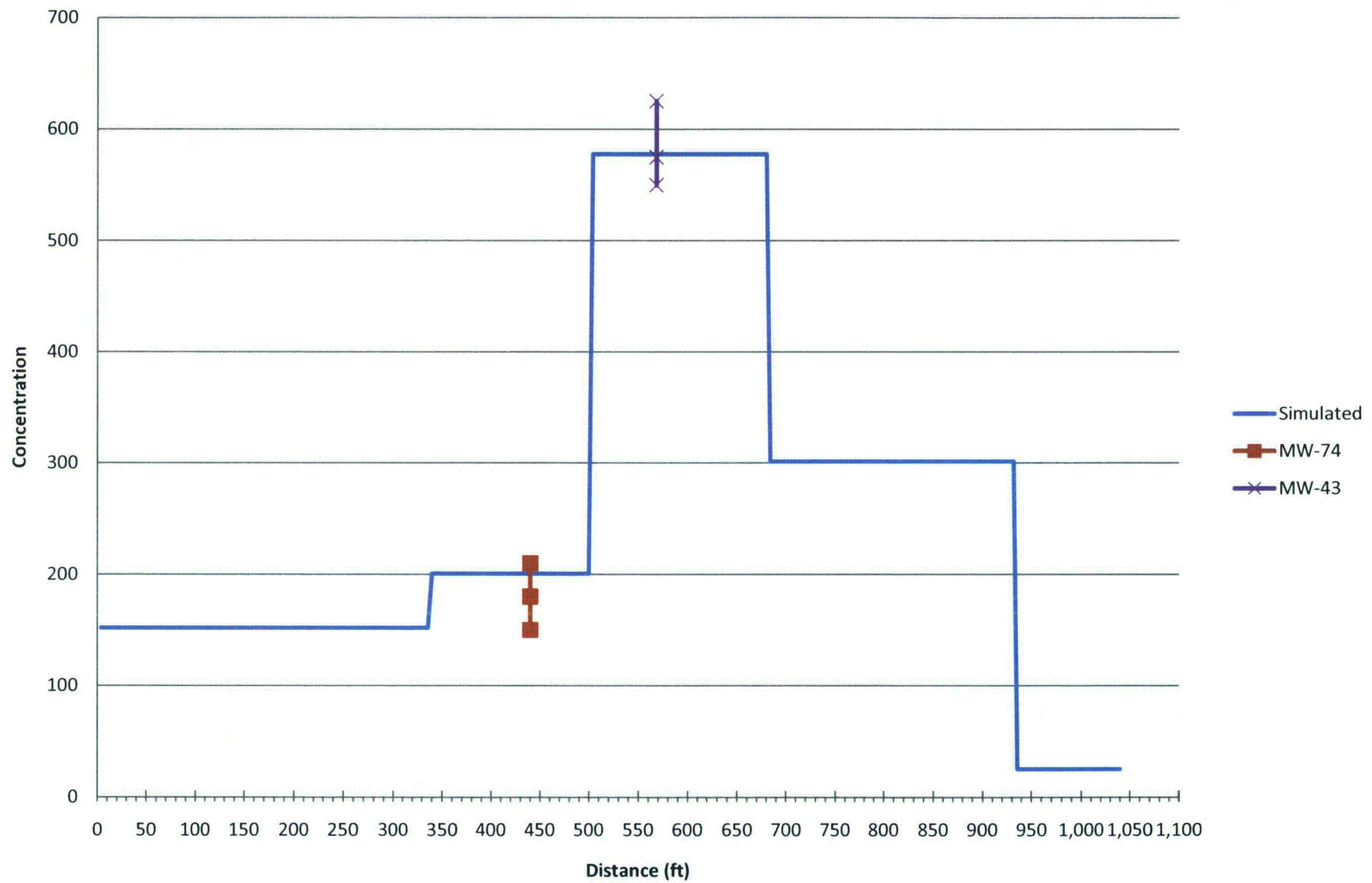


**Figure 19D. Simulated Initial Values of pH
Northern Pathway**

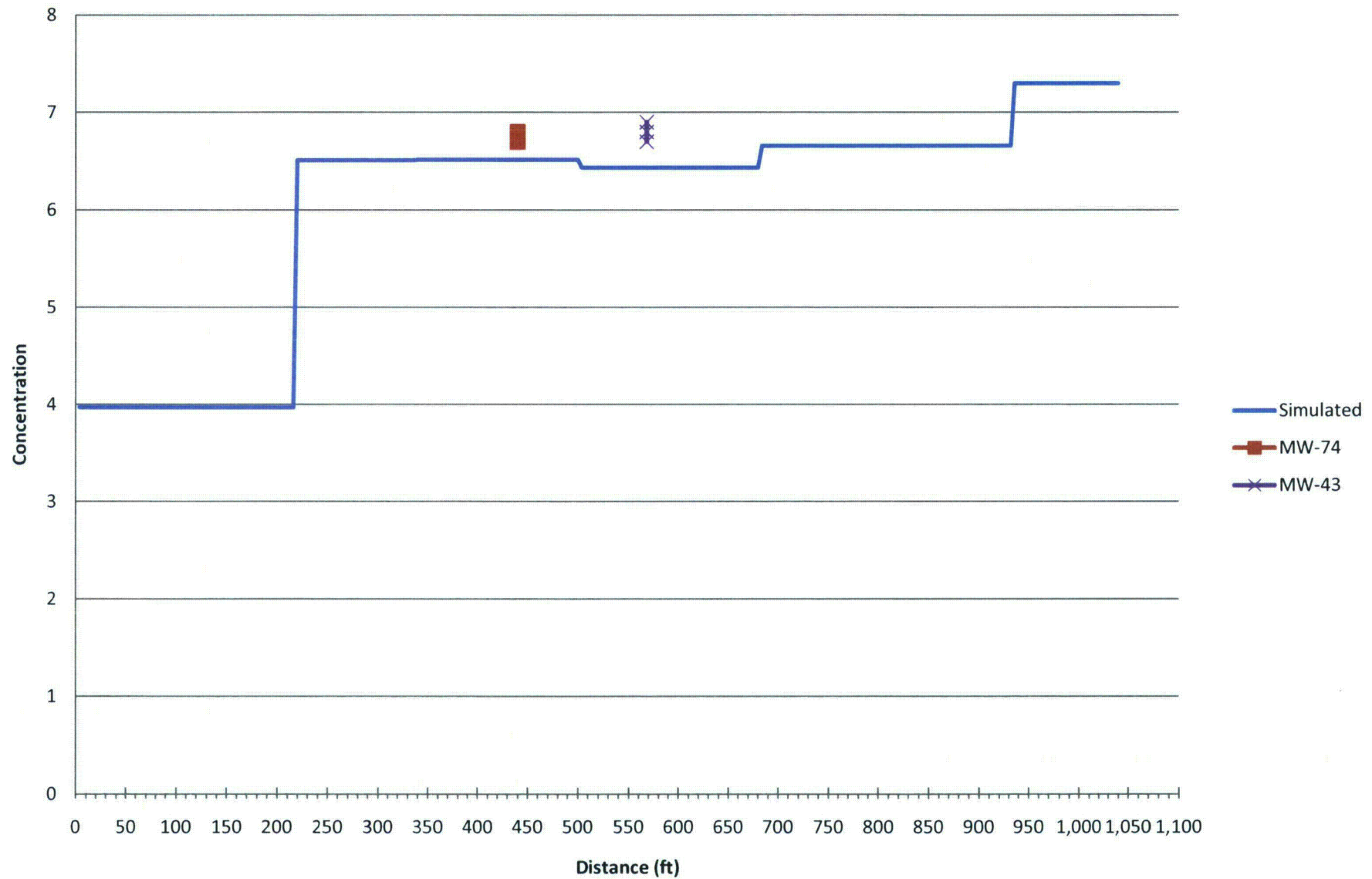


**Figure 19E. Simulated Initial Values of Radium
Northern Pathway**

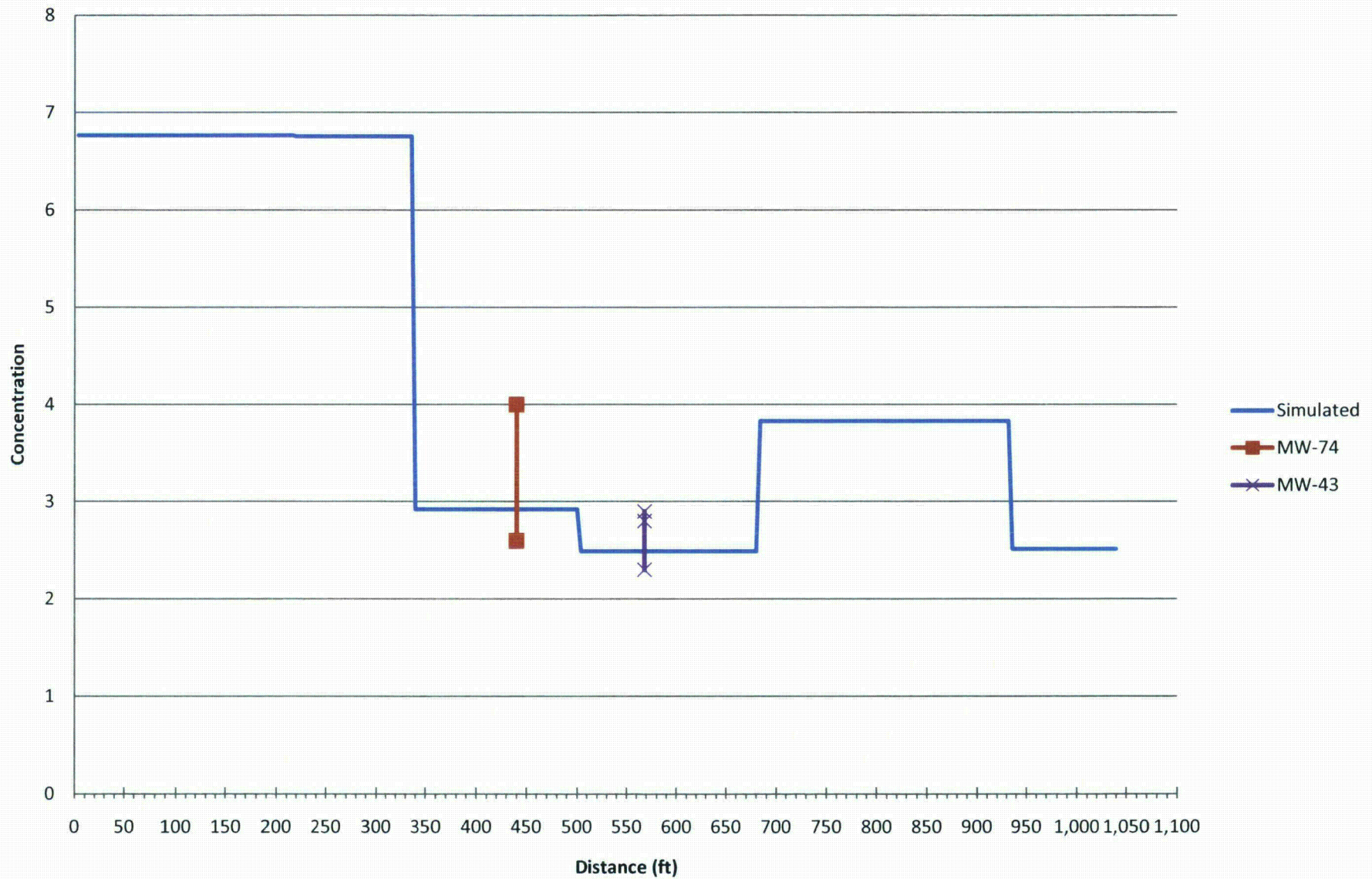


**Figure 19F. Simulated Initial Values of Nickel
Northern Pathway**

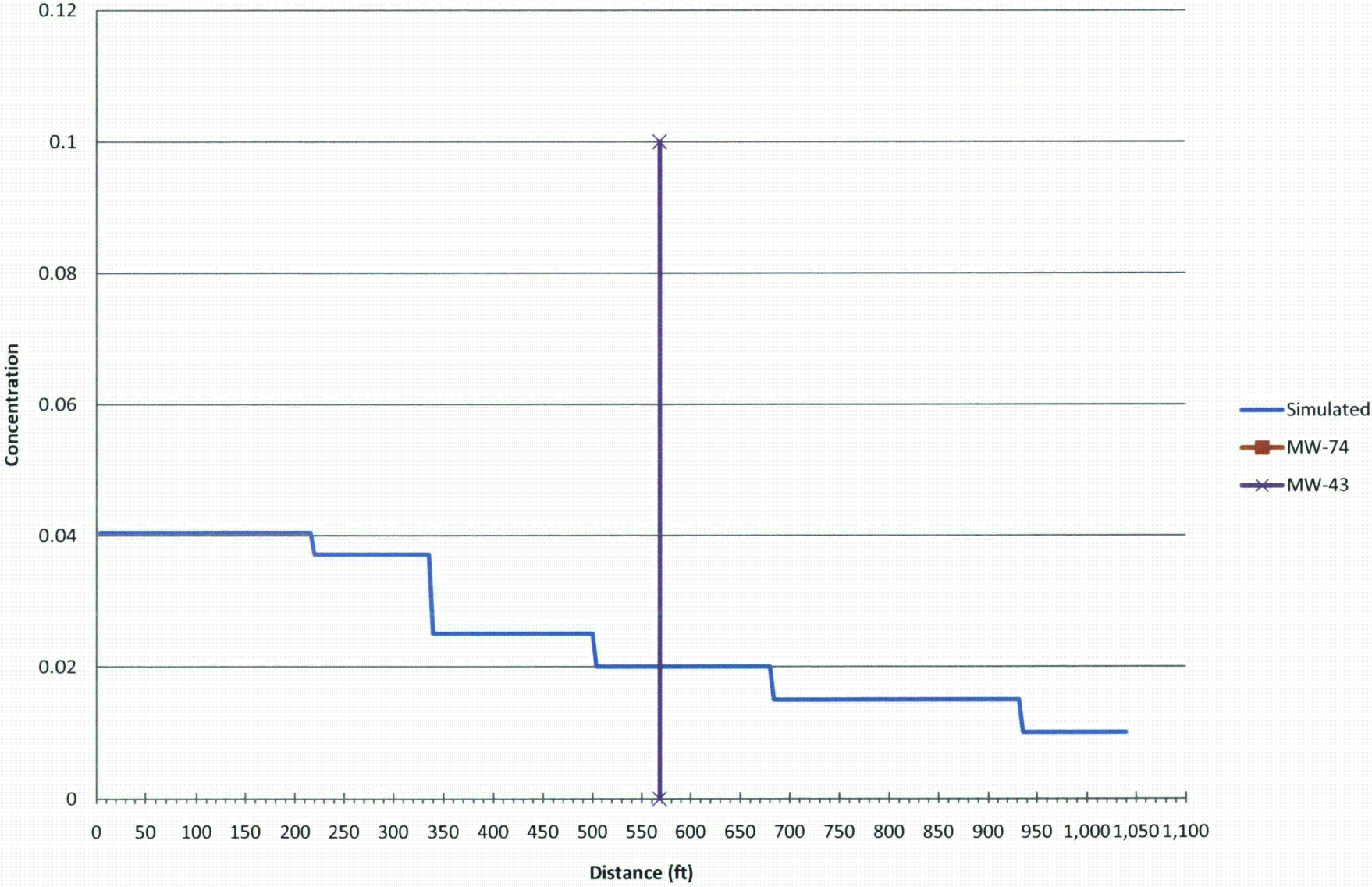


**Figure 20A. Simulated Breakthrough of Uranium
Northern Pathway**

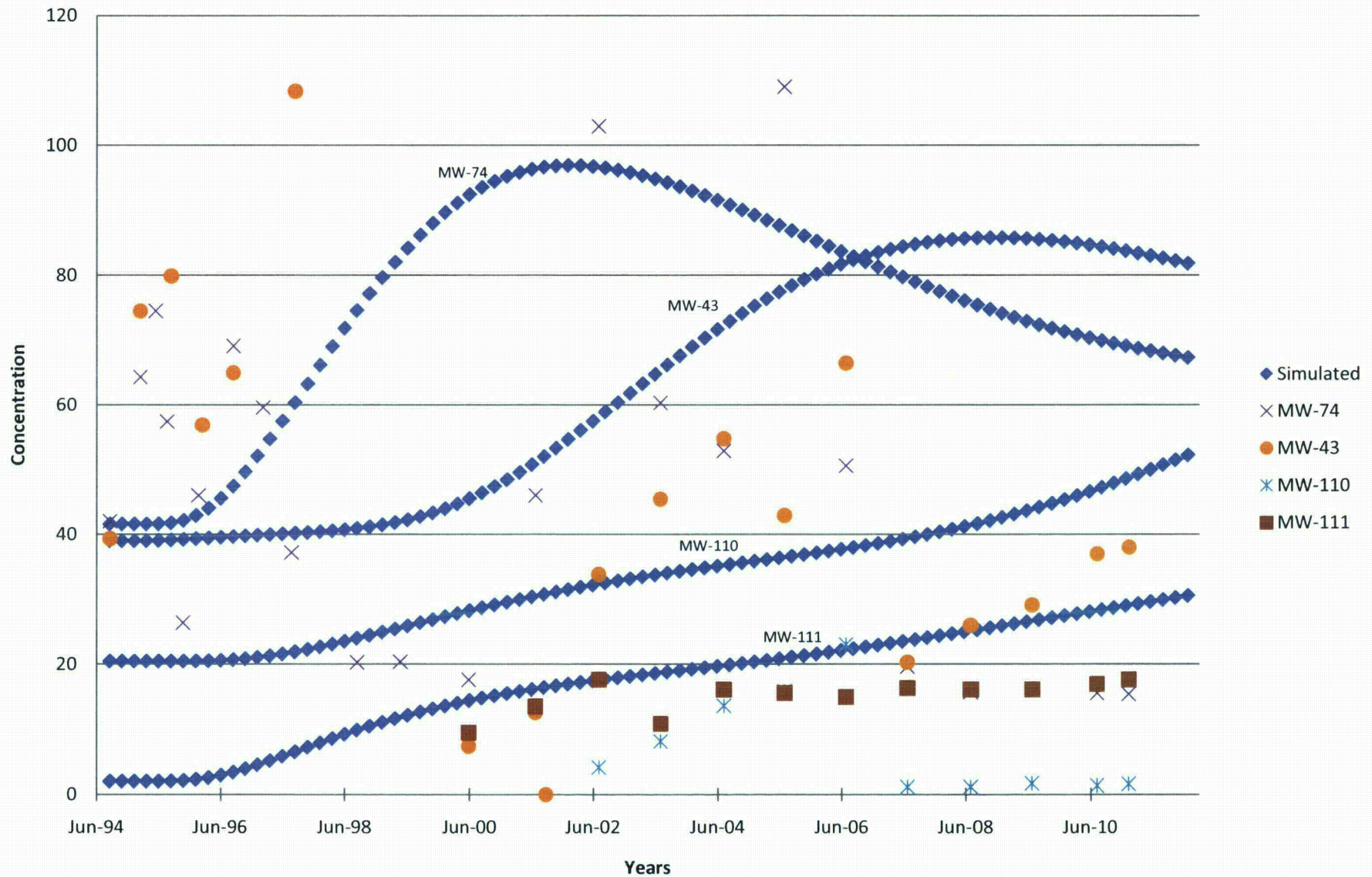


**Figure 20B. Simulated Breakthrough of Sulfate
Northern Pathway**

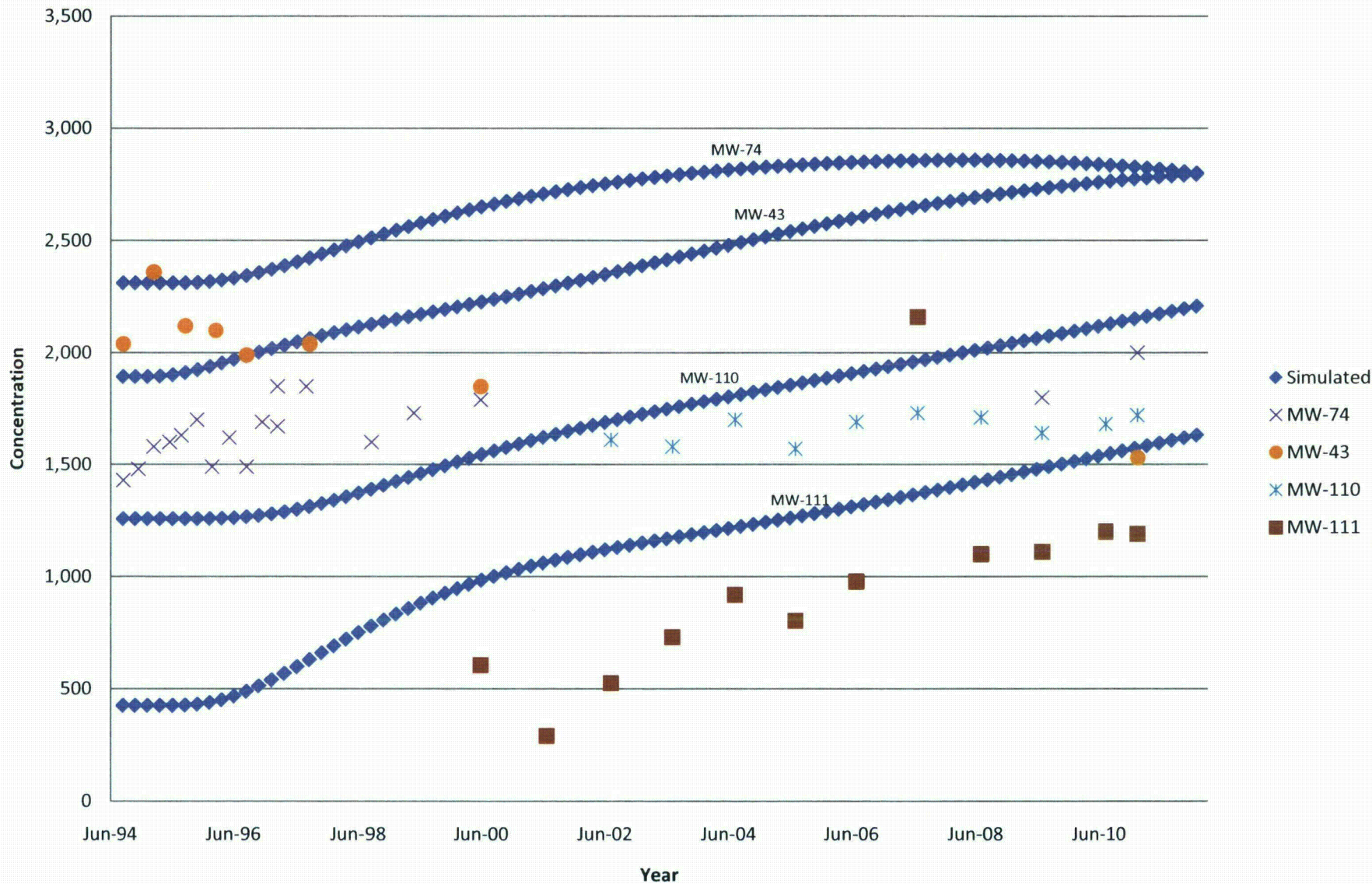


Figure 20C. Simulated Breakthrough of Chloride
Northern Pathway

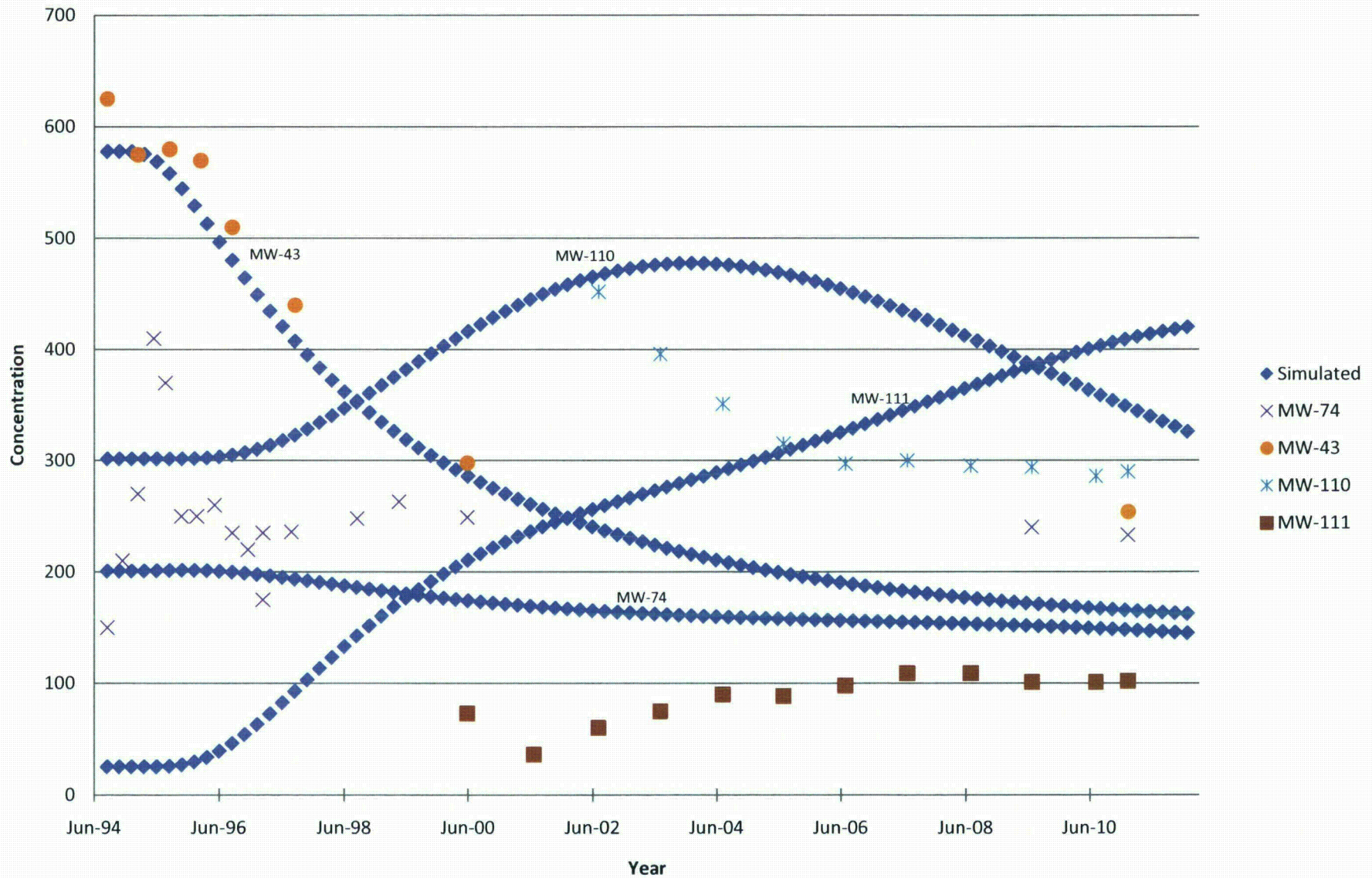
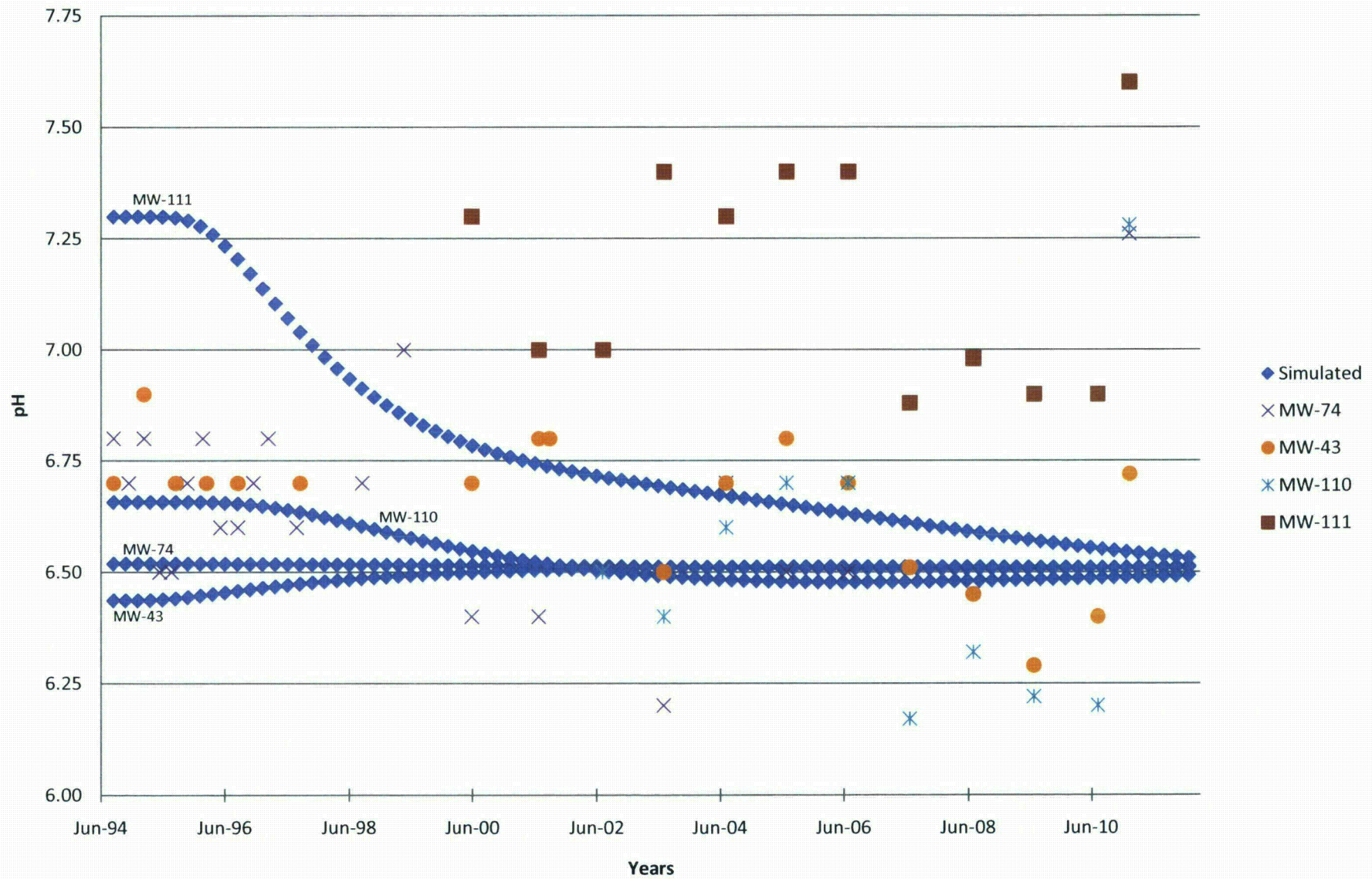
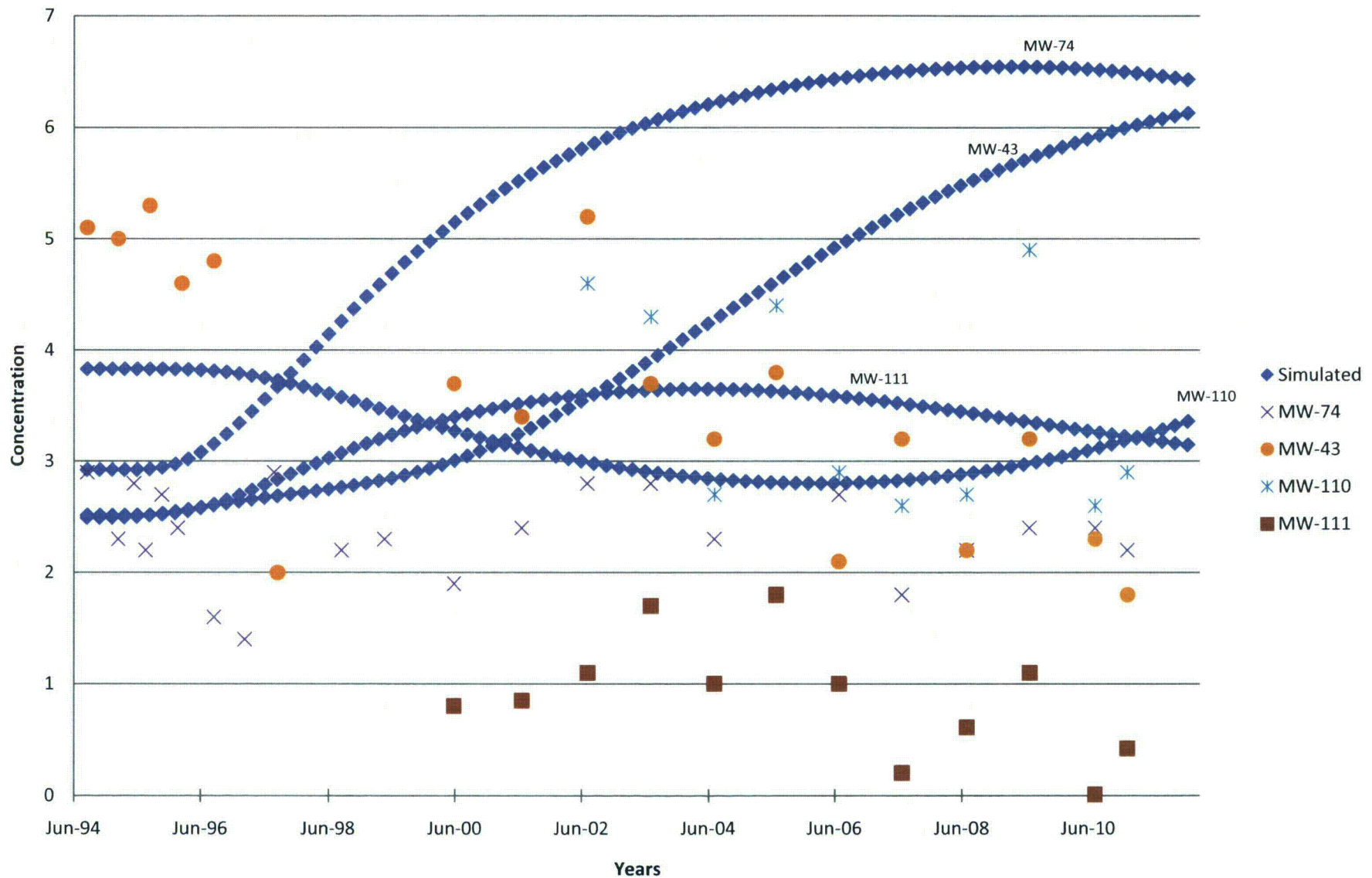


Figure 20D. Simulated Breakthrough of pH Northern Pathway



**Figure 20E. Simulated Breakthrough of Radium
Northern Pathway**



**Figure 20F. Simulated Breakthrough of Nickel
Northern Pathway**

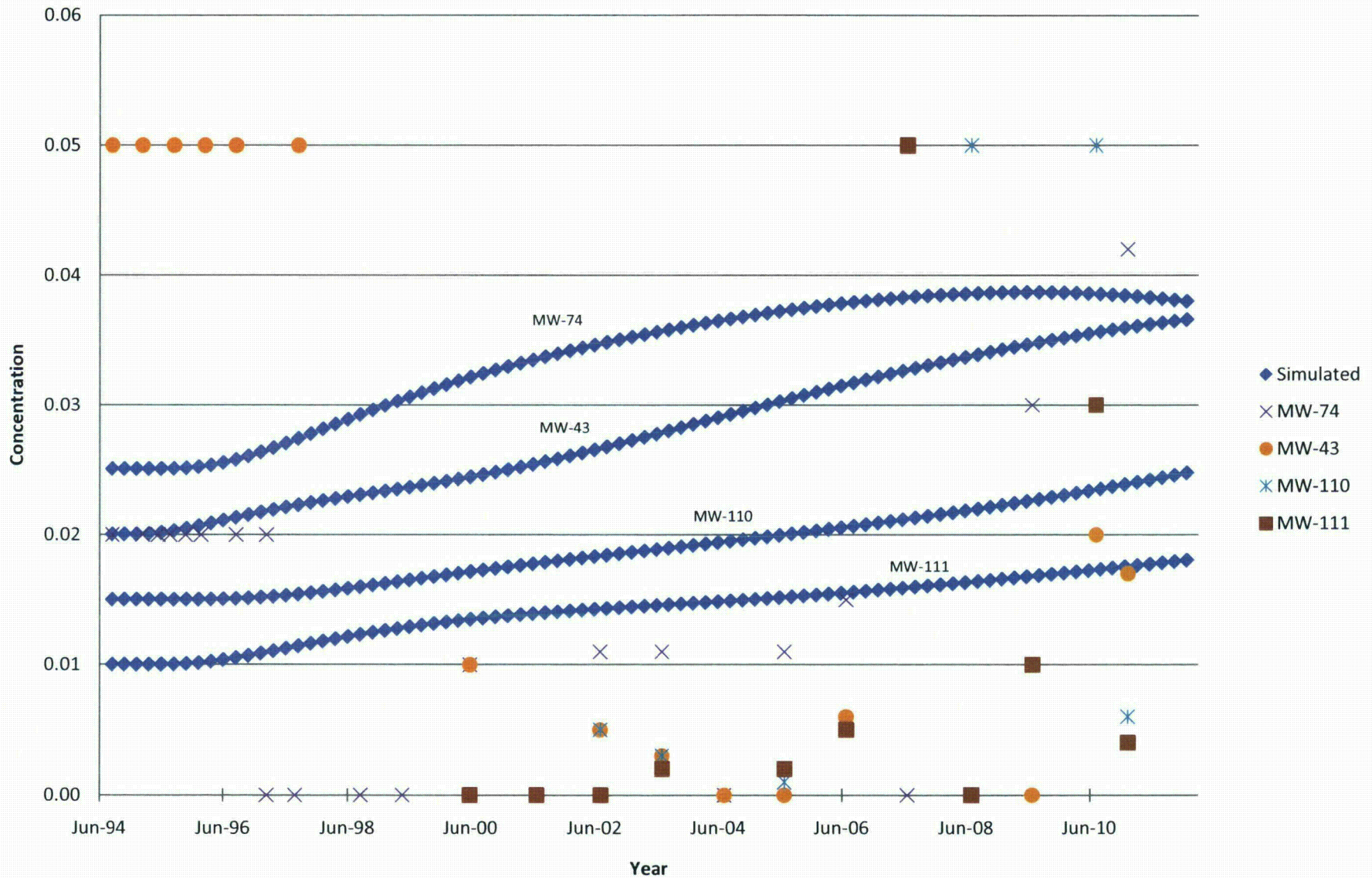


**Figure 21A. Predicted Breakthrough of Uranium
Northern Pathway**

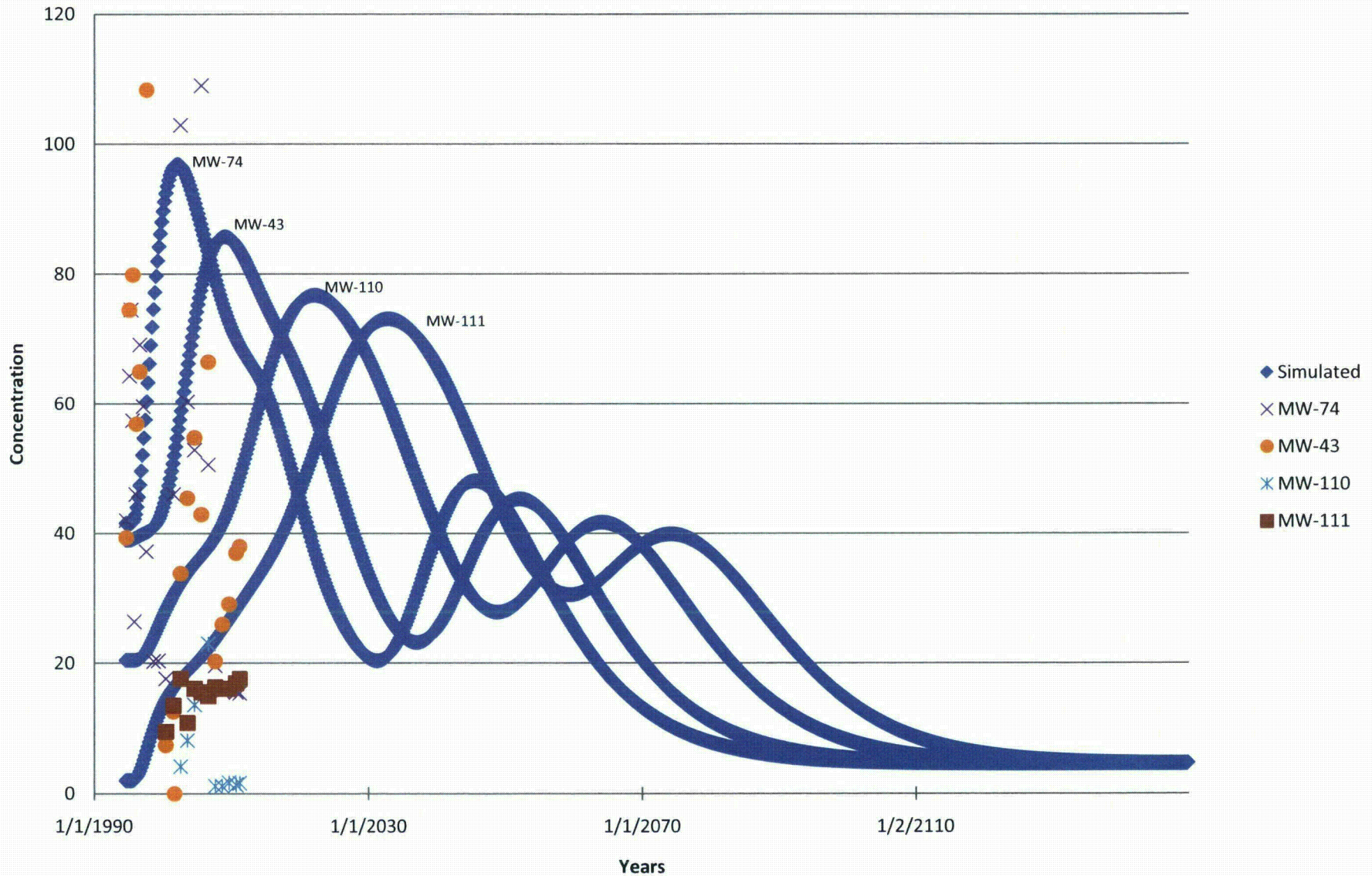
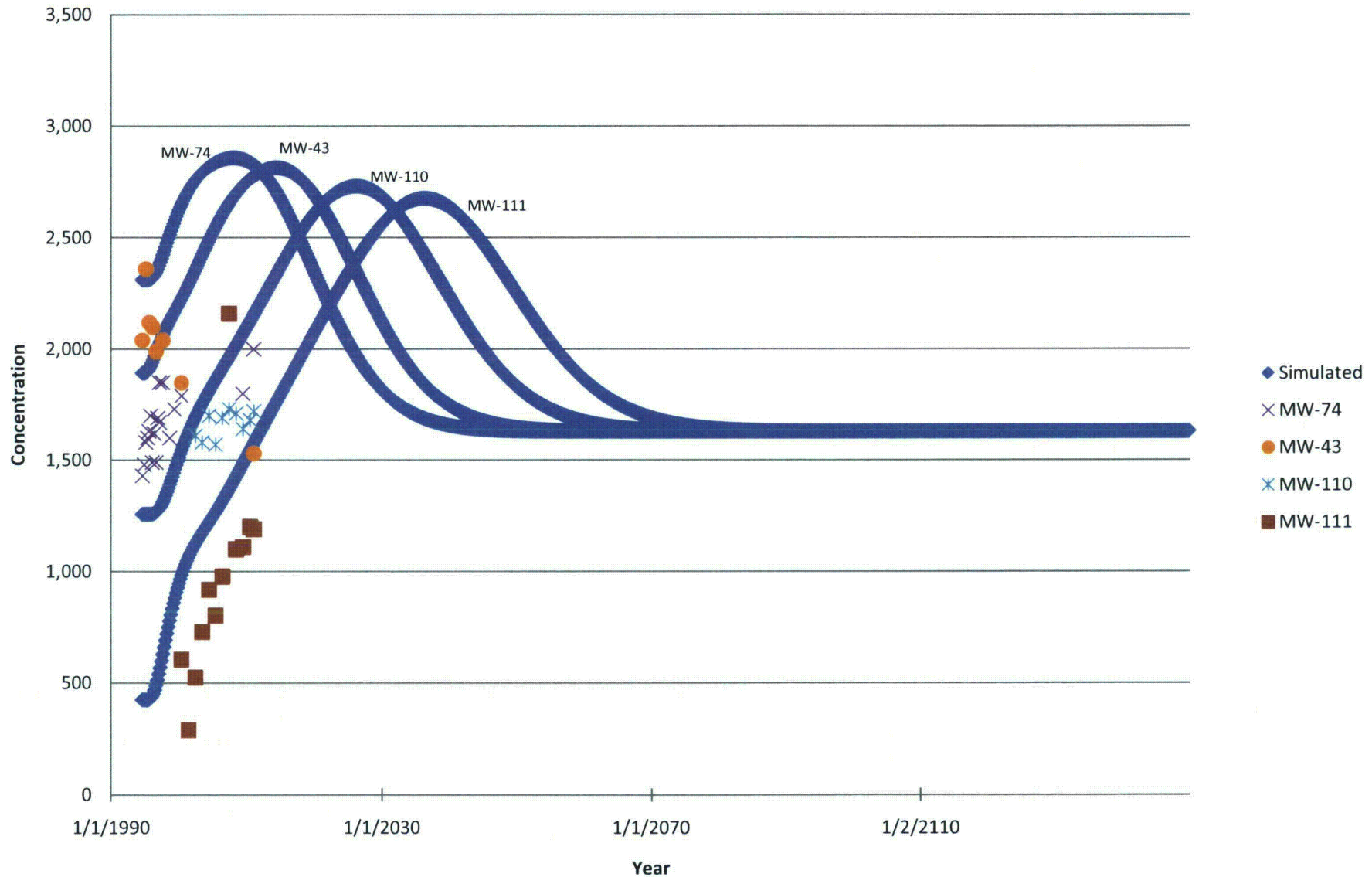


Figure 21B. Predicted Breakthrough of Sulfate
Northern Pathway



**Figure 21C. Predicted Breakthrough of Chloride
Northern Pathway**

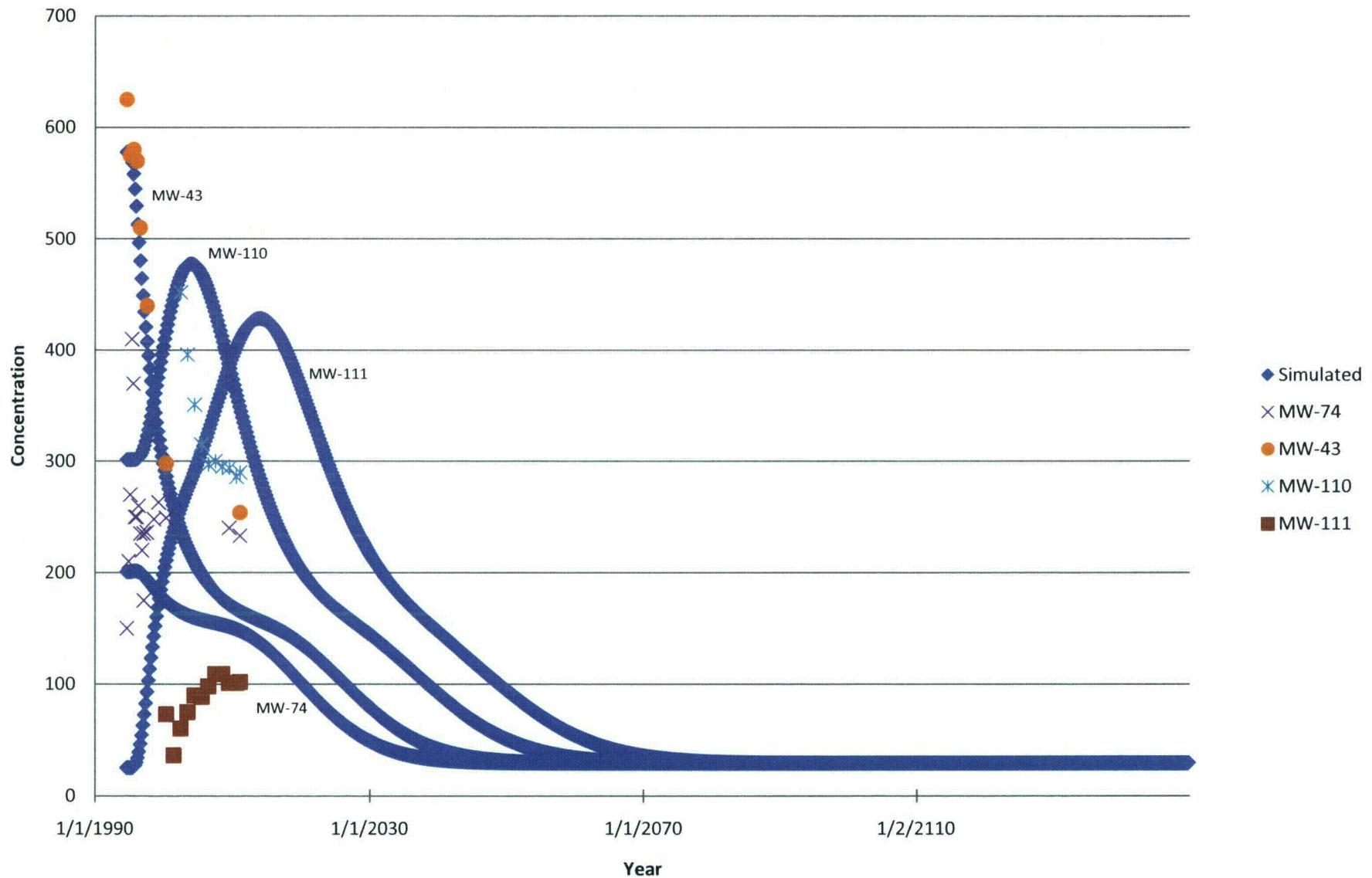
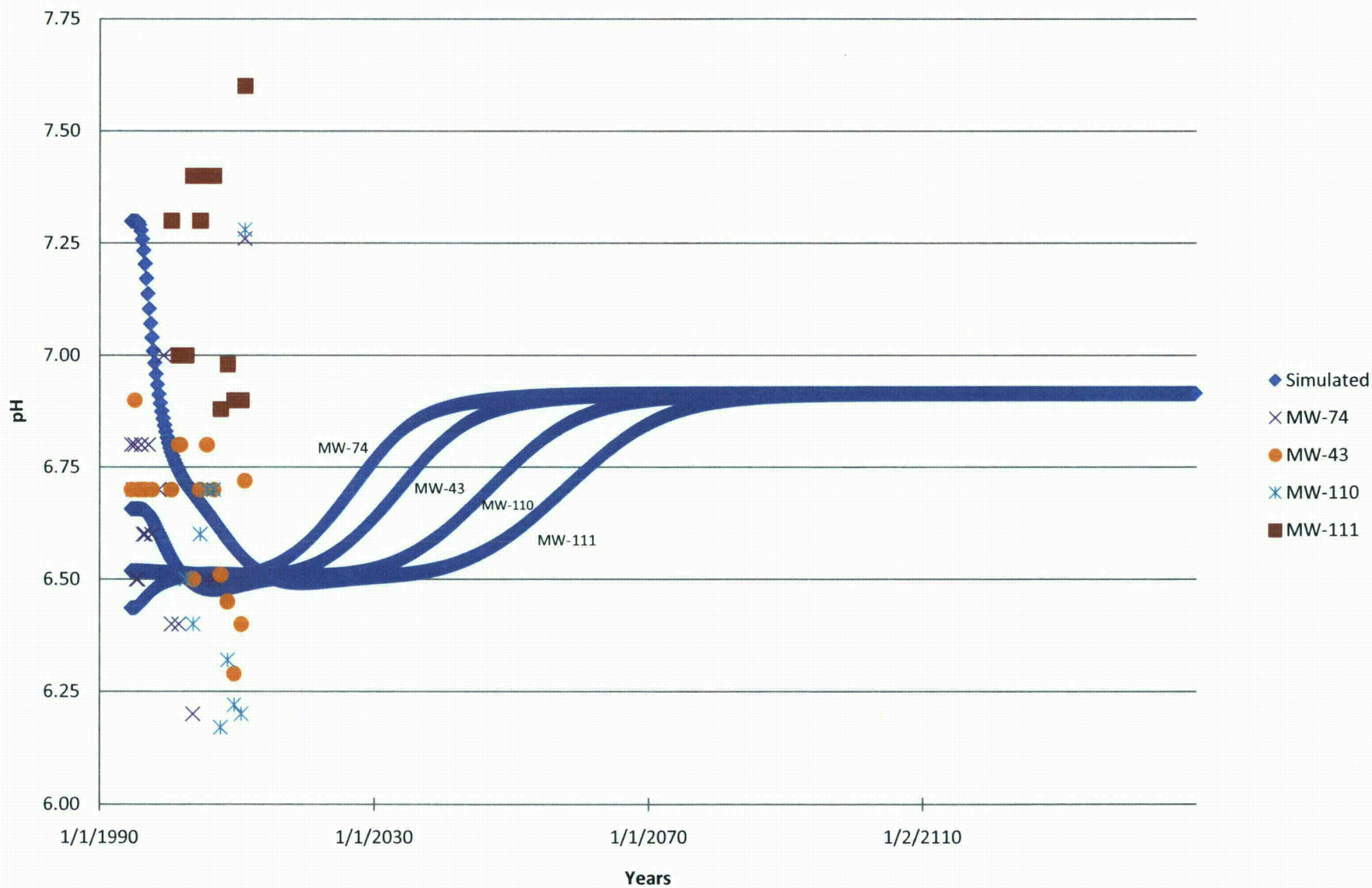


Figure 21D. Predicted Breakthrough of pH
Northern Pathway



**Figure 21E. Predicted Breakthrough of Radium
Northern Pathway**

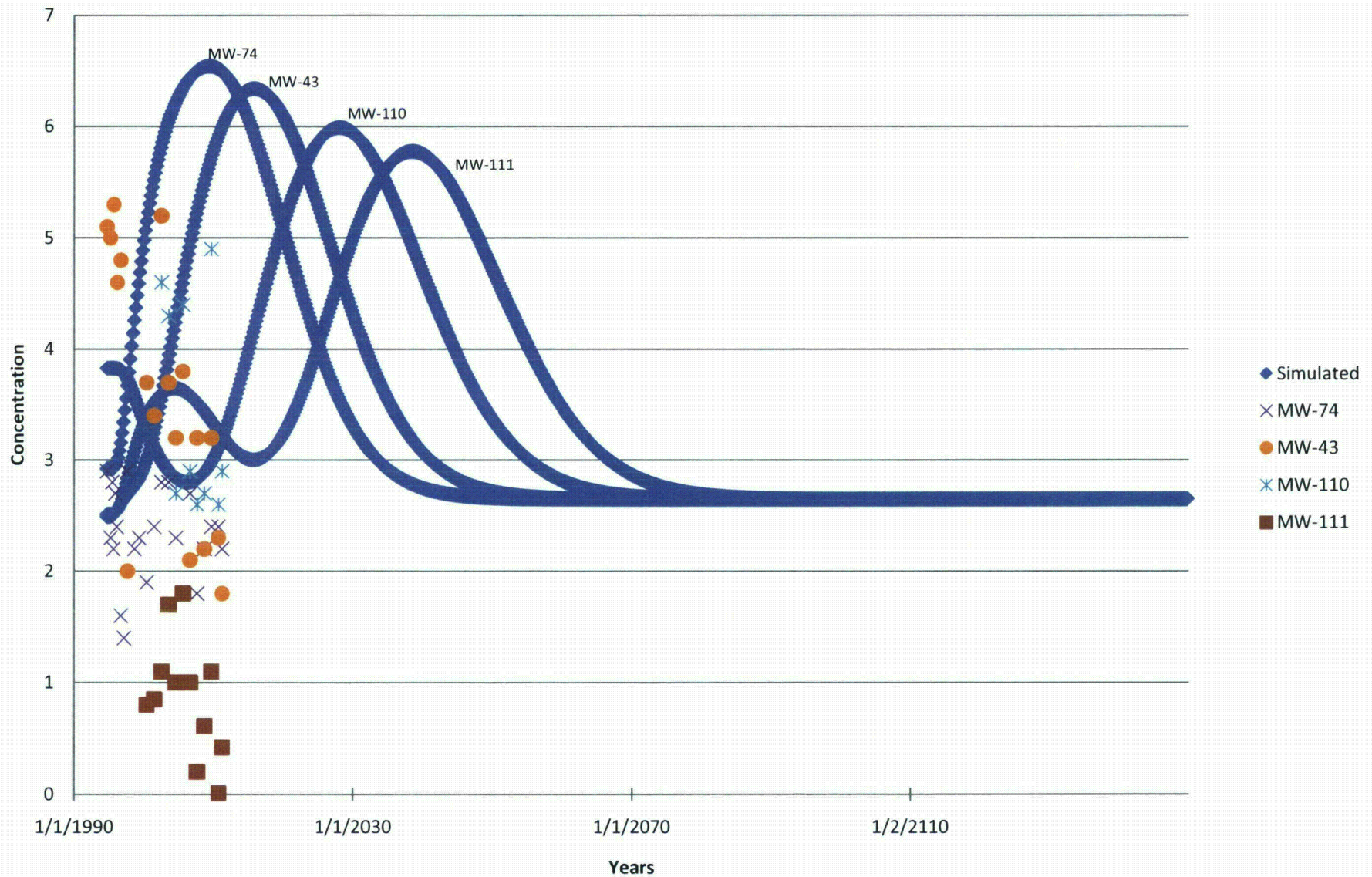


Figure 21F. Predicted Breakthrough of Nickel
Northern Pathway

